

POP Model Intercomparison Study

Stage I. Comparison of descriptions of main processes determining POP behaviour in various environmental compartments

Viktor Shatalov, Elena Mantseva, Arthur Baart, Paul Bartlett, Knut Breivik, Jesper Christensen, Sergey Dutchak, Dagmar Kallweit, Régis Farret, Mikhail Fedyunin, Sunling Gong, Kaj Mantzius Hansen, Ivan Holoubek, Ping Huang, Kevin Jones, Michael Matthies, Gerhard Petersen, Konstantinos Prevedouros, Janusz Pudykiewicz, Michael Roemer, Michael Salzmann, Martin Sheringer, Judith Stocker, Boris Strukov, Noriyuki Suzuki, Andrew Sweetman, Dirk van de Meent, Fabio Wegmann

Edited by MSC-E

METEOROLOGICAL SYNTHESIZING CENTRE - EAST

Ul. Arhitektor Vlasov, 51, Moscow 117393 Russia

tel.: +7 095 128 90 98

fax: +7 095 125 24 09

e-mail: msce@msceast.org

www.msceast.org

The authors (participants):

Arthur BAART

Delft Hydraulics
Rotterdamseweg 185
2629HD Delft
The NETHERLANDS
tel: 31 15 2858585
fax: 31 15 2858582
e-mail: Arthur.Baart@wldelft.nl

Knut BREIVIK

Norwegian Institute for Air Research (NILU)
Center for Ecological Economics, Norway
P.O. Box 100, N-2027 Kjeller,
NORWAY
tel.: + 47 63 89 80 88
fax: + 47 63 89 80 50
e-mail: knut.breivik@nilu.no
www.nilu.no

Sergey DUTCHAK

Meteorological Synthesizing Centre - EAST
Ul.Arhitektov Vlasov, 51
117394 Moscow
RUSSIA
tel: 7 095 120 02 41
fax: 7 095 125 24 09
e-mail: sergey.dutchak@msceast.org

Régis FARRET

Direction des Risques Chroniques
INERIS
Park Technologique ALATA BP no 2
65 550 Verneuil en Halatte
FRANCE
tel: 33 3 44 55 61 27
fax: 33 3 44 55 68 99
e-mail: regis.farret@ineris.fr

Sunling GONG

Air Quality Research Branch, Meteorological Service of
Canada
4905 Dufferin Street, Downsview
Ontario, M3H 5T4
CANADA
tel: 416 739 5749
fax: 416 739 5704
e-mail: Sunling.Gong@ec.gc.ca

Ivan HOLOUBEK

RECETOX - TOCOEN & Associates,
Kamenice 126/3, 625 00 Brno,
CZECH REPUBLIC
tel: +420 5 47 121 401
mobil: +420 602 753 138
fax: +420 5 47 121 431
e-mail: holoubek@recetox.muni.cz / tocoen@tocoen.cz
<http://recetox.muni.cz/>; <http://www.tocoen.cz/>

Kevin JONES

Lancaster University
Environmental Science Department
Institute of Environmental and Natural Sciences
Lancaster LA1 4YQ
UNITED KINGDOM
tel: 44 1524 59 39 72
fax: 44 1524 59 39 85
e-mail: k.c.jones@lancaster.ac.uk

Paul BARTLETT

CBNS, Queens College
City University of New York
Flushing, NY 11367
USA
tel.: 718 670 41 83
fax: 718 670 41 89
e-mail: paulwoodsbartlett@hotmail.com

Jesper CHRISTENSEN

National Environmental Research Institute
Department of Atmospheric Environment
P.O.Box 358, Frederiksborgvej 399
DK-4000 Roskilde
DENMARK
tel: +45 46 30 11 75
fax: +45 46 30 12 14
e-mail: jc@dmu.dk

Dagmar KALLWEIT

Federal Environmental Agency
II 6.2- Air Quality
POB 33 00 22, D - 14191 Berlin
GERMANY
tel.: 49 30 8903 2839
fax: 49 30 8903 2285
e-mail: dagmar.Kallweit@uba.de
<http://www.umweltbundesamt.de>

Mikhail FEDYUNIN

Meteorological Synthesizing Center "East"
Ul. Arhitektov Vlasov, 51,
Moscow 117393
RUSSIA
tel.: +7 095 128 96 21
fax: +7 095 125 24 09
e-mail: msce@msceast.org

Kaj Mantzius HANSEN

National Environmental Research Institute
Department of Atmospheric Environment
P.O.Box 358, Frederiksborgvej 399
DK-4000 Roskilde
DENMARK
tel: +45 46 30 18 72
fax: +45 46 30 12 14
e-mail: kmh@dmu.dk

Ping HUANG

Air Quality Research Branch, Meteorological
Service of Canada
4905 Dufferin Street, Downsview
Ontario, M3H 5T4
CANADA
tel: 416 739 5749
fax: 416 739 5704
e-mail: Ping.Huang@ec.gc.ca

Elena MANTSEVA

Meteorological Synthesizing Center "East"
Ul. Arhitektov Vlasov, 51,
Moscow 117393
RUSSIA
tel.: +7 095 128 96 21
fax: +7 095 125 24 09
e-mail: elena.mantseva@msceast.org

Michael MATTHIES

Institute of Environmental Systems Research
University of Osnabrueck
Artilleriestr. 34, D-49069 Osnabrueck
GERMANY
tel: 49 541 969 2576
fax: +49 541 969 2599
e-mail: matthies@usf.Uni-Osnabrueck.de

Konstantinos PREVEDOUROS

Lancaster University
Environmental Science Department
LA1 4YQ Lancaster,
UNITED KINGDOM
tel: 0044 1524 593974
e-mail: c.prevedouros@lancaster.ac.uk

Michael ROEMER

TNO-MEP
Laan van Westenenk 501
Postbus 342
7300 AH Apeldoorn
The NETHERLANDS
tel: 31 55 5493787
fax: 31 55 5493252
e-mail: M.G.M.Roemer@mep.tno.nl

Martin SCHERINGER

Swiss Federal Institute of Technology
ETH Hönggerberg
CH-8093 Zuerich
SWITZERLAND
fax: +41 1 632 11 89
e-mail: scheringer@tech.chem.ethz.ch

Judith STOCKER

Swiss Federal Institute of Technology
ETH Hönggerberg
CH-8093 Zuerich
SWITZERLAND
fax: +41 1 632 11 89
e-mail: judith.stocker@tech.chem.ethz.ch

Noriyuki SUZUKI

National Institute for Environmental Studies
16-2 Onogawa, Tsukuba, Ibaragi 305-8506
JAPAN
tel: +81-298-50-2331
fax: +81-298-50-2880
e-mail: nsuzuki@nies.go.jp

Dirk van de MEENT

RIVM Laboratory for Ecological Risk Assessment,
Postbus 1, 3720BA Bilthoven,
THE NETHERLANDS
tel: +31 30 274 3130 (3015);
fax: +31 30 274 4413
e-mail: D.van.de.Meent@rivm.nl

Gerhard PETERSEN

GKSS - Research Centre, Institute of Hydrophysics
Max-Planck-Strasse 1, D-21502 Geesthacht
GERMANY
tel: 49 41 52 87 18 47
fax: 49 41 52 87 18 88
e-mail :
petersen@gkss.de/Gerhard.Petersen@gkss.de

Janusz PUDYKIEWICZ

AES, Environment Canada Service
2121 trans-Canada Highway
Dorval, Quebec, H9P 1J3
CANADA
tel. 514 421 72 12
fax 514 421 21 06
e-mail Janusz.Pudykiewicz@ec.gc.ca

Michael SALZMANN

Swiss Federal Institute of Technology
ETH Hönggerberg
CH-8093 Zuerich
SWITZERLAND
fax: +41 1 632 11 89
e-mail: msalz@student.ethz.ch

Victor SHATALOV

Meteorological Synthesizing Center "East"
Ul. Arhitektov Vlasov, 51, Moscow 117393
RUSSIA
tel.: +7 095 128 96 21
fax: +7 095 125 24 09
e-mail: Victor.Shatalov@msceast.org

Boris STRUKOV

Meteorological Synthesizing Centre - EAST
Ul.Arhitektov Vlasov, 51, 117394 Moscow
RUSSIA
tel: 7 095 128 96 21
fax: 7 095 125 24 09
e-mail: msce@msceast.org

Andrew SWEETMAN

Environmental Science Department
Lancaster University
Lancaster, LA1 4YQ
UNITED KINGDOM
tel: 44 1524 59 33 00
fax: 44 1524 59 39 85
e-mail: a.sweetman@lancaster.ac.uk

Fabio WEGMANN

Swiss Federal Institute of Technology
ETH Hönggerberg
CH-8093 Zuerich
SWITZERLAND
fax: +41 1 632 11 89
e-mail: fwegmann@tech.chem.ethz.ch

CONTENTS

| | |
|---|-----|
| Introduction | 7 |
| <i>Chapter 1.</i> Overview of participating models | 11 |
| <i>Chapter 2.</i> Intercomparison programme | 15 |
| <i>Chapter 3.</i> Comparison of physical-chemical properties and degradation rates of PCB-153 between individual models | 19 |
| 3.1. The Henry's law constant and the air-water partition coefficient | 21 |
| 3.2. The subcooled liquid vapour pressure | 24 |
| 3.3. The octanol/water partition coefficient | 26 |
| 3.4. The octanol/air partition coefficient | 29 |
| 3.5. The organic carbon/water partition coefficient | 31 |
| 3.6. Water solubility | 32 |
| 3.7. Degradation rate constants of PCBs in the environmental media | 33 |
| <i>Chapter 4.</i> Comparison of process parameterizations and results of computational experiments for PCB-153 | 37 |
| 4.1. Gas/particle partitioning | 37 |
| 4.2. Dry deposition of the particulate phase | 42 |
| 4.3. Wet deposition | 45 |
| 4.4. Gaseous exchange between atmosphere and soil | 50 |
| 4.5. Gaseous exchange between atmosphere and water | 58 |
| 4.6. Gaseous exchange between atmosphere and vegetation | 63 |
| Conclusions | 67 |
| References | 72 |
| <i>Annex A.</i> Descriptions of the models | 77 |
| <i>Annex B.</i> Comparison of physical-chemical properties of PCB-28 and PCB-180 between individual models | 89 |
| <i>Annex C.</i> Descriptions of main processes | 111 |
| <i>Annex D.</i> Comparison of results of computational experiments for PCB-28 | 147 |
| <i>Annex E.</i> Comparison of results of computational experiments for PCB-180 | 157 |

INTRODUCTION

Environmental pollution by Persistent Organic Pollutants (POPs) (or Persistent Bio-accumulative and Toxic Substances (PBTs)) is one of the global problems to be resolved by the international community. Wide interest to problems of environmental contamination by POPs can be explained by the fact that these pollutants possess high toxicity for living organisms, persistence in the environment, and ability to be built up in food chains to levels that are harmful to human health and ecosystems. Moreover, these substances can be transported over long distances from emission sources and be distributed between different environmental compartments - air, water, soil and vegetation.

The problem of environmental pollution by POPs is in the spotlight of the Convention on Long-range Transboundary Air Pollution of 1979 and the Stockholm Convention on POPs of 2001. This problem attracts attention of numerous international programmes and organisations: the United Nations Environment Programme (UNEP), the Organisation for Economic Co-operation and Development (OECD), the World Health Organisation (WHO), the World Meteorological Organisation (WMO), the Arctic Monitoring and Assessment Programme (AMAP), the Baltic Marine Environment Protection Commission (HELCOM), the Oslo-Paris Commission for the Protection of the Marine Environment of the North-East Atlantic (OSPAR) and others.

Within the framework of the Convention on Long-range Transboundary Air Pollution of 1979 (hereinafter Convention), the Protocol on Persistent Organic Pollutants (hereinafter the Protocol on POPs) is ratified by sixteen Parties to the Convention and has entered into force in October 2003. In addition to the fulfilment of their basic obligations, Parties to the Protocol shall encourage research, development, monitoring and co-operation related, in particular, to the long-range transport and deposition levels and their modelling. In compliance with the Protocol "in good time before each annual session of the Executive Body, the Co-operative Programme for Monitoring and Evaluation of the Long-range Transmission of Air Pollutants in Europe (hereinafter EMEP) shall provide information on the long-range transport and deposition of persistent organic pollutants" (Article 9) [ECE/EB.AIR/66, 1999].

For the assessment of environmental pollution, for the risk assessment, for the evaluation of new pollutants as potential candidates to be implemented in the regulatory control activity, a number of different model approaches are under development. To review different model approaches and improve our understanding of POP behaviour in various environmental compartments, POP model intercomparison study was initiated by EMEP.

A certain experience in model intercomparison for different types of pollutants is accumulated in the Meteorological Synthesizing Centre - East of EMEP (hereinafter EMEP/MSC-E). In particular, intercomparison of transport models for heavy metals was carried out in 1996 (for lead) [Sofiev *et al.*, 1996] and in 1998 (for cadmium) [Gusev *et al.*, 2000]. Intercomparison of mercury transport models was initiated in 1999 and is now in progress with participation of many scientists from various countries [Ryaboshapko *et al.*, 2002; Ryaboshapko *et al.*, 2003]. The recommendations to carry out the comparison of different POP multicompartment models were drawn by the Executive Body for the Convention [ECE/EB.AIR/75, 2002]. Later, the necessity of performing such intercomparison was stressed at the OECD/UNEP Workshop on the Use of Multimedia Models for Estimating Overall Environmental Persistence and Long-Range Transport held in Ottawa in 2001 [ENV/JM/MONO(2002)15, 2002]. Several POP model comparisons concerning particular question of estimating overall persistence and atmospheric travel distances of some POPs were accomplished [Wania and Mackay, 2000; Wania and Dugani, 2003]. In 2002, EMEP/MSC-E initiated the intercomparison study of POP multicompartment models aimed at comparing different approaches to POP modelling both in general and in detail.

The draft programme of the intercomparison study was prepared on the basis of the discussion on POP model intercomparison issues during the third EMEP/TFMM meeting in Geneva, March 2002 [EB.AIR/GE.1/2002/4]. The first meeting on the model intercomparison with participation of national experts (both in modelling and measurements) from Canada, the Czech Republic, France, Germany, Japan, Norway, Switzerland, the United Kingdom, the USA and representatives of the OECD was organised by EMEP/MSC-E (Moscow, November 2002). Presentations of the participating models, acceptance of the Programme on intercomparison study of POP models, in-depth discussion of the goals of Stage I and elaboration of its time-schedule were the main topics at this meeting. Since that time, modellers from Denmark and the Netherlands have joined this activity.

Table 1 displays a list of the participating models together with brief descriptions of model type and resolution. The study concerns a wide spectrum of models designed for the simulation of POP behaviour in the environment. It should be mentioned that both generic and spatially resolved dynamic models are involved in this study.

Table 1. *The list of participating models*

| | Model name | Type/ resolution | Experts | Institution |
|----|---------------------------|---|--|---|
| 1 | HYSPLIT 4 | Lagrangian, regional | P. Bartlett | CBNS, Queens College, USA |
| 2 | EVN-BETR (European scale) | Dynamic box/5x5°, regional | K. Jones, A. Sweetman, C. Prevedouros | Lancaster University, UK |
| 3 | UK-MODEL (UK scale) | Dynamic, box model, regional (UK) | | |
| 4 | ELPOS | Box model, regional, parameterization close to EUSES 1.0 | M. Matthies | Univ. Osnabrück, Germany |
| 5 | ChemRange | one-dimensional, steady-state box model | M. Scheringer, F. Wegmann, M. Salzmann J. Stocker | ETH Zürich, Switzerland |
| 6 | CliMoChem | two-dimensional box model with temporal resolution | | |
| 7 | CAM/POPs | Gridded, regional/global | S. Gong, P. Huang | Air Quality Research Branch, Canada |
| 8 | G-CIEMS | multi-box with geo-referenced geographical resolution (10x10 km ²), regional | N. Suzuki | National Institute for Environmental Studies, Japan |
| 9 | INERIS | Box model, regional, parameterization close to EUSES and ChemCan | R. Farret | Chronic Risks Division, INERIS, France |
| 10 | GLOBO-POP | zonally averaged non-steady state global multimedia fate and transport model | K. Breivik | NILU, Norway |
| 11 | POPCYCLING-Baltic | regional multimedia fate and transport model | | |
| 12 | MEDIA | gridded (2x2°), global | J. Pudykiewicz | Meteorological Service of Canada |
| 13 | ADOM-POP | 3D-Eulerian atmospheric transport and chemistry model 50x50 km | G. Petersen | GKSS, Germany |
| 14 | DEHM-POP | 3D-Eulerian atmospheric transport and chemistry model, northern hemisphere: 150x150 km, EMEP: 50x50 km | J. Christensen, K.M. Hansen | National Environmental Research Institute, Denmark |
| 15 | SimpleBox | nested multimedia environmental fate model, generic, five spatial scales: regional, continental and global (arctic, moderate and tropic geographic zones) | D. van de Meent | RIVM Laboratory for Ecological Risk Assessment, the Netherlands |
| 16 | The LOTOS model | European domain, lowest 2 km of atmosphere; resolution: about 30x30 km, every hour | M.G.M. Roemer , A.C. Baart | TNO-MEP, the Netherlands |
| 17 | ADEPT | 3D atmospheric transport model for Europe | | Delft Hydraulics, the Netherlands |
| 18 | MSCE-POP | EMEP: 50x50 km or 150x150km, hemispheric: 2.5x2.5° | S. Dutchak, V. Shatalov , M. Fedyunin, E. Mantseva, B. Strukov | EMEP/MSC-E |

This report presents the results of Stage I of the POP model intercomparison study.

Chapter 1 is devoted to a brief overview of the participating models. More detailed descriptions of the models submitted by research groups involved into the intercomparison study are contained in Annex A.

Chapter 2 is devoted to the description of model intercomparison programme. Both the general programme and the programme of Stage I of the intercomparison study are presented.

Chapter 3 provides information on physical-chemical properties of PCB-153 used for calculation experiments in participating models and on “reference data set”. The tables with physical-chemical parameters used in participating models and in “reference data set” for PCB-28 and PCB-180 are presented in Annex B.

Chapter 4 comprises descriptions of main processes determining PCBs behaviour in the environment as submitted by the participants, input data and the analysis of the results of calculation experiments for PCB-153. Descriptions of main processes determining POP behaviour in the environment are summarised in Annex C. Tables with input data for calculation experiments and results of model intercomparison on PCB-28 and PCB-180 are given in Annexes D and E, respectively.

Main conclusions are drawn in the end of the Technical Report.

More detailed information on the POP model intercomparison study can be found at the MSC-E website: www.msceast.org.

OVERVIEW OF PARTICIPATING MODELS

This chapter is devoted to a brief analysis of similarities and distinctions between models participating in the intercomparison study. This analysis is used for the determination of the intercomparison procedure. A more detailed description of individual models is presented in Annex A.

Table 2 contains the list of participating models together with their main characteristics: model type and/or spatial resolution, chemicals included in modelling, list of media considered, processes taken into account, input information needed for simulations and output of the models.

It is seen that the diversity of the models taking part in the intercomparison study is very large. These models differ by their type (box models or spatially resolved models), resolution and scope (from global to regional scales). These differences are mostly explained by the diversity of main purposes for which each individual model was designed (last column of Table 2).

However, the considered models have much in common. The majority of the models take into account POP behaviour in several environmental compartments (except for four purely atmospheric models – HYSPLIT 4, ADOM-POP, ADEPT and the LOTOS model). The main environmental compartments included in all these models are the atmosphere, soil and water. Some models take into account vegetation (EVN-BETR, ELPOS, G-CIEMS, POPCYCLING-BALTIC, MSCE-POP) and sediments (EVN-BETR and UK-MODEL, ELPOS, GLOBO-POP, POPCYCLING-BALTIC, MSCE-POP). Two models (MEDIA and MSCE-POP) consider the exchange between the atmosphere and the cryosphere (sea ice and snow). Most of the models describe the same processes: gas/aerosol partitioning, deposition processes, exchange between different environmental compartments, and POP degradation in various environmental media. However, the participating models can differ substantially from one another in the degree of detail of the descriptions of these processes. To evaluate the compatibility of the results obtained by models of different types, it is important to compare model descriptions of the above processes.

Most of the models are able to simulate the environmental behaviour of a large diversity of POPs. Such substances as PCBs, PAHs, HCHs, PCDD/Fs and HCB are included in the list of chemicals for most of the participating models. Among these substances, PCBs (in particular, PCB-153) are the most investigated chemicals for which a lot of information on physical-chemical properties and environmental pollution levels is available. This group of pollutants may be a good basis for the comparison of model descriptions of POP behaviour in the environment.

All the models use similar sets of input information. The most important input parameters common for all the models are data on physical-chemical properties of the considered POPs and on their emissions. Maximum differences in the input parameters of different models are related to meteorological and geophysical information. It should be noted that, at least at the beginning of the intercomparison study, only the information on physical-chemical properties of substances is essential, since the comparison between the models can be performed for some conventional environmental conditions. At the next steps of the intercomparison study, the information on emissions and on measured environmental levels of POPs becomes necessary.

In spite of considerable differences between output parameters of compared models, some of them can be obtained with the use of almost all of the models. These are deposition/exchange fluxes between environmental compartments, contents of POPs masses in these compartments (mass

balance calculations) and overall persistence and long-range transport potential for considered POPs. The comparison between these output parameters produced by different models under the same conventional environmental conditions is a useful exercise for harmonising outputs of different models used in the study.

Below we present the program of the intercomparison study as a whole with a detailed description of its first stage (Chapter 2), an analysis of physical-chemical properties of PCB-153 used in different POP multicompartment models (Chapter 3) and a discussion on the results of computational experiments carried out at Stage I of the study (Chapter 4). The comparison between mass balances, environmental levels, overall persistence and long-range transport potentials of POPs as predicted by the participating models will be performed at subsequent stages of the intercomparison study.

Table 2. *Summary of model properties*

| Model | Type/ resolution | Chemicals | Media | Processes | Input | Output |
|------------------------------|--|--|---|---|---|--|
| HYSPLIT 4 | Lagrangian, regional | HCB, dioxin, PCBs and atrazine | Atmosphere | dispersion in the atmosphere, deposition, destruction | phys-chem properties, emissions, | depositions, source-to-receptor relationships |
| EVN-BETR (European scale) | dynamic box/5°x5°, regional | PCBs, PCDD/Fs, PAHs, Ocs, PBDEs | air, veg., soil, water, sed. | atmospheric transport, exchange | phys-chem properties, emissions, air flow balances | persistence, transport potential, |
| UK-MODEL (UK scale) | dynamic, box model, regional (UK) | PCBs, PCDD/Fs, PAHs, Ocs, PBDEs | air, soil, water, sed. | dynamic intermedia mass transfer (deposition, volatilization), gas-particle partitioning, degradation, | phys-chem properties, dynamic emissions | concentrations, mass flows, persistence |
| ELPOS | box model, regional, parameterization close to EUSES 1.0 | 109 substances (PCBs, PCDD/Fs, pesticides, industrial chemicals) | Air, water, soil, sediments, vegetation | intermedia mass transfer (deposition, volatilization), gas-particle partitioning (2 models), degradation, substance specific soil penetration depth | phys-chem properties, emissions, environmental parameters | overall persistence, CTD in air, CTD in water, mass percentages, stickiness |
| ChemRange | one-dimensional, steady-state box model | non-polar organic chemicals | air, soil, water. | degradation, transport in water and air, exchange between compartment, wet and dry deposition, partitioning, runoff from soil, leaf fall | phys-chem properties, emissions, environmental parameters | concentrations, mass fractions and mass flows, overall persistence, spatial range |
| CliMoChem | two-dimensional box model with temporal resolution | non-polar organic chemicals | air, soil, water. | degradation, transport in water and air, exchange between compartment, wet and dry deposition, partitioning, runoff from soil, leaf fall | phys-chem properties, emissions, environmental parameters | concentrations, mass fractions and mass flows, persistence, spatial ranges, cold condensation potentials |
| CAM/POPs | gridded, regional/global | PCBs | air, soil, water | gas/aerosol partitioning, transport exchange, deposition, degradation | phys-chem properties, emissions, environmental parameters | air concentrations and depositions |
| G-CIEMS | multi-box with geo-referenced geographical resolution (10x10 km ²), regional | PCDD/Fs | air, soil, rivers, coastal sea, vegetation | transport, partitioning, deposition, degradations, runoff | phys-chem properties, emissions, geographic/hydrological/ meteorological data | gross input and output between target area and outer boundary for each transport pathway |
| INERIS | box model, regional, parameterization close to EUSES and ChemCan | | | | | |
| GLOBO-POP | zonally averaged non-steady state global multimedia fate and transport model | HCHs, PCBs | air, two soils, fresh and ocean water and sediments | degradation, transport in water and air, exchange between compartment, wet and dry deposition, partitioning | phys-chem properties, emissions, monthly averaged environmental parameters | assessment of the long range transport behaviour of persistent organic chemicals |

| | | | | | | |
|-------------------|--|---|---|---|---|--|
| POPCYCLING-Baltic | regional multimedia fate and transport model | HCHs | air, two soils, fresh and sea water and sediments, vegetation | degradation, transport in water and air, exchange between compartment, wet and dry deposition, partitioning | phys-chem properties, emissions, monthly averaged environmental parameters | a quantitative understanding of the historical behavior of HCHs in Baltic region |
| MEDIA | gridded (2x2°), global | HCHs | air, soil, ocean, cryosphere | transport in air and sea, deposition, exchange, degradation | phys-chem properties, emissions, meteorological data | fields of air concentrations |
| ADOM-POP | 3D-Eulerian atmospheric transport and chemistry model 50x50 km | PAHs (B[a]P) | air | atmospheric transport and diffusion, cloud processes, physico-chemical transformations, deposition | phys-chem properties, meteorology, geophys. information, emissions | deposition and concentration fields |
| DEHM-POP | 3D-Eulerian atmospheric transport and chemistry model, northern hemisphere: 150x150 km, EMEP: 50x50 km | α -HCH | air, soil, water | atmospheric advection and diffusion, deposition, air/surface gas exchange, degradation | phys-chem properties, meteorological data, geophysical information, emissions | deposition and concentration fields |
| SimpleBox | nested multimedia environmental fate model generic, five spatial scales: regional, continental and global (arctic, moderate and tropic geographic zones) | more than 100 organic substances | air, fresh and sea water, sediment, soil, vegetation | partitioning, wet and dry deposition, intermedia transfer processes, degradation, advective and diffusive transport | phys-chem properties, emissions, environmental parameters | Overall persistence in the environment: <ul style="list-style-type: none"> • residence time at steady state ratio of inventory and input (or output) • clearance time (dynamic) Long-range transport potential: <ul style="list-style-type: none"> • transport out of regional scale as fraction of input (or output) at steady state |
| ADEPT | 3D atmospheric transport model for Europe | organic pollutants | atmosphere | partitioning; transport; wet and dry deposition | phys-chem properties, emissions | concentrations, deposition fluxes |
| The LOTOS model | European domain, lowest 2 km of atmosphere; chemistry based on ozone and aerosols; resolution: about 30x30 km, every hour | lindane | atmosphere | partitioning; transport; wet and dry deposition; | phys-chem properties; analysed meteorological fields; emissions, | deposition and concentration fields |
| MSCE-POP | EMEP: 50x50 km or 150x150km, hemispheric 2.5x2.5° | PAHs, PCBs, PCDD/Fs, γ -HCH, HCB | air, soil, water, veg., sed., cryosphere | gas/aerosol partitioning, exchange, deposition, degradation | phys-chem properties, meteorology, geophysical information, emissions | deposition and concentration fields, media distribution, long-term trends |

INTERCOMPARISON PROGRAMME

The description of the programme on the intercomparison study of POP models is presented in this Chapter. Its first section contains a brief overview of the intercomparison programme in general. The second section is devoted to a more detailed description of the programme of Stage I of the intercomparison study.

The study concerns a wide spectrum of models designed for simulating POP behaviour in the environment. These models can be spatially resolved or generic. Below, they are referred to as **POP models**.

Objectives. The main objectives of the intercomparison study are:

- to strengthen the exchange of scientific expertise between different groups working in the field of POP modelling;
- to increase the transparency of existing POP models and their results: model concept, parameterisations, temporal and spatial resolution and output and uncertainties;
- to harmonise the output parameters of POP models of different types and complexity for obtaining comparable results at different levels of regulatory activities;
- to consider model approaches to the evaluation of new substances.

Stages of the intercomparison. The model intercomparison study is performed in the following stages:

- Stage I.** Comparison of descriptions of main processes determining POP behaviour in various environmental compartments.
- Stage II.** Comparison of mass balance estimates and calculated deposition and concentration fields of POPs in different environmental compartments. Sensitivity study with respect to physical-chemical parameter values used in basic process descriptions and mass balance estimates.
- Stage III.** Comparison of calculated overall environmental persistence and long-range transport potential for evaluation of new substances.

At Stage I, model descriptions of the main processes determining POP fate in the environment (scavenging, partitioning, degradation etc.) are compared. This implies the comparison between the approaches to parameterisation of these processes by the models and between the models' operation. The latter is performed via relevant computational experiments. Details of Stage I are given below.

At Stage II, the balance values are compared (PCB masses in different environmental compartments: atmosphere, soil, water, vegetation; masses of PCB degraded in these compartments; mass fluxes of PCB transported in/out of the specified domain; mass fluxes of PCB transported from one compartment to another; and PCB concentrations at each interface). The comparison is carried out on agreed conditions (e.g., land cover data, leaf area index, organic matter content in the soil, environmental temperature regime etc.) and with the use of input data on emissions with zero initial concentrations of PCBs in environmental media and, as optional, with initial concentrations for the

specified calculation domain (35°N – 70°N; 10°W – 30°E). Additionally, the comparison between spatial distribution patterns of depositions and PCBs concentrations in various environmental compartments as predicted by different models is performed; these characteristics can be also compared with monitoring data (optional). Sensitivity studies with respect to physical-chemical parameter values used in the process descriptions and mass balance estimates are carried out. The second intermediate report can be an output of this stage.

At Stage III, model estimates of the long-range transport potential and the overall environmental persistence data on POPs are compared. Such a comparison can be performed for chemicals proposed below. The results of the study should be published in the final report including the results of all stages, conclusions and recommendations.

Pollutants selected for the intercomparison: First priority: PCB-153. Second priority: B[a]P, lindane, PCB-28, PCB-180, as a new pollutant - PBDE (proposed by R. Farret).

Computational experiments with PCB-153 are agreed to be the subject of this intercomparison study. For other selected pollutants, it is proposed to carry out computational experiments on the voluntary basis.

“Reference data set”: Taking into account recommendations of the first meeting, the internally consistent data sets of key physical-chemical properties and degradation rates of PCBs hereinafter referred to as “reference data sets” were proposed for model testing. Calculations within the sensitivity study with respect to physical-chemical parameters should be performed at Stage II with the help of these data sets. For models using “reference data sets” as own physical-chemical properties, alternative data sets based on individual data of some other participating models are proposed for this sensitivity study.

Emission data: Officially reported emission data on PCBs are still incomplete in terms of their spatial and temporal coverage to satisfy the data requirements for the calculation experiments to be performed at Stage II. Therefore, consistent global atmospheric emission estimates presented by [Breivik *et al.* 2002] (see also www.nilu.no/projects/globalpcb/) have been chosen. The higher (or worst-case) emission estimate is to be applied, as this particular scenario appears to be more reasonable on the global scale [Wania and Daly, 2002; Meijer *et al.* 2003].

Time-schedule:

Table 3. Time-table of the intercomparison study

| Stage | Time period |
|---|-------------------------------|
| I. Process descriptions | November 2002 – February 2004 |
| II. Mass balance estimates and calculated deposition and concentration fields | March 2004 –December 2004 |
| III. Overall environmental persistence and long-range transport potential | December 2004 – August 2005 |

Stage I

Stage I is aimed at the comparison of descriptions of basic processes affecting POPs fate in the environment (listed below). This comparison is based on the analysis of process descriptions (approach and parameterisation) used in different POP models coupled with the analysis of the results of computational experiments carried out by the participating POP models.

Basic processes. The following processes are considered:

- Gas/particle partitioning of POPs in the atmosphere.
- POP deposition from the atmosphere (wet deposition for gaseous and particulate phases and dry deposition of particulate phase onto forest, grass, bare soil, and water surfaces).
- Gas exchange processes between the atmosphere and different types of underlying surface (soil, water, vegetation).
- POP degradation in various environmental compartments (the atmosphere, soil, vegetation, water).

Physical-chemical properties. Within the framework of Stage I, it was agreed to carry out computational experiments for the considered PCB congeners on the basis of physical-chemical data sets applied by the individual models. Physical-chemical parameters used in the description of the above processes were submitted by the participating models. This information is analysed in Chapter 3 and Annex B.

Computational experiments. The following computational experiments have been performed:

- Calculations of POP gas/particle partitioning in the atmosphere (particulate fraction for a range of temperatures).
- Calculations of dry deposition fluxes to agreed types of underlying surfaces (forest, grass, bare soil, seawater).
- Calculations of wet deposition fluxes both for gaseous and particulate phases and total POP concentrations in precipitation.
- Calculations of POP concentrations in different environmental media and/or gaseous fluxes from and to underlying surfaces (soil, water, vegetation) at given atmospheric concentrations.
- Calculations of temporal trends characterising POP concentrations in the soil at the stages of their accumulation and clearance (optional additional experiment).

The input data for modelling include several sets of given PCB air concentrations in different phases (if needed) and environmental conditions (averaged ambient temperatures, organic content in the atmospheric aerosol, TSP, precipitation intensity, mean wind velocity, etc.) relevant for each of the experiments.

A more detailed description of the input data for computational experiments and the analysis of their results are presented in Chapter 4.

COMPARISON OF PHYSICAL-CHEMICAL PROPERTIES AND DEGRADATION RATES OF PCB-153 BETWEEN INDIVIDUAL MODELS

This Chapter provides an overview of physical-chemical properties and degradation rates used in the participating models and in the “reference data set” of PCB-153. The latter is an agreed set of physical-chemical properties for model testing. Appropriate data on PCB-28 and PCB-180 are given in Annex B. Individual data sets have been presented by the following models: CAM/POPs (Canada), DEHM-POP (Denmark), G-CIEMS (Japan), EVN-BETR and UK-MODEL (UK), CliMoChem (Switzerland), and MSCE-POP (EMEP).

Model parameterization of the basic environmental processes (degradation in various media, partitioning between different phases, removal from the atmosphere, and gaseous exchange with underlying surfaces) considered at Stage I can be described with the help of the following physical-chemical properties of PCBs:

- Henry’s law constant (or air/water partition coefficient);
- subcooled liquid vapour pressure;
- octanol/water partition coefficient;
- octanol/air partition coefficient;
- organic carbon/water partition coefficient;
- water solubility;
- degradation rate constants in the environmental media.

The comparison of these parameters base values and coefficients of their temperature dependencies for PCB-153 is made in the appropriate subsections (Similar comparison on PCB-28 and PCB-180 can be found in Annex B). One can see that base values of some physical-chemical properties and/or coefficients of temperature dependencies) vary substantially between different models. The scattering of the values reported by the participants for each parameter can to some extent characterize its uncertainty. To evaluate the uncertainty, a number of statistical parameters (the maximum, the minimum, the arithmetic mean, the median and the geometric mean) are calculated. The plots comparing temperature dependencies of the considered parameters for PCB-153 are presented in Figs. 1-6 (for PCB-28 and PCB-180 – in Figs. B.1-B.12. in Annex B).

The POP Model Intercomparison Study involves models that are fundamentally different in terms of overall modelling approach and objectives. This includes differences in process descriptions as well as variability in their spatial and temporal resolutions. Comparisons of the model results are therefore considered difficult without some sort of harmonisation of input parameters. In order to make the comparison of model outputs more easily to comprehend, it has therefore been decided to standardise certain common input parameters in Stage II of the model intercomparison. The data to be harmonised at follow-up stage include the information on physical-chemical properties (including degradation rates) as well as the emission estimates as these are input parameters that are common to all models. This Chapter contains information on reference data set of PCB-153 physical-chemical properties selected for the calculations within this intercomparison study.

Many studies report data on experimentally determined or theoretically derived physical-chemical properties of individual POPs, but it is difficult to judge which data in the literature that are the more reliable or accurate. However, vapour pressure, Henry's law constant, water solubility, octanol/water and octanol/air partition coefficients should preferably adhere to thermodynamic constraints and be internally consistent [Beyer *et al.*, 2002]. As reference sets for the calculation experiments at Stage II to be carried out for PCBs (153 with 28 and 180 as optional) we have chosen to rely on information presented by Li *et al.* [2003] as this comprehensive data set and compilation fulfill the criteria of internally consistency. For the recalculation of organic carbon/water partition coefficient from octanol/water coefficient, the values of coefficients of regression relation most frequently used by the models are proposed for the "reference data sets". For the sake of simplicity, degradation rate constants in various environmental media are assumed seasonally independent. These values were taken from [Mackay *et al.* 1992].

The "reference data sets" are prepared for the three PCB congeners. Proposed "reference data set" for PCB-153 is presented in Table 4 (data on other PCBs - see Table B.1. in Annex B).

Table 4. "Reference data set" of physical-chemical properties and degradation rates of PCB-153*

| Description | Numerical values | | Comments | Ref. |
|---|--|----------|--|-----------------------|
| Air/water Henry's law constant, H (Pa·m ³ /mol) | | | | |
| Temperature dependent: $H = H_0 \exp (-a_H(1/T - 1/T_0))$ where T - temperature (K), H_0 is the value at the reference temperature T_0 , and a_H is a parameter of temperature dependence. | $H_0(T_0)$, Pa·m ³ /mol | 4.91E+00 | Coefficients are recalculated from the following temperature dependence: $\log H = \log H(25^\circ\text{C}) - (\Delta U_{aw} + R \cdot 298.15)/(\ln(10) \cdot R) \cdot (1/T - 1/298.15)$ where: T - temperature; R - Universal Gas Constant; ΔU_{aw} - internal energy of phase transfer, kJ/mol (for PCB-153: 62.8). $H(25^\circ\text{C})$ - Henry 's law constant at 25°C, Pa·m ³ /mol (PCB-153: 19.8). | Li et al., 2003 |
| | a_H | 7851.7 | | |
| Air/water partition coefficient, K_{aw} (dimensionless) | | | | |
| Temperature dependent: $K_{aw} = K_{aw}^0 \exp (-a_{Kaw}(1/T - 1/T_0))$ where T - temperature (K), K_{aw}^0 is the value at the reference temperature T_0 , and a_{Kaw} is a parameter of temperature dependence. | $K_{aw}^0(T_0)$, dimensionless | 2.09E-03 | Coefficients are recalculated from the following temperature dependence: $\log K_{aw} = \log K_{aw}(25^\circ\text{C}) - \Delta U_{aw}/(\ln(10) \cdot R) \cdot (1/T - 1/298.15)$ where: T - temperature; R - Universal Gas Constant; ΔU_{aw} - internal energy of phase transfer, kJ/mol (for PCB-153: 62.8). $K_{aw}(25^\circ\text{C})$ - dimensionless air/water partition coefficient at 25°C, estimated from: $K_{aw}(25^\circ\text{C}) = H(25^\circ\text{C})/(R \cdot 298.15)$ | Li et al., 2003 |
| | a_{Kaw} | 7553.5 | | |
| Subcooled liquid vapour pressure, p_{ol} (Pa) | | | | |
| Temperature dependent: $p_{ol} = p_{ol}^0 \exp (-a_p(1/T - 1/T_0))$ where T - temperature (K), p_{ol}^0 is the value at the reference temperature T_0 , and a_p is a parameter of temperature dependence. | $p_{ol}^0(T_0)$, Pa | 8.82E-05 | Coefficients are recalculated from the following temperature dependence: $\log p_{ol} = \log p_{ol}(25^\circ\text{C}) - (\Delta U_a + R \cdot 298.15)/(\ln(10) \cdot R) \cdot (1/T - 1/298.15)$ where: T - temperature; R - Universal Gas Constant; ΔU_a - internal energy of phase transfer, kJ/mol (for PCB-153: 87.7). $p_{ol}(25^\circ\text{C})$ - vapour pressure at 25°C, Pa (for PCB-153: 6.06E-4) | Li et al., 2003 |
| | a_p | 10846.6 | | |
| Octanol/water partition coefficient, K_{ow} (dimensionless) | | | | |
| Temperature dependent: $K_{ow} = K_{ow}^0 \exp (a_{Kow}(1/T - 1/T_0))$ where T - temperature (K), K_{ow}^0 is the value at the reference temperature T_0 , and a_{Kow} is a parameter of temperature dependence. | $K_{ow}^0(T_0)$, dimensionless | 1.45E+07 | Coefficients are recalculated from the following temperature dependence: $\log K_{ow} = \log K_{ow}(25^\circ\text{C}) - \Delta U_{ow}/(\ln(10) \cdot R) \cdot (1/T - 1/298.15)$ where: T - temperature; R - Universal Gas Constant; ΔU_{ow} - internal energy of phase transfer, kJ/mol (for PCB-153: -31.1). $K_{ow}(25^\circ\text{C})$ - octanol/water partition coefficient at 25°C, dimensionless (for PCB-153: 7.44E+6) | Li et al., 2003 |
| | a_{Kow} | 3740.7 | | |
| Octanol/air partition coefficient, K_{oa} (dimensionless) | | | | |
| Temperature dependent: $K_{oa} = K_{oa}^0 \exp (a_{Koa}(1/T - 1/T_0))$ where T - temperature (K), K_{oa}^0 is the value at the reference temperature T_0 , and a_{Koa} is a parameter of temperature dependence. | $K_{oa}^0(T_0)$, dimensionless | 2.05E+10 | Coefficients are recalculated from the following temperature dependence: $\log K_{oa} = \log K_{oa}(25^\circ\text{C}) - \Delta U_{oa}/(\ln(10) \cdot R) \cdot (1/T - 1/298.15)$ where: T - temperature; R - Universal Gas Constant; ΔU_{oa} - internal energy of phase transfer, kJ/mol (for PCB-153: -93.9). $K_{oa}(25^\circ\text{C})$ - octanol/air partition coefficient at 25°C, dimensionless (for PCB-153: 2.76E+9); | Li et al., 2003 |
| | a_{Koa} | 11294.2 | | |

| Description | Numerical values | | Comments | Ref. |
|--|----------------------------------|----------|---|--------------------|
| Organic carbon/water partition coefficient, K_{oc} (dimensionless) | | | | |
| Regression relation: $K_{oc} = regc K_{ow}^b$ where $regc$ and b are regression coefficients | $regc$ | 0.41 | K_{oc} is calculated from K_{ow} , where K_{ow} is the temperature dependent octanol-water partitioning coefficient | Karickhoff, 1981 |
| | b | 1 | | |
| Water solubility, S_{WL} (mol/m ³) | | | | |
| Temperature independent | $S_{WL}(T)$, mol/m ³ | 1.80E-05 | Values are calculated for T = 283.15 with the help of the following temperature dependence: log S_{WL} = log $S_{WL}(25^{\circ}C)$ - $\Delta U_W/(\ln(10) \cdot R) \cdot (1/T - 1/298.15)$ where: R - Universal Gas Constant; ΔU_W - internal energy of phase transfer, kJ/mol (for PCB-153: 25.0). $S_{WL}(25^{\circ}C)$ - water solubility, mol/m ³ at 25°C (PCB-153: 3.07E-5); | Li et al., 2003 |
| Degradation rate constants, k_d (1/s) | | | | |
| Degradation in atmosphere: Temperature independent | k_{air} , 1/s | 3.50E-08 | Degradation rate constant in the air is converted from half-life values, h (PCB-153: 5500): $k_d = 0.693/ t_{1/2}$ where k_d is the first-order rate constant (s ⁻¹) and $t_{1/2}$ is the half-life (s). | Mackay et al, 1992 |
| Degradation in soil: Temperature independent | k_{soil} , 1/s | 3.50E-09 | Degradation rate constant in soil is converted from half-life values (PCB-153: 55000): $k_d = 0.693/ t_{1/2}$ where k_d is the first-order rate constant (s ⁻¹) and $t_{1/2}$ is the half-life (s). | |
| Degradation in water: Temperature independent | k_{water} , 1/s | 3.50E-09 | Degradation rate constant in water is converted from half-life values (PCB-153: 55000): $k_d = 0.693/ t_{1/2}$ where k_d is the first-order rate constant (s ⁻¹) and $t_{1/2}$ is the half-life (s). | |
| Degradation in sediment: Temperature independent | k_{sed} , 1/s | 3.50E-09 | Degradation rate constant in sediment is converted from half-life values (PCB-153: 55000): $k_d = 0.693/ t_{1/2}$ where k_d is the first-order rate constant (s ⁻¹) and $t_{1/2}$ is the half-life (s). | |

* - for the sake of comparability, the base values and coefficients of temperature dependences of the considered parameters are given here at the temperature 283.15 K (T_0) and the way they were recalculated from original dependencies is specified in the field "Comments".

The comparison of values of physical-chemical properties and degradation rates of PCB-153 used in data sets of the participating models and "reference data set" is also performed in this Chapter (for PCB-28 and PCB-180 similar comparison is presented in Annex B). Temperature dependencies of the considered parameters from "reference data set" are given in red in Figs. 1-6. Of note that G-CIEMS and SimpleBox models have done the calculations of Stage I with the help of mentioned physical-chemical properties from "reference data sets". The exception is in the selection of K_{oc} - K_{ow} relationship by G-CIEMS. Besides individual/own data sets of EVN-BETR and UK-MODEL are extremely close to the "reference data sets".

3.1. The Henry's law constant and the air/water partition coefficient

Relation between the air-water Henry's law constant, (H or K_H , Pa·m³/mol) and the air/water partition coefficient (K_{aw} , dimensionless) is as follows:

$$K_{aw} = \frac{H}{RT}, \quad (1)$$

where T - temperature, K;

$R = 8.314$ J/(mol·K) - universal gas constant.

Coefficients K_{aw} and H are mainly used in the description of the gaseous exchange process between the atmosphere and soil, and between the atmosphere and water, as well as of wet deposition of the POP gaseous phase. Besides, EVN-BETR and UK-MODEL and CliMoChem models also use K_{aw} for the evaluation the octanol/air partition coefficient (K_{oa}):

$$K_{oa} = K_{ow}/K_{aw}. \quad (2)$$

Temperature dependence of K_{aw} and H is included practically in all participating models (except H value of EVN-BETR and UK-MODEL) (Table 5). Comparison of these dependencies for PCB-153 (used in calculations at Stage I by the participating POP models and in "reference data set") is given in Figs.1a and 1b.

Table 5. The Henry's law constant and the air/water partition coefficient of PCB-153 (data sets of the participating POP models)*

| Model | Description | Numerical values | | Comments | Reference |
|-----------------------|---|-----------------------------------|----------|--|--|
| CAM/POPs | Temperature dependent: $H = H_0 \exp (- a_H (1/T - 1/T_0))$ where T - temperature ($^{\circ}\text{K}$), H_0 is the value at the reference temperature T_0 , and a is a parameter of temperature dependence. Temperature dependent: $K_{aw} = H / (R \cdot T)$ | H_0 , Pa·m ³ /mol | 6.09E-01 | Coefficient a_H of the exponential equation are recalculated from the coefficient of the following temperature dependence: $H = H_0 \cdot 10^{(-3416 (1/T - 1/T_0))}$ with the help of the following formula: $a_H = \ln(10) \cdot 3416$, It was obtained from the following temperature dependence: $\log(H/H(25^{\circ}\text{C}))= \text{slop} (1/T - 1/ 298)$ $H(25^{\circ}\text{C})$ - Henry 's law constant at 25°C , Pa·m ³ /mol (PCB-153: 2.43) | <i>Achman et al.</i> , 1993 |
| | | a_H | 7865.6 | | |
| | | T_0 , $^{\circ}\text{K}$ | 283.15 | | |
| G-CIEMS | Temperature dependent: $H = H_0 \exp (- a_H (1/T - 1/T_0))$ where T - temperature (K), H_0 is the value at the reference temperature T_0 , and a_H is a parameter of temperature dependence. | H_0 , Pa·m ³ /mol | 4.91E+00 | Same to the "reference data set" The value a_H can be put directly as input data. When the input data is not given, temperature dependence of vapour pressure is used as surrogate, assuming the temperature-independent water solubility | <i>Li et al.</i> , 2003 |
| | | a_H | 7851.7 | | |
| | | T_0 , $^{\circ}\text{K}$ | 283.15 | | |
| SimpleBox | Temperature dependent: $H = H_0 \exp (- a_H (1/T - 1/T_0))$ where T - temperature (K), H_0 is the value at the reference temperature T_0 , and a_H is a parameter of temperature dependence. | H_0 , Pa·m ³ /mol | 4.91E+00 | Same to the "reference data set" | <i>Li et al.</i> , 2003 |
| | | a_H | 7851.7 | | |
| | | T_0 , $^{\circ}\text{K}$ | 283.15 | | |
| EVN-BETR and UK-MODEL | Temperature independent: | H , Pa·m ³ /mol | 19.8 | Calculated as H = Vapour Pressure (Pa) / Water Solubility (mol/m ³) at 25°C | <i>Li et al.</i> , 2003 |
| | Temperature dependent: $K_{aw} = K_{aw}^0 \exp (- a_{Kaw} (1/T - 1/T_0))$ where T - temperature (K), K_{aw}^0 is the value at the reference temperature T_0 , and a_{Kaw} is a parameter of temperature dependence. | K_{aw} , dimensionless | 2.08E-03 | At 10°C , calculated as $K_{aw} (T_0) = 10^{\log K_{aw}} \cdot a$, $a = \exp[(\Delta H_{vap} / R) \cdot (1 / T_0 - 1 / T)]$. $\Delta H_{vap} = 62.8$ KJ/mol: Enthalpy of vaporisation (from water to air) here: $a_{Kaw} = \Delta H_{vap} / R$ | |
| | | a_{Kaw} | 7553.5 | | |
| | | T_0 , $^{\circ}\text{K}$ | 283.15 | | |
| ClimoChem | Temperature dependent: $K_{aw} = K_{aw}^0 \exp (- a_{Kaw} (1/T - 1/T_0))$ where T - temperature (K), K_{aw}^0 is the value at the reference temperature T_0 , and a_{Kaw} is a parameter of temperature dependence. | K_{aw}^0 , dimensionless | 2.01E-03 | $K_{aw}(T) = K_{aw}(T_{ref}) \exp(dH_{Kaw}/R(1/T_{ref} - 1/T))$ (dimensionless) T = temperature (283.15 K); T_{ref} = reference temperature (298.15 K) $K_{aw}(T_{ref})$ =Henry 's law constant at T_{ref} (dimensionless): PCB 153: 9.18E-3 dH_{Kaw} = phase transfer enthalpy (J/mol): PCB 153: 71000 R = universal gas constant (8.3145 J/molK) | <i>Beyer et al.</i> , 2002 |
| | | a_{Kaw} | 8540 | | |
| | | T_0 , $^{\circ}\text{K}$ | 283.15 | | |
| DEHM-POP | Temperature dependent: $K_{aw} = K_{aw}^0 \exp (- a_{Kaw} (1/T - 1/T_0))$ where T - temperature (K), K_{aw}^0 is the value at the reference temperature T_0 , and a_{Kaw} is a parameter of temperature dependence. | K_{aw}^0 , dimensionless | 2.01E-03 | $K_{aw}(283.15) = K_{aw}^0(298.15) \exp(- a_{Kaw} (1/T - 1/T_0))$, where $K_{aw}^0(298.15) = 9.18\text{E-}3$ for PCB 153 | <i>Beyer et al.</i> , 2002 |
| | | a_{Kaw} | 8536 | | |
| | | T_0 , $^{\circ}\text{K}$ | 283.15 | | |
| MSCE-POP | Temperature dependent: $H = H_0 \exp (- a_H (1/T - 1/T_0))$ where T - temperature (K), H_0 is the value at the reference temperature T_0 , and a_H is a parameter of temperature dependence. Temperature dependent: $K_{aw} = H / (R \cdot T)$ | H_0 , Pa·m ³ /mol | 3.781 | Coefficients of the exponential equation are recalculated from the standard form of temperature dependence: $\log H = -A/T(\text{K}) + B$ with the help of the following formulas: $a_H = \ln(10) \cdot A$, $H_0 = 10^{(-A/T_0 + B)}$, where $A = \Delta H_W / 2.303R$; $B = \log H_{298} + \Delta H_W / 2.303R(298)$. H_{298} is Henry's law constant (Pa·m ³ /mol) at 25°C (for PCB-153: 16.48); ΔH_W is the enthalpy of volatilization from water, kJ/mol (for PCB-153: 69.4) | <i>Burkhard et al.</i> , 1985; <i>Dunnivant et al.</i> , 1992 |
| | | a_H , K | 8347 | | |
| | | T_0 , K | 283.15 | | |

* - for the sake of comparability, the base values and coefficients of temperature dependences of the considered parameters are given here at the temperature 283.15 K (T_0) and the way they were recalculated from original dependencies is specified in the field "Comments".

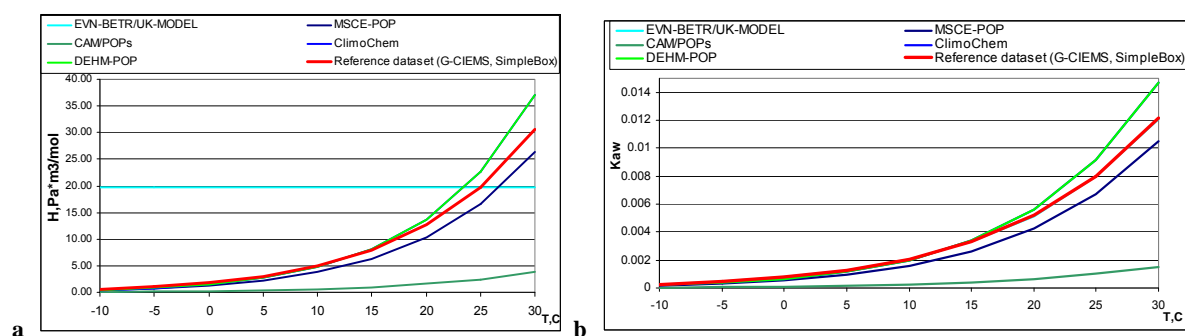


Fig. 1. Comparison of temperature dependencies of Henry's law constant (H , $\text{Pa}\cdot\text{m}^3/\text{mol}$) and air/water partition coefficient (K_{aw} , dimensionless) of PCB-153.

For the computations at Stage I, G-CIEMS and SimpleBox exploit temperature dependencies of Henry's law constant and air/water partition coefficient of PCB-153 presented in "reference data set". EVN-BETR and UK-MODEL also use one and the same temperature dependence of K_{aw} with "reference data set" and the constant value of H calculated for 25 °C with the help of data from [Li *et al.*, 2003]. CliMoChem and DEHM-POP models have performed calculation experiments with equal values of these parameters from [Beyer *et al.*, 2002]. These models present maximum values of K_{aw} among all the models. According to the data reported, there is similarity in temperature dependencies used in CliMoChem, DEHM-POP, MSCE-POP and "reference data set". CAM/POPs uses lower values of these parameters than other participating models. The difference in absolute values of H and K_{aw} calculated from various types of temperature dependencies, used by the participants in Stage I calculations, is rather large. To illustrate this statement, statistical parameters characterizing the scattering of the values of Henry's law constant and air/water partition coefficient between all models are given in Table 6 for three arbitrary temperatures (-10°C, 10°C and 25°C) and for coefficients of temperature dependencies.

Table 6. Absolute values and statistical parameters of Henry's law constant (H , $\text{Pa}\cdot\text{m}^3/\text{mol}$) and air/water partition coefficient (K_{aw} , dimensionless) of PCB-153 for three arbitrary temperatures (-10 °C, 10 °C and 25 °C) and coefficients of temperature dependencies

| | H , $\text{Pa}\cdot\text{m}^3/\text{mol}$ | | | | K_{aw} , dimensionless | | | |
|-----------------------|---|-----------|----------|--------|--------------------------|------------|------------|-----------|
| | -10°C | 10°C | 25°C | a_H | -10°C | 10°C | 25°C | a_{Kaw} |
| CAM/POPs | 7.37E-02 | 6.09E-01 | 2.46E+00 | 7865.6 | 3.37E-05 | 2.59E-04 | 9.94E-04 | - |
| G-CIEMS | 5.97E-01 | 4.91E+00 | 1.98E+01 | 7851.7 | 2.75E-04** | 2.09E-03** | 8.00E-03** | 7553.5 |
| SimpleBox | 5.97E-01 | 4.91E+00 | 1.98E+01 | 7851.7 | 2.75E-04** | 2.09E-03** | 8.00E-03** | 7553.5 |
| EVN-BETR and UK-MODEL | 19.8 | 19.8 | 19.8 | - | 2.74E-04** | 2.08E-03** | 7.96E-03** | 7553.5 |
| CliMoChem | 4.44E-01* | 4.73E+00 | 2.27E+01 | - | 2.03E-04 | 2.01E-03 | 9.17E-03* | 8540* |
| DEHM-POP | 4.45E-01* | 4.73E+00 | 2.27E+01 | - | 2.03E-04 | 2.01E-03 | 9.16E-03* | 8536* |
| MSCE-POP | 4.02E-01 | 3.78E+00 | 1.67E+01 | 8347 | 1.84E-04 | 1.61E-03 | 6.72E-03 | - |
| "Reference data set" | 5.97E-01 | 4.91E+00 | 1.98E+01 | 7851.7 | 2.75E-04** | 2.09E-03** | 8.00E-03** | 7553.5 |
| <i>min</i> | 7.37E-02 | 6.09E-01 | 2.46E+00 | 7851.7 | 3.37E-05 | 2.59E-04 | 9.94E-04 | 7553.5 |
| <i>max</i> | 1.98E+01 | 1.98E+01 | 2.27E+01 | 8347.0 | 2.75E-04 | 2.09E-03 | 9.17E-03 | 8540.0 |
| <i>arith. mean</i> | 2.87E+00 | 6.05E+00 | 1.80E+01 | 7953.5 | 2.15E-04 | 1.78E-03 | 7.25E-03 | 7881.7 |
| <i>median</i> | 5.21E-01 | 4.82E+00 | 1.98E+01 | 7851.7 | 2.39E-04 | 2.05E-03 | 8.00E-03 | 7553.5 |
| <i>geom. mean</i> | 6.30E-01 | 4.32E+00 | 1.55E+01 | 7951.2 | 1.86E-04 | 1.54E-03 | 6.24E-03 | 7868.4 |
| <i>max/min</i> | 8 / 269*** | 8 / 33*** | 9 | 1.1 | 8 | 8 | 9 | 1.1 |

*, ** - difference in absolute values obtained from identical temperature dependencies can be explained by accuracy of coefficient recalculation.

*** - the first value is calculated without the temperature independent value of H (EVN-BETR and UK-MODEL), the second value is calculated taking it into account.

There is a substantial difference between highest and lowest absolute values of H (CAM/POPs and EVN-BETR and UK-MODEL) both at -10°C and 10°C. These values differ from each other more than an order of magnitude. It can be explained by the fact that EVN-BETR and UK-MODEL use the

constant value of H calculated for 25 °C. That is why scattering of H values is going down with temperature increase. If not take into account this temperature independent value, max/min ratio for this parameter is equal to 8-9. Differences in absolute values of K_{aw} between G-CIEMS, SimpleBox, CliMoChem, DEHM-POP, MSCE-POP and “reference data set” are also not high. In this case scattering of both parameters values is slightly increasing with temperature. It is seen that median values of Henry's law constant and air-water partition coefficient used in models is very close to those used in “reference data set”.

Comparison of Henry's law constant and air/water partition coefficient of PCB-28 and PCB-180 used in the participating models and “reference data sets” are presented in Fig. B.1 and B.2. in Annex B. There is also statistical evaluation of absolute values and coefficients of temperature dependencies in Table B.3 and B.4.

It is seen that the difference in highest and lowest absolute values of H between all models is also very large for PCB-180. Similar to that for PCB-153, scattering is going down with temperature increase. But if not take into account temperature independent H value of PCB-180, max/min ratio for this parameter and for K_{aw} lies within factor 12-22. At that scattering of both parameters values is growing with temperature increase more substantial.

Henry's law constant and air/water partition coefficient values of PCB-28 used by all models are closer than those data on above two congeners. Difference in H values between all models for PCB-28 is much less than for other congeners. Scattering is going down with temperature. If not take into account temperature independent H value of PCB-28, max/min ratio for this parameter and for K_{aw} lies within factor 2. Scattering of both parameters values is going down with temperature increase.

3.2. The subcooled liquid vapour pressure

The value of subcooled liquid-vapour pressure (p_{oL} , Pa) is used in the modelling of the process of POP partitioning between its particulate and gaseous phase in the atmosphere in accordance with the Junge-Pankow adsorption model [Junge, 1977; Pankow, 1987]. Thus, in this cases the value of p_{oL} determining the particle-bound fraction of a pollutant in air strongly influences such subsequent important processes as dry and wet particle deposition and degradation in air.

CliMoChem and DEHM-POP models do not use subcooled liquid vapour pressure for model calculations. EVN-BETR and UK-MODEL assumes this parameter temperature-independent. Other models use temperature dependence of this parameter. The coefficients of temperature dependencies for PCB-153 are presented in Table 7.

As seen from the Table, the participating models use two types of temperature dependence coefficients of p_{oi} which do not differ from each other very much. The first type of this dependence is taken from “reference data set” and it is also used by G-CIEMS and SimpleBox. The second one is utilised by CAM/POPs and MSCE-POP. Comparison of these temperature dependencies of p_{oi} is presented in Fig. 2. The “reference data set” shows slightly less values of this parameter.

Table 7. The subcooled liquid vapour pressure of PCB-153 (data sets of the participating POP models)*

| Model | Description | Numerical values | | Comments | Reference |
|-----------------------|--|------------------|----------|--|--|
| CAM/POPs | Temperature dependent: $p_{ol} = p_{ol}^0 \exp(-a_p(1/T - 1/T_0))$ where T - temperature (K), p_{ol}^0 is the value at the reference temperature T_0 , and a_p is a parameter of temperature dependence. | p_{ol}^0 , Pa | 9.69E-05 | Coefficients of the exponential equation are recalculated from the standard form of temperature dependence: $p_{ol} = 10^{(m/T + b)}$, $a_p = \ln(10) \cdot m$; $p_{ol}^0 = 10^{(m/T_0 + b)}$ where T - temperature ($^{\circ}$ K); $m = -4775$: parameter of temperature dependence, and $b = 12.85$: parameter depended on molecular weight. It was obtained from the following original equation: $\log(p_{ol}) = -Q / (2.303 RT) + b$ where: T - temperature; R - Universal Gas Constant Q - the heat of vaporisation (KJ/mol) | Harner et al., 1996; Falconer et al., 1995 |
| | | a_p | 10995 | | |
| | | T_0 , K | 283.15 | | |
| SimpleBox | Temperature dependent: $p_{ol} = p_{ol}^0 \exp(-a_p(1/T - 1/T_0))$ where T - temperature (K), p_{ol}^0 is the value at the reference temperature T_0 , and a_p is a parameter of temperature dependence. | p_{ol}^0 , Pa | 8.82E-05 | Same to the "reference data set" | Li et al., 2003 |
| | | a_p | 10846.6 | | |
| | | T_0 , K | 283.15 | | |
| G-CIEMS | Temperature dependent: $p_{ol} = p_{ol}^0 \exp(-a_p(1/T - 1/T_0))$ where T - temperature (K), p_{ol}^0 is the value at the reference temperature T_0 , and a_p is a parameter of temperature dependence. | p_{ol}^0 , Pa | 8.82E-05 | Same to the "reference data set" | Li et al., 2003 |
| | | a_p | 10846.6 | | |
| | | T_0 , K | 283.15 | | |
| EVN-BETR and UK-MODEL | Temperature independent: | p_{ol} , Pa | 6.60E-04 | $T = 25^{\circ}\text{C}$ | Li et al., 2003 |
| MSCE-POP | Temperature dependent: $p_{ol} = p_{ol}^0 \exp(-a_p(1/T - 1/T_0))$ where T - temperature (K), p_{ol}^0 is the value at the reference temperature T_0 , and a_p is a parameter of temperature dependence. | p_{ol}^0 , Pa | 9.69E-05 | Coefficients of the exponential equation are recalculated from the standard form of temperature dependence: $\log p_{ol}(\text{Pa}) = -4775/T(\text{K}) + 12.85$ with the help of the following formulas: $a_p = \ln(10) \cdot 4775$, $p_{ol}^0 = 10^{(-4775/T_0 + 12.85)}$ | Falconer and Bidleman, 1994 |
| | | a_p | 10995 | | |
| | | T_0 , K | 283.15 | | |

* - for the sake of comparability, the base values and coefficients of temperature dependences of the considered parameters are given here at the temperature 283.15 K (T_0) and the way they were recalculated from original dependencies is specified in the field "Comments".

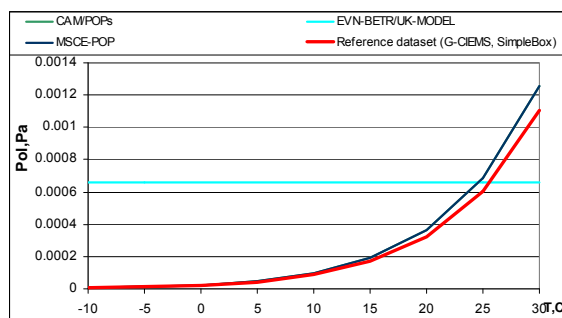


Fig. 2. Comparison of temperature dependencies of subcooled liquid vapour pressure of PCB-153 used in data sets of the participating POP models and in "reference data set"

The dispersion of the subcooled liquid vapour pressure of PCB-153 can be characterized by the comparison of its absolute values at -10°C , 10°C and 25°C and coefficients of temperature dependence used by the participating models. Above mentioned values and corresponding statistical parameters are given in Table 8.

Table 8. Absolute values, coefficients of temperature dependence and statistical parameters of subcooled liquid vapour pressure of PCB-153 for three arbitrary temperatures (-10 °C, 10 °C and 25 °C)

| | p_{OL} , Pa | | | a_p |
|--------------------|---------------|------------|----------|---------|
| | -10°C | 10°C | 25°C | |
| CAM/POPs | 5.07E-06 | 9.69E-05 | 6.84E-04 | 10995 |
| G-CIEMS | 4.80E-06 | 8.82E-05 | 6.06E-04 | 10846.6 |
| SimpleBox | 4.80E-06 | 8.82E-05 | 6.06E-04 | 10846.6 |
| EVN-BETR/UK-MODEL | 6.60E-04 | 6.60E-04 | 6.60E-04 | - |
| MSCE-POP | 5.07E-06 | 9.69E-05 | 6.84E-04 | 10995 |
| Reference data set | 4.80E-06 | 8.82E-05 | 6.06E-04 | 10846.6 |
| <i>min</i> | 4.80E-06 | 8.82E-05 | 6.06E-04 | 10846.6 |
| <i>max</i> | 6.60E-04 | 6.60E-04 | 6.84E-04 | 10995.0 |
| <i>arith. mean</i> | 1.14E-04 | 1.86E-04 | 6.41E-04 | 10906.0 |
| <i>median</i> | 4.93E-06 | 9.26E-05 | 6.33E-04 | 10846.6 |
| <i>geom. mean</i> | 1.11E-05 | 1.27E-04 | 6.40E-04 | 10905.7 |
| <i>max/min</i> | 1.1 / 137.6* | 1.1 / 7.5* | 1.1 | 1.0 |

* - the first value is calculated without the temperature independent value of p_{OL} (EVN-BETR and UK-MODEL), the second value is calculated taking it into account

If not take into account temperature independent value of subcooled liquid vapour pressure of PCB-153 included in EVN-BETR and UK-MODEL, all the rest models use close temperature dependencies of p_{ol} . Scattering between its values at all considered temperatures (-10, 10 and 25 °C) is about 1.1. However, considering temperature independent value of p_{ol} of EVN-BETR and UK-MODEL, one can see that for all three temperatures the difference between maximum and minimum values increases up to several order of magnitude. For the first given temperature (-10 °C) it is rather high (max/min ratio equals to 138). At 10 °C, it is considerably smaller (max/min ratio equals to 7.5). For all models max/min ratio for coefficients of temperature dependence equals practically to 1.0.

Comparison of subcooled liquid vapour pressure values of PCB-28 and PCB-180 used in the participating models and “reference data sets” are presented in Fig. B.3 and B.4 in Annex B. Statistical evaluation of absolute values and coefficients of temperature dependencies is given in Table B.6 and B.7.

For all three temperatures the difference in maximum and minimum values of p_{ol} between all models is less for PCB-28 than that for PCB-153 and PCB-180. If not taking into account temperature independent value of p_{ol} , max/min ratio for PCB-28 varies within factor 1.3. For PCB-180 max/min ratio of p_{ol} values lies within factor 7.

3.3. The octanol/water partition coefficient

The octanol/water partition coefficient (K_{ow} , dimensionless) is used in the participating models for the estimation of the POP partitioning in the organic carbon/water system (K_{oc}) on the basis of regression dependencies and of the partition coefficient in the octanol/air system (K_{oa}) (Subsections 3.4 and 3.5). Thus, this parameter mainly influences on the description of the following processes: gas-particle partitioning in the atmosphere (in accordance with absorption model), gaseous exchange between the atmosphere and soil (partitioning in soil compartment), and gaseous exchange between the atmosphere and vegetation (partitioning among vegetation compartment). K_{ow} is also included by CliMoChem models in the calculation of the water particle-bound fraction of a pollutant for modelling diffusion process from seawater to atmosphere.

The most part of participating models (CAM/POPs, SimpleBox, G-CIEMS, EVN-BETR and UK-MODEL CliMoChem and DEHM-POP) involve the octanol/water partition coefficient of the considered PCBs in the form of the temperature dependence. As usual the temperature dependencies of this parameter are equated by downward exponents with different values of K_{ow} at reference temperature (for example at 10°C) as the pre-exponential multiplier and with the values of

the second - temperature coefficient of these dependencies defined with the help of the enthalpy or the internal energy of phase transfer. The exception is CAM/POPs model, in which the temperature dependence of K_{ow} is recalculated from temperature dependencies of the Henry's law constant and the octanol/air partition coefficient. MSCE-POP model contents temperature independent values of K_{ow} . These data together with coefficients of K_{ow} temperature dependencies for PCB-153 are presented in Table 9.

Temperature dependencies of the octanol/water partition coefficient of PCB-153 used in the calculations by the participating models and in "reference data set" are compared in Fig.3.

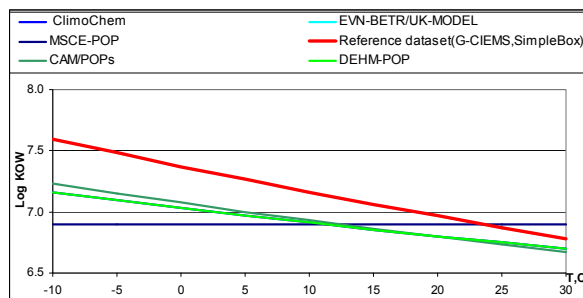


Fig. 3. Comparison of temperature dependencies of $\log K_{ow}$ of PCB-153 used in the models and in "reference data set"

Table 9. The octanol/water partition coefficient of PCB-153 (data sets of the participating POP models)*

| Model | Description | Numerical values | | Comments | Reference |
|-----------------------|--|---------------------------------|----------|---|---------------------------|
| CAM/POPs | Temperature dependent: $K_{ow} = K_{oa} \cdot H/RT$ where T - temperature ($^{\circ}K$); R - Universal Gas Constant; H - Henry's law constant; K_{oa} - Octanol/air partition coefficient (dimensionless) | - | - | These values are calculated with the help of temperature dependencies of H and K_{oa} . | This study |
| SimpleBox | Temperature dependent: $K_{ow} = K_{ow}^0 \exp(a_{Kow}(1/T - 1/T_0))$ where T - temperature (K), K_{ow}^0 is the value at the reference temperature T_0 , and a_{Kow} is a parameter of temperature dependence. | $K_{ow}^0(T_0)$, dimensionless | 1.45E+07 | Same to the "reference data set" | Li et al., 2003 |
| | | a_{Kow} | 3740.7 | | |
| | | T_0, K | 283.15 | | |
| G-CIEMS | Temperature dependent: $K_{ow} = K_{ow}^0 \exp(a_{Kow}(1/T - 1/T_0))$ where T - temperature (K), K_{ow}^0 is the value at the reference temperature T_0 , and a_{Kow} is a parameter of temperature dependence. | $K_{ow}^0(T_0)$, dimensionless | 1.45E+07 | Same to the "reference data set" | Li et al., 2003 |
| | | a_{Kow} | 3740.7 | | |
| | | T_0, K | 283.15 | | |
| EVN-BETR and UK-MODEL | Temperature dependent: $K_{ow} = K_{ow}^0 \exp(a_{Kow}(1/T - 1/T_0))$ where T - temperature (K), K_{ow}^0 is the value at the reference temperature T_0 , and a_{Kow} is a parameter of temperature dependence. | K_{ow}^0 , dimensionless | 1.45E+07 | For $10^{\circ}C$, calculated as $K_{ow}(T_0) = 10^{\log K_{ow}} \cdot a$, $a = \exp[(\Delta H_{sol}/R) \cdot (1/T_0 - 1/T)]$. $\Delta H_{sol} = -31.1$ KJ/mol: Enthalpy of solution (from octanol to water) here: $a_{Kow} = \Delta H_{sol}/R$ | Li et al., 2003 |
| | | a_{Kow} | 3740.5 | | |
| | | T_0, K | 283.15 | | |
| ClimoChem | Temperature dependent: $K_{ow} = K_{ow}^0 \exp(a_{Kow}(1/T - 1/T_0))$ where T - temperature (K), K_{ow}^0 is the value at the reference temperature T_0 , and a_{Kow} is a parameter of temperature dependence ($-dH/R$) | K_{ow}^0 , dimensionless | 8.17E+06 | $K_{ow}(T) = K_{ow}(T_{ref}) \exp((dH_{Kow}/R)(1/T_{ref} - 1/T))$ dimensionless T = temperature (283.15K); T_{ref} = reference temperature (298.15 K) $K_{ow}(T_{ref})$ = Octanol/water partition coefficient at T_{ref} PCB 153: 5.62E+6; dH_{Kow} = phase transfer enthalpy (J/mol) PCB 153: -17500 R = universal gas constant (8.3145 J/mol K) | Beyer et al., 2002 |
| | | a_{Kow} | 2104.8 | | |
| | | T_0, K | 283.15 | | |
| DEHM-POP | Temperature dependent: $K_{ow} = K_{ow}^0 \exp(a_{Kow}(1/T - 1/T_0))$ where T - temperature (K), K_{ow}^0 is the value at the reference temperature T_0 , and a_{Kow} is a parameter of temperature dependence ($-dH/R$) | K_{ow}^0 , dimensionless | 8.17E+06 | $K_{ow}(283.15) = K_{ow}^0(298.15) \exp(a_{Kow}(1/T - 1/T_0))$, where $K_{ow}^0(298.15) = 5.62E+6$ for PCB 153 $a_{Kow} = dH_{Kow}/R$ dH_{Kow} = phase transfer enthalpy (J/mol) PCB 153: -17500 R = universal gas constant (8.3145 J/mol K) | Beyer et al., 2002 |
| | | a_{Kow} | 2102.4 | | |
| | | T_0, K | 283.15 | | |
| MSCE-POP | Temperature independent | K_{ow} , dimensionless | 7.94E+6 | $\log K_{ow} = 6.9$ | Mackay et al., v.1., 1992 |

* - for the sake of comparability, the base values and coefficients of temperature dependences of the considered parameters are given here for the temperature 283.15 K (T_0) and the way they were recalculated from original dependencies is specified in the field "Comments".

Comparison of the plots of temperature dependencies of the octanol/water partition coefficient of PCB-153 used in CAM/POPs, CliMoChem, DEHM-POP models and in “reference data set” (also in SimpleBox, G-CIEMS, and EVN-BETR/UK-MODEL) shows not substantial differences between values of $\log K_{ow}$ used by the models (except temperature independent value presented by MSCE-POP). To evaluate the scattering of K_{ow} , the variability of this parameter values used by the participating models is determined at three fixed temperature (-10°C, 10°C and 25°C). Absolute values, coefficients of temperature dependence and statistical parameters of octanol/water partition coefficient of PCB-153 for three arbitrary temperatures are given in Table 10.

The difference between all models in terms of absolute values of octanol/water partition coefficient of PCB-153 used for modelling is not large for all considered temperatures (max/min ratios of K_{ow} vary from 5 to 2). If not take into account the temperature independent value of MSCE-POP, max/min ratio at -10°C comes down to 3. Besides, the difference between statistical parameters characterizing the values averaged between models at three various temperatures (arithmetic and geometric means, and median) is not substantial (factor 3-4) within the temperature interval (-10 - 25°C). It is seen that the values of this parameter at all considered temperatures are the largest for “reference data set” including SimpleBox, G-CIEMS and EVN-BETR/UK-MODEL respectively. At the same time, CAM/POPs, CliMoChem, and DEHM-POP have close values between one another which are lower than the first ones. For all these models and “reference data set” scattering of this parameter at 25°C is minimum. For the models max/min ratio of coefficients of temperature dependences equals to 2.0.

Table 10. Absolute values, coefficients of temperature dependence and statistical parameters of octanol/water partition coefficient of PCB-153 for three arbitrary temperatures (-10 °C, 10 °C and 25 °C)

| | K_{ow} | | | a_{Kow} |
|--------------------|------------|------------|------------|-----------|
| | -10°C | 10°C | 25°C | |
| CAM/POPs | 1.72E+07 | 8.51E+06 | 5.42E+06 | - |
| SimpleBox | 3.96E+07 | 1.45E+07 | 7.46E+06 | 3740.7* |
| G-CIEMS | 3.96E+07 | 1.45E+07 | 7.46E+06 | 3740.7* |
| EVN-BETR/UK-MODEL | 3.96E+07 | 1.45E+07 | 7.46E+06 | 3740.5* |
| CliMoChem | 1.44E+07 | 8.17E+06 | 5.62E+06 | 2104.8** |
| DEHM-POP | 1.44E+07 | 8.17E+06 | 5.62E+06 | 2102.4** |
| MSCE-POP | 7.94E+06 | 7.94E+06 | 7.94E+06 | - |
| Reference data set | 3.96E+07 | 1.45E+07 | 7.46E+06 | 3740.7* |
| <i>min</i> | 7.94E+06 | 7.94E+06 | 5.42E+06 | 2102.4 |
| <i>max</i> | 3.96E+07 | 1.45E+07 | 7.94E+06 | 3740.7 |
| <i>arith. mean</i> | 2.59E+07 | 1.13E+07 | 6.93E+06 | 3085.8 |
| <i>median</i> | 2.70E+07 | 1.13E+07 | 7.46E+06 | 3740.5 |
| <i>geom. mean</i> | 2.16E+07 | 1.08E+07 | 6.86E+06 | 2971.3 |
| <i>max/min</i> | 2.8/5.0*** | 1.8/1.8*** | 1.4/1.5*** | 1.8 |

*, ** - difference in absolute values obtained from identical temperature dependencies can be explained by accuracy of coefficient recalculation

*** - the first value is calculated without the temperature independent value of K_{ow} (MSCE-POP), the second value is calculated taking it into account

Comparison of octanol/water partition coefficient values of PCB-28 and PCB-180 used in the participating models and “reference data sets” are presented in Fig. B.5 and B.6 in Annex B. Statistical evaluation of absolute values and coefficients of temperature dependencies is given in Table B.9 and B.10.

Differences in absolute values of octanol/water partition coefficient between all models for PCB-28 and PCB-180 are also not large. Max/min ratio of K_{ow} values for PCB-28 varies from 2 to 4; and for PCB-180 – from 2 to 3. If the temperature independent values of MSCE-POP are not taken into account, max/min ratio for PCB-28 lies within factor 1.2 and for PCB-180 – within factor 1-3. For these congeners, K_{ow} values are changing with temperature increase within factor 3-4 for considered interval of temperatures (-10-25°C). Scattering of coefficients of temperature dependences among all models for PCB-28 lies within factors 1 and for PCB-180 – within factor 4.

3.4. The octanol/air partition coefficient

The octanol/air partition coefficient (K_{oa} , dimensionless) is used by EVN-BETR and UK-MODEL, G-CIEMS and DEHM-POP in the description of POP gas-particle partitioning in the atmosphere as absorption from air into an octanol-like film of particle phase according to [Finizio *et al.*, 1997; Falconer and Harner, 2000]. Besides, this parameter is included into descriptions of the gaseous exchange between air and vegetation. It should be mentioned that EVN-BETR and UK-MODEL and CliMoChem models do not use K_{oa} parameter straight as input information for modelling but recalculate it from K_{ow} and K_{aw} .

The participating models and “reference data set” contain this parameter in the form of temperature dependence. Coefficients of these dependencies are presented in Table 11.

Table 11. The octanol/air partition coefficient of PCB-153 (data sets of the participating POP models)*

| Model | Description | Numerical values | | Comments | Reference |
|-----------------------|---|------------------------------------|---------------------|--|-----------------------------------|
| CAM/POPs | Temperature dependent: $K_{oa} = 10^{(a/T + b)}$ where: T - temperature; P - liquid vapour pressure p_{oi} (Pa) | a | -529-19.25 logP | These values are calculated with the help of temperature dependencies of p_{oi} | Harner <i>et al.</i> , 1996; 1998 |
| | | b | 8.2995-0.95 logP | | |
| SimpleBox | Temperature dependent: $K_{oa} = K_{oa}^0 \exp(a_{K_{oa}}(1/T - 1/T_0))$ where T - temperature (K), K_{oa}^0 is the value at the reference temperature T_0 , and $a_{K_{oa}}$ is a parameter of temperature dependence. | $K_{oa}^0(T_0)$, dimensionless | 2.05E+10 | Same to the “reference data set” | Li <i>et al.</i> , 2003 |
| | | $a_{K_{oa}}$ | 11294.2 | | |
| | | T_0, K | 283.15 | | |
| G-CIEMS | Temperature dependent: $K_{oa} = K_{oa}^0 \exp(a_{K_{oa}}(1/T - 1/T_0))$ where T - temperature (K), K_{oa}^0 is the value at the reference temperature T_0 , and $a_{K_{oa}}$ is a parameter of temperature dependence. | $K_{oa}^0(T_0)$, dimensionless | 2.05E+10 | Same to the “reference data set” K_{oa} is used as optional only when the input value is given. | Li <i>et al.</i> , 2003 |
| | | $a_{K_{oa}}$ | 11294.2 | | |
| | | T_0, K | 283.15 | | |
| EVN-BETR and UK-MODEL | Temperature dependent: $K_{oa} = K_{ow} / K_{aw}$ | $K_{oa}^0(T_0)$, dimensionless | 6.97E+09 | At 10°C, calculated as $K_{oa} = K_{ow} / K_{aw}$ | |
| | | T_0, K | 283.15 | | |
| DEHM-POP | Temperature dependent: $K_{oa} = K_{oa}^0 \exp(a_{K_{oa}}(1/T - 1/T_0))$ where T - temperature (K), K_{oa}^0 is the value at the reference temperature T_0 , and $a_{K_{oa}}$ is a parameter of temperature dependence. | $K_{oa}^0(T_0)$, dimensionless | 2.74E+10 | $K_{oa}(283.15) = K_{oa}^0(298.15) \exp(a_{K_{oa}}(1/T - 1/T_0))$, where $K_{oa}^0(298.15) = 4.14E+9, 1.16E+8, 1.68E+10$ for PCB 153, 28 and 180 respectively $a_{K_{oa}} = dHK_{oa}/R$ $dH K_{oa}$ = phase transfer enthalpy (J/mol) PCB 153: -88400 R = universal gas constant (8.3145 J/mol K) | Beyer <i>et al.</i> , 2002 |
| | | $a_{K_{oa}}$ | 10636.8 | | |
| | | T_0, K | 283.15 | | |
| MSCE-POP | Temperature dependent: $K_{oa} = K_{oa}^0 \exp(a_{K_{oa}}(1/T - 1/T_0))$ where T - temperature (K), K_{oa}^0 is the value at the reference temperature T_0 , and $a_{K_{oa}}$ is a parameter of temperature dependence. | $K_{oa}^0(T_0)$, dimensionless | 3.64E+10 | Coefficients of the exponential equation are recalculated from the standard form of temperature dependence: $\log K_{oa} = 4695/T(K) - 6.02$ with the help of the following formulas: $a_p = \ln(10) \cdot 4695$, $K_{oa}^0(T_0) = 10^{(4695/T_0 - 6.02)}$ | Harner and Bidleman, 1996 |
| | | $a_{K_{oa}}$ | 10811 | | |
| | | T_0, K | 283.15 | | |

* - for the sake of comparability, the base values and coefficients of temperature dependencies of the considered parameters are given here for the temperature 283.15 K (T_0) and the way they were recalculated from original dependencies is specified in the field “Comments”.

Following the data submitted comparison of temperature dependencies of the octanol/air partition coefficient used by the models and in “reference data set” is presented in Fig. 4.

MSCE-POP has performed the calculations with the help of the highest values of octanol/air partition coefficient of PCB-153 among other participating models. Describing equations of temperature dependence of K_{oa} in different ways, CAM/POPs and DEHM-POP nevertheless use practically similar values of this parameters for PCB-153. The values of K_{oa} calculated with “reference data set” (also SimpleBox, G-CIEMS) are somewhat lower than previous ones. EVN-BETR/UK-MODEL uses the lowest values of this parameter than other participating models.

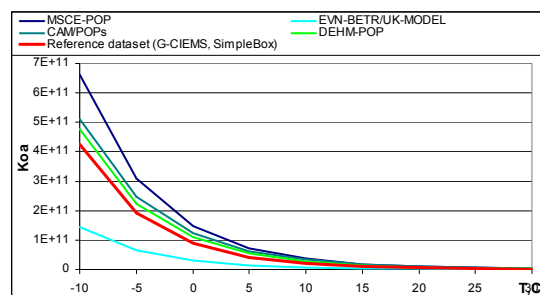


Fig. 4. Comparison of temperature dependencies of octanol/air partition coefficient of PCB-153 used in the participating POP models and in “reference data set”

In order to characterize the spread of octanol/air partition coefficient of PCB-153, the comparison of its absolute values at three arbitrary temperatures (-10°C, 10°C and 25°C) between the participating models is made. Absolute values of K_{oa} , coefficients of temperature dependencies and their statistical parameters are presented in Table 12.

Table 12. Absolute values, coefficients of temperature dependencies and statistical parameters of octanol/air partition coefficient of PCB-153 for three arbitrary temperatures (-10 °C, 10 °C and 25 °C)

| | K_{oa} | | | $a_{K_{oa}}$ |
|--------------------|----------|----------|----------|--------------|
| | -10°C | 10°C | 25°C | |
| CAM/POPs | 5.10E+11 | 3.29E+10 | 5.45E+09 | - |
| SimpleBox | 4.25E+11 | 2.05E+10 | 2.76E+09 | 11294.2 |
| G-CIEMS | 4.25E+11 | 2.05E+10 | 2.76E+09 | 11294.2 |
| EVN-BETR/UK-MODEL | 1.45E+11 | 6.97E+09 | 9.37E+08 | - |
| DEHM-POP | 4.76E+11 | 2.74E+10 | 4.14E+09 | 10636.8 |
| MSCE-POP | 6.63E+11 | 3.64E+10 | 5.33E+09 | 10811 |
| Reference data set | 4.25E+11 | 2.05E+10 | 2.76E+09 | 11294.2 |
| <i>min</i> | 1.45E+11 | 6.97E+09 | 9.37E+08 | 10636.8 |
| <i>max</i> | 6.63E+11 | 3.64E+10 | 5.45E+09 | 11294.2 |
| <i>arith. mean</i> | 4.38E+11 | 2.36E+10 | 3.45E+09 | 11066.1 |
| <i>mediana</i> | 4.25E+11 | 2.05E+10 | 2.76E+09 | 11294.2 |
| <i>geom. mean</i> | 4.05E+11 | 2.13E+10 | 3.03E+09 | 11062.4 |
| <i>max/min</i> | 5 | 5 | 6 | 1 |

At all considered temperatures there is not a large difference in values of K_{oa} obtained with the use of existing temperature dependencies. The difference between absolute values of this parameter used by the participants at the first two temperatures is smaller than it is at the last one (max/min ratios come up from 5 to 6). Max/min ratio of coefficients of temperature dependencies of K_{oa} equals to 1.0.

Comparison of octanol/air partition coefficient values of PCB-28 and PCB-180 used in the participating models and in “reference data sets” are presented in Fig. B.7 and B.8 in Annex B. Statistical evaluation of absolute values and coefficients of temperature dependencies is given in Table B.12 and B.13.

Differences in absolute values of octanol/water partition coefficient between all models for PCB-28 are less than that for PCB-153 and PCB-180. Max/min ratios between absolute values of K_{oa} used by all models at the three considered temperatures range from 2 to 5 for PCB-28 and from 6 to 8 for PCB-180. Max/min ratio of coefficients of temperature dependencies of K_{oa} for these congeners equals practically to 1.0.

3.5. The organic carbon/water partition coefficient

The organic carbon/water partition coefficient (K_{oc} , L/kg) strongly influences on the description of processes of POP sorption by soil and sediments. Partition coefficients in the “organic carbon-water” system selected by the participating models for modelling of PCB-153 are presented in Table 13.

Table 13. The organic carbon/water partition coefficient of PCBs, dm^3/kg (data sets of the participating POP models)

| Model | Description | Numerical values | | Comments | Reference |
|-----------------------|--|------------------|------|--|---|
| CAM/POPs | Regression relation: $K_{oc} = regc K_{ow}^b$ where $regc$ and b are regression coefficients | $regc$ | 0.41 | K_{oc} is calculated from K_{ow} , where K_{ow} is the temperature dependent octanol-water partitioning coefficient | Karickhoff, 1981 Mackay, 1991 Schnoor, 1996 |
| | | b | 1 | | |
| SimpleBox | Regression relation: $K_{oc} = regc K_{ow}^b$ where $regc$ and b are regression coefficients | $regc$ | 0.41 | Same to the “reference data set” K_{oc} is calculated from K_{ow} , where K_{ow} is the temperature dependent octanol-water partition coefficient | Karickhoff, 1981 |
| | | b | 1 | | |
| G-CIEMS | Regression relation: $K_{oc} = regc K_{ow}^b$ where $regc$ and b are regression coefficients | $regc$ | 1.26 | | |
| | | b | 0.81 | | |
| EVN-BETR and UK-MODEL | Regression relation: $K_{oc} = regc K_{ow}^b$ where $regc$ and b are regression coefficients | $regc$ | 0.41 | | Karickhoff, 1981 |
| | | b | 1 | | |
| CliMoChem | Regression relation: $K_{oc} = regc K_{ow}^b$ where $regc$ and b are regression coefficients | $regc$ | 0.35 | K_{oc} is calculated from K_{ow} , where K_{ow} is the temperature dependent octanol-water partition coefficient | Seth et al., 1999 |
| | | b | 1 | | |
| DEHM-POP | Regression relation: $K_{oc} = regc K_{ow}^b$ where $regc$ and b are regression coefficients | $regc$ | 0.41 | | Mackay, 1999 |
| | | b | 1 | | |
| MSCE-POP | Regression relation: $K_{oc} = regc K_{ow}^b$ where $regc$ and b are regression coefficients | $regc$ | 0.41 | | Karickhoff, 1981 |
| | | b | 1 | | |

All models use one and the same approach to estimate this parameter – recalculation from octanol/water partition coefficient with the use of simple regression relationships. It is seen that for determination of K_{oc} , regression coefficient equals to 0.41 is most frequently used. G-CIEMS uses regression equation different from other models. Hence, final value of K_{oc} is most substantially affected by the difference in K_{ow} values. Temperature dependencies of organic carbon/water partition coefficient of PCB-153 used in the calculations by the participating models and in “reference data set” are compared in Fig.5.

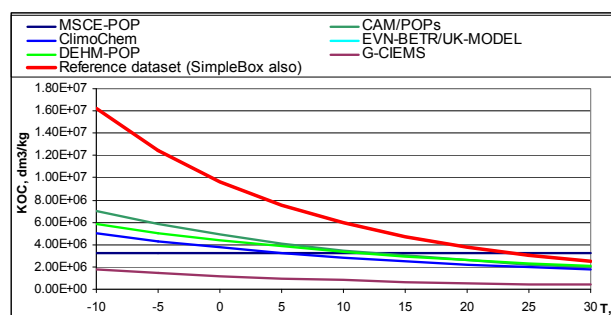


Fig. 5. Comparison of temperature dependencies of organic carbon/water partition coefficient of PCB-153 used in the participating POP models and in “reference data set”

Values of K_{oc} used in “reference data set” and also in EVN-BETR/UK-MODEL and SimpleBox models are the highest among all models practically within the whole considered temperature interval. For CAM/POPs, CliMoChem, and DEHM-POP (including MSCE-POP temperature independent value of K_{oc}) its values differ from each other not substantially. Values of this parameter used in G-CIEMS are lower than those used in other models. Table 14 presents the range of absolute values of organic

carbon/water partition coefficient of PCB-153 recalculated from K_{ow} values taken at three arbitrary temperatures (-10°C, 10°C and 25°C).

The difference between the highest and the lowest values of K_{oc} used by all participating models is less than an order of magnitude (max/min ratio comes down from 9 to 7 for the considered temperatures). Although, in the case of K_{ow} at these temperatures the max/min ratio decreases from 5 to 2. For models using one and the same approach to determination of K_{oc} (all models except for G-CIEMS), its values differ within factors of 2-5.

Table 14. Absolute values and statistical parameters of organic carbon/water partition coefficient of PCB-153 for three arbitrary temperatures (-10 °C, 10 °C and 25 °C).

| | K_{oc} , dm ³ /kg | | |
|--------------------|--------------------------------|----------|----------|
| | -10°C | 10°C | 25°C |
| CAM/POPs | 7.06E+06 | 3.50E+06 | 2.23E+06 |
| SimpleBox | 1.62E+07 | 5.95E+06 | 3.06E+06 |
| G-CIEMS | 1.80E+06 | 7.96E+05 | 4.65E+05 |
| EVN-BETR/UK-MODEL | 1.62E+07 | 5.95E+06 | 3.06E+06 |
| CliMoChem | 5.03E+06 | 2.86E+06 | 1.97E+06 |
| DEHM-POP | 5.89E+06 | 3.35E+06 | 2.31E+06 |
| MSCE-POP | 3.26E+06 | 3.26E+06 | 3.26E+06 |
| Reference data set | 1.62E+07 | 5.95E+06 | 3.06E+06 |
| <i>min</i> | 1.80E+06 | 7.96E+05 | 4.65E+05 |
| <i>max</i> | 1.62E+07 | 5.95E+06 | 3.26E+06 |
| <i>arith. mean</i> | 8.96E+06 | 3.95E+06 | 2.42E+06 |
| <i>mediana</i> | 6.47E+06 | 3.42E+06 | 2.68E+06 |
| <i>geom. mean</i> | 6.91E+06 | 3.41E+06 | 2.14E+06 |
| <i>max/min</i> | 5.0/9.0 * | 2.1/7.5* | 1.7/7.0* |

* - the first value is calculated without the values of K_{oc} used in G-CIEMS, the second value is calculated taking it into account.

Comparison of organic carbon/water partition coefficient temperature dependencies of PCB-28 and PCB-180 used in the participating models and “reference data sets” are presented in Fig. B.9 and B.10 in Annex B. Statistical evaluation of absolute values and coefficients of temperature dependencies is given in Table B.15 and B.16.

Difference between the highest and the lowest values of organic carbon/water partition coefficient is less than an order of magnitude. For the considered temperature interval, max/min ratios for PCB-28 and PCB-180 come down from 4 to 2.

3.6. Water solubility

Solubility in water (S_w , mol/m³) is an important characteristic of a pollutant defining its behaviour in the atmosphere, precipitation, soils and water. The data on water solubility of PCB-153 used by EVN-BETR/UK-MODEL, G-CIEMS and SimpleBox models which contain this parameter temperature independent are presented in Table 15. With the help of subcooled liquid-vapour pressure, this parameter can be used for estimation of Henry’s law constant if the latter is not available as input data. CAM/POPs, CliMoChem, DEHM-POP, and MSCE-POP do not include this parameter as input data in the calculations. Values of water solubility of PCB-153 used in the participating models and in “reference data set” are of the same order.

Table 15. Water solubility of PCB-153 (data sets of the participating POP models)

| Model | Description | Numerical values | | Comments | Reference |
|-----------------------|--------------------------|----------------------------------|----------|--|-----------------|
| G-CIEMS | Temperature independent. | $S_{WL}(T)$, mol/m ³ | 1.80E-05 | Same to the "reference data set" $T = 10^{\circ}\text{C}$ When Henry's law constants is not given as input, water solubility is used to estimate Henry's law constant | Li et al., 2003 |
| SimpleBox | Temperature independent | $S_{WL}(T)$, mol/m ³ | 1.80E-05 | Same to the "reference data set" $T = 10^{\circ}\text{C}$ | Li et al., 2003 |
| EVN-BETR/ UK-MODEL | Temperature independent | $S_{WL}(T)$, mol/m ³ | 3.07E-05 | $T = 25^{\circ}\text{C}$ | Li et al., 2003 |

The data on water solubility of PCB-28 and PCB-180 used in EVN-BETR/UK-MODEL and SimpleBox models which contain this parameter temperature independent are given in Table B.17 in Annex B. Values of S_{WL} used in EVN-BETR/UK-MODEL exceed those of SimpleBox about 2 times.

3.7. Degradation rate constants of PCBs in the environmental media

The multi-compartment models contain a different number of the environmental media included in their descriptions (See Chapter 2). The degradation process of POP in each medium is characterised by the values of its half-life ($t_{1/2}$) or degradation rate constant (k_d) which are connected with each other. Models CAM/POPs, G-CIEMS, EVN-BETR and UK-MODEL, CliMoChem and MSCE-POP use information on separate degradation rate constants (or half-lives) for the three environmental compartments (air, soil, and water). Degradation process in vegetation is considered by EVN-BETR, G-CIEMS and CliMoChem models. In EVN-BETR and UK-MODEL, degradation processes in sediment is also taken into account.

The degradation process in the atmosphere is mainly considered as the gas-phase reaction of a pollutant with hydroxyl radicals and all other reactions are neglected. The temperature-dependent second order rate constants of this reaction are used by CAM/POPs, CliMoChem and MSCE-POP models. Values of the pre-exponential multiplier and coefficients of temperature dependence for PCB-153 rate constant in the atmosphere are displayed in Table 16. No temperature dependence of degradation rate constants in air is used by EVN-BETR and UK-MODEL, SimpleBox and G-CIEMS.

In all models except for CliMoChem degradation processes in other media than air are temperature independent. Degradation of POPs in soil, water, sediment and vegetation are described as a first-order process. These data are also presented in Table 16.

Table 16. Degradation rate constants (or half-lives) of PCB-153 in the environmental media (data sets of the participating POP models)*

| Model | Description | Numerical values | | Comments | Reference |
|-----------|--|--|----------|--|--------------------|
| CAM/ POPs | Degradation in atmosphere: Temperature dependent: $k_{air} = k_{air}^0 \exp(-a_{kair}(1/T - 1/T_0))$ where T - temperature (K), k_{air}^0 is the value at the reference temperature T_0 , and a_{kair} is a parameter of temperature dependence | $k_{air}^0(T_0)$, cm ³ / (molec·s) | 2.11E-13 | Coefficients of the exponential equation are recalculated from the following temperature dependence: $K_{OH} = K_{OH}^0 \exp(a(1/T_0 - 1/T))$ where $K_{OH}^0 = 2.7\text{E-}13$ is the value at the reference temperature T_0 (298 K), $a = 1400$ is parameter of temperature dependence. | This study |
| | | a_{kair} | 1400 | | |
| | | T_0 , K | 283.15 | | |
| CliMoChem | Degradation in atmosphere: Temperature dependent: $k_{air} = k_{air}^0 \exp(-a_{kair}(1/T - 1/T_0))$ where T - temperature (K), k_{air}^0 is the value at the reference temperature T_0 , and a_{kair} is a parameter of temperature dependence | $k_{air}^0(T_0)$, cm ³ / (molec·s) | 1.18E-13 | $k_{air}(T) = k_{air}(T_{ref}) \exp((-E_{air}/R)(1/T - 1/T_0))$ T = temperature (283.15 K), T_0 = reference temperature (298.15 K) $k_{air}(T_0)$ = degradation rate constant at T_0 (cm ³ /d), PCB 153: 1.42E-8; E_{air} = activation energy (J/mol), PCB 153: 15400; R = universal gas constant (8.3145 J/mol K) k_{air}^0 = degradation rate constant at 283.15 (cm ³ /d), PCB 153: 1.02E-08 $a_{kair} = E_a/R$ | Beyer et al., 2002 |
| | | a_{kair} | 1852.2 | | |
| | | T_0 , K | 283.15 | | |

| Model | Description | Numerical values | | Comments | Reference | | |
|--|---|--|--|---|---|--|--------------------------------|
| | Degradation in soil: Temperature dependent: $k_{soil} = k_{soil}^0 \exp(-a_{ksoil}(1/T - 1/T_0))$ where T - temperature (K), k_{soil}^0 is the value at the reference temperature T_0 , and a_{ksoil} is a parameter of temperature dependence | $k_{soil}^0(T_0)$, 1/s | 6.16E-10 | $k_{soil}(T) = k_{soil}(T_{ref}) \exp((-E_{asoil}/R)(1/T - 1/T_0))$ T = temperature (283.15 K), T_0 = reference temperature (298.15 K) $k_{soil}(T_0)$ = degradation rate constant at T_0 (1/d), PCB 153: 1.01E-4; E_{asoil} = activation energy (J/mol) PCB 153: 30000 R = universal gas constant (8.3145 J/mol K) k_{soil}^0 = degradation rate constant at 283.15 (1/d), PCB 153: 5.32E-05 $a_{ksoil} = E_{asoil}/R$ | | | |
| | | a_{ksoil} | 3608.2 | | | | |
| | | T_0, K | 283.15 | | | | |
| | Degradation in water: Temperature dependent: $k_{water} = k_{water}^0 \exp(-a_{kwater}(1/T - 1/T_0))$ where T - temperature (K), k_{water}^0 is the value at the reference temperature T_0 , and a_{kwater} is a parameter of temperature dependence | $k_{water}^0(T_0)$, 1/s | 8.47E-10 | $k_{water}(T) = k_{water}(T_{ref}) \exp((-E_{awater}/R)(1/T - 1/T_0))$ T = temperature (283.15 K), T_0 = reference temperature (298.15 K) $k_{water}(T_0)$ = degradation rate constant at T_0 (1/d), PCB 153: 1.39E-4; E_{awater} =activation energy (J/mol), PCB 153: 30000 R = universal gas constant (8.3145 J/mol K) k_{water}^0 =degradation rate constant at 283.15 (1/d), PCB 153: 7.32E-05; $a_{kwater} = E_{awater}/R$ | | | |
| | | a_{kwater} | 3608.2 | | | | |
| | | T_0, K | 283.15 | | | | |
| | Degradation in vegetation**: Temperature dependent: $k_{veg} = k_{veg}^0 \exp(-a_{kveg}(1/T - 1/T_0))$ where T - temperature (K), k_{veg}^0 is the value at the reference temperature T_0 , and a_{kveg} is a parameter of temperature dependence | $k_{veg}^0(T_0)$, 1/s | 1.14E-07 | $k_{veg}(T) = k_{veg}(T_{ref}) \exp((-E_{aveg}/R)(1/T - 1/T_0))$ T = temperature (283.15 K), T_0 = reference temperature (298.15 K) $k_{veg}(T_0)$ = degradation rate constant at T_0 (1/d), PCB 153: 1.37E-2; E_{aveg} = activation energy (J/mol), PCB 153: 15400 R = universal gas constant (8.3145 J/mol K) $k_{veg}(T_0)$ = degradation rate constant at T_0 (1/d), PCB 153: 9.86E-03; $a_{kveg} = E_{aveg}/R$ | | | |
| | | a_{kveg} | 1852.2 | | | | |
| | | T_0, K | 283.15 | | | | |
| | MSCE-POP | Degradation in atmosphere: Temperature dependent: $k_{air} = k_{air}^0 \exp(-a_{kair}(1/T - 1/T_0))$ where T - temperature (K), k_{air}^0 is the value at the reference temperature T_0 , and a_{kair} is a parameter of temperature dependence | $k_{air}^0(T_0)$, cm ³ / (molec.s) | 1.18E-13 | | Coefficients of the exponential equation are recalculated from the following temperature dependence: $k_{air} = A \cdot \exp(-E_a/RT)$ with the help of the following formulas: $a_{kair}=E_a/R$, $k_{air}^0 = A \cdot \exp(-E_a/RT_0)$, where $A = 8.12 \text{ E-11}$ is the pre-exponential multiplier value, cm ³ /(molec·s); $E_a = 15380$ is the activation energy of interaction with OH-radical in air, J/mol | Beyer and Matthies, 2001 |
| | | | a_{kair} | 1849.8 | | | |
| | | | T_0, K | 283.15 | | | |
| Degradation in soil: Temperature independent | | k_{soil} , 1/s | 1.17E-09 | Degradation rate constant in soil is conversed from half-life values (PCB-153: 165000 hours): $k_d = 0.693/ t_{1/2}$, where k_d is the first-order rate constant (s ⁻¹) and $t_{1/2}$ is the half-life (s). | Sinkkonen and Paasivirta, 2000 | | |
| Degradation in water: Temperature independent | k_{water} , 1/s | 1.6E-09 | Degradation rate constant in water is conversed from half-life values (PCB-153: 120000 hours): $k_d = 0.693/ t_{1/2}$, where k_d is the first-order rate constant (s ⁻¹) and $t_{1/2}$ is the half-life (s). | | | | |
| SimpleBox | Degradation in atmosphere: Temperature independent | k_{air} , 1/s | 3.50E-08 | Same half-lives as in "reference data set" : PCB-153: 5500 hours | Mackay et al., 1992 | | |
| | Degradation in soil: Temperature independent | k_{soil} , 1/s | 3.50E-09 | Same half-lives as in "reference data set" : PCB-153: 55000 hours | | | |
| | Degradation in water: Temperature independent | k_{water} , 1/s | 3.50E-09 | Same half-lives as in "reference data set" : PCB-153: 55000 hours | | | |
| G-CIEMS | Degradation in atmosphere: Temperature independent | k_{air} , 1/s | 3.50E-08 | Same half-lives as in "reference data set" : PCB-153: 5500 hours | Mackay et al., 1992 | | |
| | Degradation in soil: Temperature independent | k_{soil} , 1/s | 3.50E-09 | Same half-lives as in "reference data set" : PCB-153: 55000 hours | | | |
| | Degradation in water: Temperature independent | k_{water} , 1/s | 3.50E-09 | Same half-lives as in "reference data set" : PCB-153: 55000 hours | | | |
| EVN-BETR and UK- MODEL | Degradation in atmosphere: Temperature independent | k_{air} , 1/s | 3.50E-08 | Same half-lives as in "reference data set" : PCB-153: 5500 hours | Mackay et al., 1992 | | |
| | Degradation in soil: Temperature independent | k_{soil} , 1/s | 3.50E-09 | Same half-lives as in "reference data set" : PCB-153: 55000 hours | | | |
| | Degradation in water: Temperature independent | k_{water} , 1/s | 3.50E-09 | Same half-lives as in "reference data set" : PCB-153: 55000 hours | | | |
| | Degradation in sediment: Temperature independent | k_{sed} , 1/s | 3.50E-09 | Same half-lives as in "reference data set" : PCB-153: 55000 hours | | | |
| | Degradation in vegetation: Temperature independent | k_{veg} , 1/s | 1.13E-08 | PCB-153 half-life in vegetation: 17000 hours | | | |

* - for the sake of comparability, the base values and coefficients of temperature dependences of the considered parameters are given here for the temperature 283.15 K (T_0) and the way they were recalculated from original dependencies is specified in the field "Comments".

** - because of insufficient data on degradation rate constants in vegetation, the values are taken from atmospheric degradation [Möller, 2002] and multiplied with an average OH-radical concentration of 970000 1/cm³ [Beyer et al., 2002].

The second-order rate constants of PCB-153 degradation process in the air in the form of temperature dependencies are compared in Fig. 6.

Following the data reported, CliMoChem and MSCE-POP models use one and the same values of temperature dependent rate constants of PCB-153 degradation in the atmosphere. CAM/POPs provides the highest values.

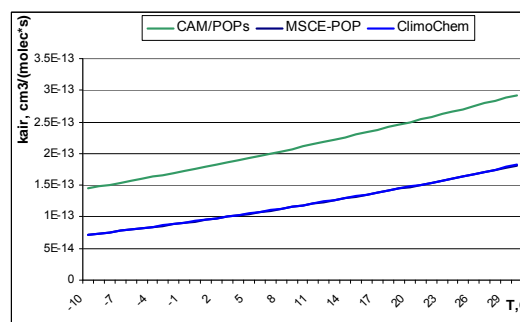


Fig. 6. Comparison of temperature dependencies of degradation rate constant of PCB-153 in the atmosphere

The comparison of temperature dependencies of second-order rate constants of PCB-28 and PCB-180 used in the participating models are presented in Fig. B.11 and B.12 in Annex B.

CliMoChem and MSCE-POP models also use one and the same values of degradation rate constants in the atmosphere for PCB-28 and PCB-180.

In the “reference data set” the rate constants of degradation processes in all environmental media are assumed temperature independent. For these purpose data on suggested half-life groups were taken from [Mackay *et al.* 1992] and converted into the first-order degradation rate constants. In order to have possibility to compare values of degradation rate constant of PCB-153 used in all participating models and in the “reference data set”, the rate constants of the second order degradation process in air were yearly averaged for the models which keep this parameter temperature dependent. This calculation was made with the use of monthly averaged temperatures calculated on the basis of meteorological data for 1997, 1998 and 1999 in Europe. Then multiplying the second order rate constants by mean annual OH-radical concentration in the surface layer of 2 km depth at the latitude of 45°N ($0.8 \cdot 10^6$ mole/cm³) [Yu Lu and Khall, 1991], the first order degradation rate constants were calculated for CAM/POPs, CliMoChem, and MSCE-POP models. The results on PCB-153 are presented in Table 17 (for results on PCB-28 and PCB-180 see Tables B.19 and B.21 in Annex B). However, the usage of the mean annual OH-radical concentration for all the models which in reality include this parameter in different ways is rather rough assumption. For an example, in CliMoChem it varies depending on the temperature and in MSCE-POP - depending on the season.

Table 17. Monthly averaged temperatures calculated on the basis of meteorological data for 1997, 1998 and 1999 in Europe and the yearly average degradation rate constants of PCB-153 for the models which use temperature dependence of these parameters

| Month | Temperatures, °C | | | CAM/POPs air, cm ³ ·mole ⁻¹ ·s ⁻¹ | MSCE-POP air, cm ³ ·mole ⁻¹ ·s ⁻¹ | CliMoChem | | |
|--|------------------|----------|---------|--|--|--|---|---|
| | Over land | Over sea | Average | | | air, cm ³ ·mole ⁻¹ ·s ⁻¹ | soil, s ⁻¹ (for Over land temp) | sea, s ⁻¹ (for Over sea temp) |
| Jan | 4 | 4 | 4 | 1.90E-13 | 1.02E-13 | 1.03E-13 | 4.67E-10 | 6.43E-10 |
| Feb | 4 | 3 | 4 | 1.90E-13 | 1.02E-13 | 1.03E-13 | 4.67E-10 | 6.13E-10 |
| Mar | 7 | 5 | 6 | 1.97E-13 | 1.07E-13 | 1.08E-13 | 5.37E-10 | 6.74E-10 |
| Apr | 11 | 6 | 9 | 2.07E-13 | 1.15E-13 | 1.16E-13 | 6.44E-10 | 7.06E-10 |
| May | 17 | 10 | 13 | 2.22E-13 | 1.26E-13 | 1.27E-13 | 8.37E-10 | 8.47E-10 |
| Jun | 21 | 14 | 17 | 2.38E-13 | 1.38E-13 | 1.38E-13 | 9.92E-10 | 1.01E-09 |
| Jul | 22 | 16 | 19 | 2.46E-13 | 1.44E-13 | 1.45E-13 | 1.03E-09 | 1.10E-09 |
| Aug | 22 | 16 | 19 | 2.46E-13 | 1.44E-13 | 1.45E-13 | 1.03E-09 | 1.10E-09 |
| Sep | 18 | 13 | 15 | 2.30E-13 | 1.32E-13 | 1.32E-13 | 8.74E-10 | 9.68E-10 |
| Oct | 14 | 10 | 12 | 2.18E-13 | 1.24E-13 | 1.24E-13 | 7.35E-10 | 8.47E-10 |
| Nov | 10 | 7 | 9 | 2.07E-13 | 1.15E-13 | 1.16E-13 | 6.16E-10 | 7.39E-10 |
| Dec | 6 | 5 | 6 | 1.97E-13 | 1.07E-13 | 1.08E-13 | 5.13E-10 | 6.74E-10 |
| Averaged second-order rate constants, cm ³ ·mole ⁻¹ ·s ⁻¹ | | | | 2.16E-13 | 1.22E-13 | 1.22E-13 | - | - |
| Averaged first-order rate constants, s ⁻¹ | | | | 1.72E-07 | 9.73E-08 | 9.78E-08 | 7.29E-10 | 8.27E-10 |

The rate constants of the first order degradation process in soil, sea and vegetation used in CliMoChem model which keeps these parameters temperature dependent were yearly averaged. This calculation was also made with the use of monthly averaged temperatures calculated on the basis of meteorological data for 1997, 1998 and 1999 in Europe.

To illustrate the dispersion of absolute values of the first-order degradation rate constants of PCB-153 in the atmosphere and in other media used in the participating models and in the “reference data set”, statistical treatment of these parameters is made and some statistics are given in Table 18.

Table 18. Absolute values and statistical parameters of degradation rate constants of first order (PCB-153)

| | k_{air}, s^{-1} | k_{soil}, s^{-1} | k_{water}, s^{-1} | $k_{sediment}, s^{-1}$ | k_{veg}, s^{-1} |
|--------------------|-------------------|--------------------|---------------------|------------------------|-------------------|
| CAM/POPs | 1.72E-07 | - | - | - | - |
| CliMoChem | 9.78E-08 | 7.29E-10 | 8.27E-10 | - | 1.18E-07 |
| MSCE-POP | 9.73E-08 | 1.17E-09 | 1.60E-09 | - | - |
| SimpleBox | 3.50E-08 | 3.50E-09 | 3.50E-09 | - | - |
| G-CIEMS | 3.50E-08 | 3.50E-09 | 3.50E-09 | - | - |
| EVN-BETR/UK-MODEL | 3.50E-08 | 3.50E-09 | 3.50E-09 | 3.50E-09 | 1.13E-08 |
| Reference data set | 3.50E-08 | 3.50E-09 | 3.50E-09 | 3.50E-09 | - |
| <i>min</i> | 3.50E-08 | 7.29E-10 | 8.27E-10 | - | - |
| <i>max</i> | 1.72E-07 | 3.50E-09 | 3.50E-09 | - | - |
| <i>arith. mean</i> | 7.25E-08 | 2.65E-09 | 2.74E-09 | - | - |
| <i>median</i> | 3.50E-08 | 3.50E-09 | 3.50E-09 | - | - |
| <i>geom.mean</i> | 5.89E-08 | 2.24E-09 | 2.42E-09 | - | - |
| <i>max/min</i> | 4.9 | 4.8 | 4.2 | 1.0 | 10.4 |

There is a large difference in absolute values of degradation rate constant of PCB-153 (s^{-1}) between the models which are using and not using its temperature dependencies of degradation rate constants. It is exemplified by the differences in highest and lowest values of these parameters for degradation processes in air, soil, and water, sediments and vegetation. Max/min ratios for degradation processes in air, soil, and water vary within factor of 4-5. The difference between temperature dependent values of degradation rate constant of PCB-153 in air is within a factor of 2. EVN-BETR and UK-MODEL, SimpleBox, G-CIEMS and the “reference data set” contain one and the same values of temperature independent rate constants taken from [Mackay *et al.* 1992]. The difference of degradation rate constant in vegetation between EVN-BETR and UK-MODEL and CliMoChem models (max/min ratio) is around 10. Degradation in sediments is considered in EVN-BETR and UK-MODEL only.

Statistical evaluation of absolute values of the first-order degradation rate constants of PCB-28 and PCB-180 in the atmosphere and in other media used in the participating models and in the “reference data set” are presented in Table B.20 and B.22 in Annex B.

Among all media the largest difference in the values of first-order rate constants between the models for PCB-28 is observed for the degradation in water and for PCB-180 - for the degradation in soil. Max/min ratios of degradation rate constant values in air, soil and water for PCB-28 vary from 2 to 12; and for PCB-180 – from 3 to 10. Max/min ratio of rate constants for degradation in vegetation between CliMoChem and EVN-BETR and UK-MODEL for PCB-28 equals to 7 and for PCB-180 it is around 6. Degradation in sediments is considered in EVN-BETR and UK-MODEL only.

Difference in temperature dependent values of degradation rate constant in air between CAM/POPs, CliMoChem and MSCE-POP models for PCB-180 is within factor 2. In CliMoChem and MSCE-POP models these values for PCB-28 are equal.

COMPARISON OF PROCESS PARAMETERIZATIONS AND RESULTS OF COMPUTATIONAL EXPERIMENTS FOR PCB-153

This Chapter is devoted to the analysis of model approaches to the description of main processes determining PCBs behaviour in the environment. These are gas/particle partitioning, dry deposition of particulate phase, wet deposition, gaseous exchange between the atmosphere and different types of underlying surface (soil, water, vegetation) and degradation processes. The comparison of the results of calculation experiments obtained by different models is presented here together with brief description of model approaches to the parameterization of the considered processes used in the participating models. More detailed description of these approaches is presented in Annex C. An overview of descriptions of degradation processes used for PCB modelling is given above in Chapter 3. The presentation in this Chapter concerns mainly PCB-153 (substance of the first priority), appropriate data on other considered pollutants (PCB-28 and PCB-180) are presented in Annexes D and E. The exposition in subsequent Sections devoted to each of the above processes (except for degradation) has one and the same structure which goes as follows.

First, we present short summary of the descriptions of the considered process submitted by participants (at present descriptions of considered processes is available for seven models: EVN-BETR and UK-MODEL, CliMoChem, G-CIEMS, DEHM-POP, SimpleBox, CAM/POPs and MSCE-POP).

Second, the description of input data used for calculation experiments with PCB – 153 on each basic process is presented. The input data for modelling include several sets of given air concentrations in different phases (if needed) and environmental conditions (averaged ambient temperatures, organic content in the atmospheric aerosol, TSP, precipitation intensity, mean wind velocity, etc.) relevant for each experiment.

Third, the intercomparison of results of computation experiment carried out by the participating models is presented. This analysis consists of two parts. The first part concerns the comparison of obtained absolute values and some statistical parameters for each experiment included in this process. The second is devoted to the pairwise comparison of the model output. The set of statistical parameters used for the comparison is different for different processes.

4.1. Gas/particle partitioning

4.1.1. Model approaches

Basically, there exist two approaches to model evaluation of the fraction of particulate phase of a pollutant in the atmosphere. The first is based on the Junge-Pankow adsorption model [Junge, 1977; Pankow, 1987]. In this case POP fraction ϕ adsorbed on the atmospheric aerosol particles is calculated using vapor pressure of the subcooled liquid p_{oi} :

$$\varphi = \frac{c \cdot \theta}{p_{ol} + c \cdot \theta} \quad (3)$$

where c is the constant depending on thermodynamic parameters of adsorption process and on properties of aerosol particle surface;

θ is the specific surface of aerosol particles, m^2/m^3 .

This approach is used in SimpleBox, CAM/POPs and MSCE-POP models. In all these models the temperature dependence of p_{ol} is taken into account. Besides, CAM/POPs model additionally uses 12-bin structure of sulphate aerosol for calculations of gas/aerosol partitioning.

The second is based on absorption model of gas/aerosol partitioning [Finizio *et al.*, 1997; Falconer and Harner, 2000]. Under this approach the fraction of POPs absorbed by organic matter of aerosol particles is calculated with the use of particle/gas partitioning coefficient K_{PA} defined via octanol/air partitioning coefficient K_{oa} :

$$\varphi = \frac{K_{PA} \cdot TSP}{(K_{PA} \cdot TSP + 1)} \quad (4)$$

Here φ is the fraction of compound sorbed to particles, K_{PA} is the gas-particle partitioning coefficient, and TSP is the total suspended particle concentration. K_{PA} is calculated using different regression relations via K_{oa} , in particular [Falconer and Harner, 2000]:

$$\log K_{PA} = m_r \log K_{oa} + \log f_{om} - 11.91, \quad (5)$$

where m_r - constant expected to have a value close to +1 for equilibrium partitioning;

K_{oa} - octanol-air partition coefficient;

f_{om} - fraction of organic matter in the particles.

This approach is used in DEHM-POP and experimental version of MSCE-POP.

To calculate gas-particle partitioning coefficient CliMoChem used another equation taken from [Finizio *et al.* 1997]:

$$K_{PA} = K_{oa}^{0.55} \cdot 10^{-8.23} \quad (6)$$

EVN-BETR and UK-MODEL and G-CIEMS calculated this coefficient with the help of equations (7) and (8), respectively:

$$K_{PA} = 3.5 \cdot K_{oa} \quad (7)$$

$$K_{PA} = y \cdot K_{oa} / (\tilde{\rho} \cdot 1000), \quad (8)$$

where y is the organic matter mass fraction, and $\tilde{\rho}$ is the density of aerosol particles.

Below the results of calculations of φ for different environmental conditions carried out by the above seven models are analyzed.

4.1.2. Input data

Nine sets of input data (different ambient temperatures in the range from -12°C to 32°C) are proposed for modelling experiments with PCB-153.

Table 19. Input data for computation experiments with PCB-153 describing gas/particle partitioning

| N | Experiment 1 | Experiment 2 | Experiment 3 | Experiment 4 | Experiment 5 | Experiment 6 | Experiment 7 | Experiment 8 | Experiment 9 |
|---|--------------|--------------|--------------|--------------|--------------|--------------|--------------|--------------|--------------|
| Averaged ambient temperature, C | -12 | -5 | 0 | 6 | 10 | 15 | 20 | 26 | 32 |
| Total Suspended Matter, TSP, $\mu\text{g}/\text{m}^3$ | 30 | 30 | 30 | 30 | 30 | 30 | 30 | 49 | 66 |
| Organic content in the aerosol, % | 20 | 20 | 20 | 20 | 20 | 20 | 20 | 20 | 20 |

Output of computation experiments describing gas/particle partitioning process is PCB particulate fraction in the atmosphere.

4.1.3. Comparison of the results

This section contains the analysis of the results of experiments on the calculations of particulate fraction φ of the considered pollutants obtained by the participating models. Here we present numerical results for the first priority substance (PCB-153) only. The corresponding results for substances of the second priority (PCB-28 and PCB-180) can be found in Annexes D and E.

The analysis is performed into two stages. At the first stage we present an analysis of the values of calculated fractions of particulate phase and characterize the spread in these values between models in each of the experiments. At the second stage we analyze pairwise differences between participating models using the regression analysis.

Analysis of the experiments. Here we use the following statistical parameters for each experiment:

- the value m_φ of fractions of particulate phase averaged between participating models;
- the value of square deviation σ_φ between results obtained by different models;

First of the above parameters illustrates the level of particulate phase fraction calculated by all considered models. The second parameter characterizes the dispersion of this fraction between the models.

Calculation results for PCB-153 together with m_φ and σ_φ are presented in Table 20. In Table 21 short comments to the calculations made by participants can be found. For two models (G-CIEMS and MSCE-POP) two versions of calculations are presented. Namely, for G-CIEMS calculations of gas-particle partitioning using molecular weight only (G-CIEMS 1) and using absorption scheme (G-CIEMS 2) were carried out. For MSCE-POP model calculations based on the adsorption (based on p_{oi} values; MSCE-POP 1) and absorption (based on K_{oa} values; MSCE-POP 2) schemes are presented. The comparison of calculated fractions of the particulate phase is illustrated also by the plot below.

Table 20. Calculation results: fractions of particulate phase of PCB-153 calculated by models and statistical parameters used for evaluation

| Exp. No | T (°C) | EVN-BETR and UK-MODEL | DEHM-POP | G-CIEMS | | CAM/POPs | MSCE-POP | | CliMoChem | SimpleBox* | m_φ | σ_φ |
|---------|--------|-----------------------|----------|---------|-------|----------|----------|-------|-----------|------------|-------------|------------------|
| | | | | 1 | 2 | | 1 | 2 | | | | |
| 1 | -12 | 0.93 | 0.83 | 0.96 | 0.78 | 0.94 | 0.874 | 0.869 | 0.163 | 0.978 | 0.81 | 0.25 |
| 2 | -5 | 0.75 | 0.62 | 0.89 | 0.53 | 0.85 | 0.698 | 0.693 | 0.098 | 0.939 | 0.67 | 0.25 |
| 3 | 0 | 0.68 | 0.44 | 0.79 | 0.35 | 0.73 | 0.522 | 0.519 | 0.068 | 0.882 | 0.55 | 0.25 |
| 4 | 6 | 0.46 | 0.26 | 0.61 | 0.18 | 0.53 | 0.315 | 0.315 | 0.044 | 0.765 | 0.39 | 0.23 |
| 5 | 10 | 0.33 | 0.17 | 0.48 | 0.11 | 0.39 | 0.208 | 0.21 | 0.033 | 0.656 | 0.29 | 0.20 |
| 6 | 15 | 0.19 | 0.095 | 0.32 | 0.058 | 0.24 | 0.118 | 0.121 | 0.023 | 0.500 | 0.19 | 0.15 |
| 7 | 20 | 0.11 | 0.053 | 0.21 | 0.031 | 0.14 | 0.065 | 0.068 | 0.017 | 0.349 | 0.12 | 0.11 |
| 8 | 26 | 0.086 | 0.042 | 0.12 | 0.014 | 0.12 | 0.032 | 0.053 | 0.018 | - | 0.06 | 0.04 |
| 9 | 32 | 0.057 | 0.029 | 0.063 | 0.007 | 0.078 | 0.016 | 0.036 | 0.017 | - | 0.04 | 0.03 |

* - only 7 experiments for Simple Box

Table 21. Comments

| Model assumptions | Models | Physical-chemical data set | Other Comments |
|---------------------|-----------------------|----------------------------|--|
| Adsorption approach | CAM/POPs | Own | equation (3); c is 0.172 Pa·m [Pankow, 1987; Falconer et al., 1994; Bidleman et al., 1998] Additional input data of 12 size-bin structure is applied on the TSP in the experiment |
| | SimpleBox | "Reference" | equation (3); JungeConst = 0.172 Pa·m by default; P_L = liquid-phase vapor pressure at ambient temperature T (Pa) = P_L (25C) · exp($(H_{vap}^0/8.314) · (1/298 - 1/T)$) H_{vap}^0 = Enthalpy of vaporization (J/mol) = ΔU_{aw} in "reference data set"; SimpleBox takes specific aerosol surface as input; calculations done only for 'standard' aerosol characteristics (TSP 30 mg/m ³ ; f_{oc} 20%), with aerosol surface set to $1.5 \cdot 10^{-4}$ m ² /m ³ |
| | MSCE-POP 1 | Own | current version – equation (3); Assumed that c = 0.172 Pa·m [Junge, 1977] for background aerosol and θ = $1.5 \cdot 10^{-4}$ m ² /m ³ [Whitby, 1978]. |
| Absorption approach | EVN-BETR and UK-MODEL | Own | equation (7); own dataset of EVN-BETR and UK-MODEL is extremely close to the "reference dataset"; K_{oa} was calculated from K_{ow}/K_{aw} |
| | CliMoChem | Own | equations (4) and (6); K_{oa} was calculated from K_{ow}/K_{aw} |
| | DEHM-POP | Own | equations (4) and (5) |
| | G-CIEMS 2 | "Reference" | equation (8) |
| | MSCE-POP 2 | Own | experimental version – equations (4) and (5); |
| Other | G-CIEMS 1 | "Reference" | Gas/particle partitioning is calculated from only molecular weight (for preliminary assessment purpose) |

The plot of dependence of φ on T calculated by participating models is presented in Fig. 7.

It is seen that practically all models (except CliMoChem) closely describe temperature dependence of particulate fraction. For the lower temperatures, values of fraction of particulate phase of PCB-153 calculated by CliMoChem are much lower than ones calculated by other participating models. Considering results of the first seven of the experiments, the highest results of this parameter are obtained by SimpleBox model.

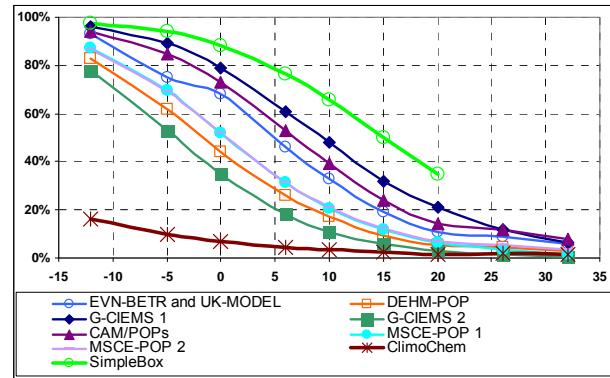


Fig. 7. Calculation results of the participating models (gas-particle partitioning)

We recall that the experiments differ mainly by ambient air temperature T (and some other parameters, see Section 4.1.2). For each temperature within the considered interval of temperatures (-12°C - 32°C), square deviation σ_φ between different model calculations (see last column in Table 20) do not exceed the averaged value of particulate phase fractions. It is testify that all models give close enough results in terms of absolute values.

Pairwise comparison of model results. Here the analysis of pairwise differences between calculation results obtained by different models by means of the regression analysis is presented. Namely, the relation between calculated fractions φ_T^1 and φ_T^2 obtained by each two models for different values of temperature T is supposed to be:

$$\varphi_T^2 = \alpha_{12} \varphi_T^1 + \beta_{12} + \omega_{12}, \quad (9)$$

where α_{12} and β_{12} are regression coefficients;
 ω_{12} is the random component of the regression relation ("white noise").

For evaluation of closeness of calculated results obtained by models, we shall use regression coefficients α_{12} and β_{12} (characterizing a non-random component of the regression relation), the *residual square deviation*, that is, square deviation σ_{12}^{res} of ω_{12} (characterizing the magnitude of random component) and the correlation coefficient r_{12} .

Table 22 contains the values of regression coefficients α and β calculated for all pairs of models. The differences between the models are explained mainly by scaling coefficients α ranging from 0.13 to 3.78. For the most part of the models (not including CliMoChem results), α varies far less (from 0.71 to 1.15). Coefficients β are not very large for all pairs of models (lying in the range from – 0.13 to 0.48). This is a numerical expression of the fact that shapes of curves expressing temperature dependencies of φ (Fig. 7) are similar for these models.

Table 22. Coefficients of regression dependence between the models (α / β)

| | DEHM-POP | G-CIEMS 1 | G-CIEMS 2 | CAM/POPs | MSCE-POP1 | MSCE-POP2 | CliMoChem | SimpleBox* |
|-----------------------|--------------|-------------|--------------|--------------|--------------|--------------|--------------|-------------|
| EVN-BETR and UK-MODEL | 0.87 / –0.07 | 1.03 / 0.08 | 0.81 / –0.09 | 1.02 / 0.04 | 0.96 / –0.07 | 0.94 / –0.05 | 0.14 / 0.00 | 0.75 / 0.36 |
| DEHM-POP | – | 1.11 / 0.18 | 0.94 / –0.04 | 1.11 / 0.13 | 1.09 / 0.01 | 1.06 / 0.02 | 0.17 / 0.01 | 0.73 / 0.47 |
| G-CIEMS 1 | – | – | 0.73 / –0.13 | 0.97 / –0.03 | 0.89 / –0.12 | 0.87 / –0.11 | 0.13 / –0.01 | 0.81 / 0.23 |
| G-CIEMS 2 | – | – | – | 1.15 / 0.18 | 1.14 / 0.06 | 1.11 / 0.07 | 0.18 / 0.01 | 0.73 / 0.51 |
| CAM/POPs | – | – | – | – | 0.93 / –0.10 | 0.91 / –0.08 | 0.14 / –0.01 | 0.75 / 0.31 |
| MSCE-POP 1 | – | – | – | – | – | 0.98 / 0.01 | 0.15 / 0.01 | 0.71 / 0.44 |
| MSCE-POP 2 | – | – | – | – | – | – | 0.16 / 0.00 | 0.72 / 0.44 |
| CliMoChem | – | – | – | – | – | – | – | 3.78 / 0.48 |

* - by 7 experiments only

This fact is once more confirmed by calculated correlation coefficients (Table 23) which is very high for all pairs of models (from 0.83 to 1.00).

Table 23. Correlation coefficients σ

| | DEHM-POP | G-CIEMS 1 | G-CIEMS 2 | CAM/POPs | MSCE-POP 1 | MSCE-POP 2 | CliMoChem | SimpleBox* |
|-----------------------|----------|-----------|-----------|----------|------------|------------|-----------|------------|
| EVN-BETR and UK-MODEL | 0.98 | 0.99 | 0.96 | 1.00 | 0.99 | 0.99 | 0.93 | 0.97 |
| DEHM-POP | – | 0.94 | 1.00 | 0.97 | 1.00 | 1.00 | 0.98 | 0.91 |
| G-CIEMS 1 | – | – | 0.91 | 0.99 | 0.96 | 0.96 | 0.87 | 0.99 |
| G-CIEMS 2 | – | – | – | 0.94 | 0.99 | 0.99 | 0.99 | 0.87 |
| CAM/POPs | – | – | – | – | 0.98 | 0.98 | 0.91 | 0.98 |
| MSCE-POP 1 | – | – | – | – | – | 1.00 | 0.97 | 0.93 |
| MSCE-POP 2 | – | – | – | – | – | – | 0.97 | 0.93 |
| CliMoChem | – | – | – | – | – | – | – | 0.83 |

* - by 7 experiments only

Thus, all models describe temperature dependence of the fraction of particulate phase of PCB-153 in the atmosphere similarly. The difference of model results can be explained by difference in base values of K_{oa} or p_{ol} since the change of these values leads to scaling of calculated values of φ .

To assess the reliability of comparative analysis given above calculations of pairwise residual square deviation σ were done (Table 24).

Table 24. Residual square deviation, σ

| | DEHM-POP | G-CIEMS 1 | G-CIEMS 2 | CAM/POPs | MSCE-POP 1 | MSCE-POP 2 | CliMoChem | SimpleBox* |
|-----------------------|----------|-----------|-----------|----------|------------|------------|-----------|------------|
| EVN-BETR and UK-MODEL | 0.167 | 0.157 | 0.214 | 0.075 | 0.124 | 0.130 | 0.050 | 0.146 |
| DEHM-POP | – | 0.321 | 0.063 | 0.237 | 0.069 | 0.056 | 0.027 | 0.245 |
| G-CIEMS 1 | – | – | 0.312 | 0.105 | 0.236 | 0.244 | 0.068 | 0.084 |
| G-CIEMS 2 | – | – | – | 0.309 | 0.139 | 0.126 | 0.017 | 0.286 |
| CAM/POPs | – | – | – | – | 0.161 | 0.167 | 0.058 | 0.112 |
| MSCE-POP 1 | – | – | – | – | – | 0.018 | 0.036 | 0.216 |
| MSCE-POP 2 | – | – | – | – | – | – | 0.035 | 0.216 |
| CliMoChem | – | – | – | – | – | – | – | 0.320 |

* - by 7 experiments only

It is seen that the values of σ range from 0.017 to 0.32. This testify the possibility of usage regression analysis for evaluation of the difference between model calculations. Maximum values of the random component are characteristic of the comparisons between G-CIEMS 1 and G-CIEMS 2, between G-CIEMS 1 and DEHM-POP, between EVN-BETR and UK-MODEL and G-CIEMS 2, between CAM/POPs and G-CIEMS 2, between G-CIEMS 1 and MSCE-POP and between SimpleBox and following models: DEHM-POP, G-CIEMS 2, MSCE-POP and CliMoChem.

The results obtained for PCB-180 are similar to the results on PCB-153. Values of fraction of particulate phase of PCB-180 calculated by CliMoChem are much lower than ones calculated by other participating models. We remark also that taking into account the real dispersion of TSP in the atmosphere can essentially affect the calculations (see plots of temperature dependence of φ for PCB-180 in Annex E). Correlation coefficients for all models vary from 0.75 to 1.00.

Results on PCB-28 (Annex D) to some extent differ from the results on above two congeners. The highest values of this parameter are obtained by SimpleBox model. Fractions of particulate phase calculated by EVN-BETR and UK model are also larger than those calculated by DEHM-POP, CliMoChem and MSCE-POP. The results obtained by other models are close to one another. Correlation coefficients for all models vary from 0.98 to 1.00.

4.2. Dry deposition of the particulate phase

4.2.1. Model approaches

Dry deposition velocity v_d is used in all models for the description of dry deposition flux of the particulate phase to different types of underlying surface:

$$F_{dep} = v_d \cdot C_{part}, \quad (10)$$

where F_{dep} is the deposition flux of POP particulate phase to a given type of underlying surface;

C_{part} is the concentration of POP particulate phase in the atmosphere.

The differences between models in the description of this process lie in the method of calculation of deposition velocity. SimpleBox, EVN-BETR and UK-MODEL and G-CIEMS models use one and the same value of dry deposition velocity for all considered types of underlying surfaces. CliMoChem model takes into account the dependence of dry deposition velocity on underlying surface type and its seasonal variations. DEHM-POP, CAM/POPs and MSCE-POP models calculate dry deposition velocity to different types of underlying surface on the basis of current meteorological conditions (such as the friction velocity, the Monin-Obukhov length and the roughness parameter). Due to high scattering of dry deposition velocity values used by the participating models (see Table 25), large range of calculated values of dry deposition flux takes place.

Table 25. Dry deposition velocity, m/s

| Type of underlying surface | EVN-BETR and UK-MODEL | DEHM-POP | | | G-CIEMS | CAM/POPs | MSCE-POP | | | CliMoChem | SimpleBox |
|----------------------------|-----------------------|----------|--------|--------|---------|----------|----------|--------|--------|-----------------------------------|-----------|
| | | Min | Max | Aver | | | Min | Max | Aver | | |
| Grass | 0.003 | 0.0003 | 0.0194 | 0.0100 | 0.0025 | 0.0042 | 0.0007 | 0.0023 | 0.0015 | 0.000647 | 0.001 |
| Forest | 0.003 | 0.0058 | 0.0172 | 0.0117 | 0.0025 | 0.0750 | 0.0005 | 0.0175 | 0.0090 | 0.0005 (conif) 0.00518 (decid) | 0.001 |
| Bare soil | 0.003 | 0.0003 | 0.0250 | 0.0125 | 0.0025 | 0.0039 | 0.0007 | 0.0023 | 0.0015 | 0.003009 | 0.001 |
| Seawater | 0.003 | 0.0002 | 0.0128 | 0.0064 | 0.0025 | 0.0017 | 0.0001 | 0.0010 | 0.0006 | 0.003009 | 0.001 |

Below we compare ranges of calculated values of dry deposition flux obtained by all participating models.

4.2.2. Input data

The following four sets of input data are proposed for modelling experiments with PCB-153.

Table 26. Input data for computation experiments with PCB-153 describing dry deposition of particulate phase

| N | Experiment 1 | Experiment 2 | Experiment 3 | Experiment 4 |
|---|--------------|--------------|--------------|--------------|
| Type of underlying surfaces | Grass | Forest | Bare soil | Seawater |
| Mean wind velocity, m/sec | 4 | 4 | 4 | 4 |
| Air concentration of particulate phase, ng/m ³ | 1 | 1 | 1 | 1 |

Output: calculated PCB dry deposition fluxes to grass, forest, bare soil, and seawater, ng/m²/h.

4.2.3. Comparison of the results

The results of calculation of particulate dry deposition flux for PCB-153 were presented by seven models: EVN-BETR and UK-MODEL, DEHM-POP, G-CIEMS, CliMoChem, SimpleBox, CAM/POPs and MSCE-POP. According to descriptions of dry deposition accepted in these models parameterizations of the flux are one and the same for all PCB congeners so that the results concern also congeners PCB-28 and PCB-180.

Three of the seven participated models (EVN-BETR and UK-MODEL, SimpleBox and G-CIEMS) do not distinguish different types of underlying surface in calculation of particulate dry deposition fluxes. For two models (DEHM-POP and MSCE-POP) range of calculated values depending on environmental parameters not included into the formulation of calculation experiment is presented.

The plot of calculation results for the particulate dry deposition flux to different type of underlying surface are presented in Fig. 8. Of note that mean deposition flux to forest (10.23 ng/m²/h) given in the plot for CliMoChem model was calculated for the sake of comparison as arithmetic mean of fluxes to coniferous and deciduous forest obtained by the model (presented in the plot as bars). The corresponding numerical values are given in Table 27.

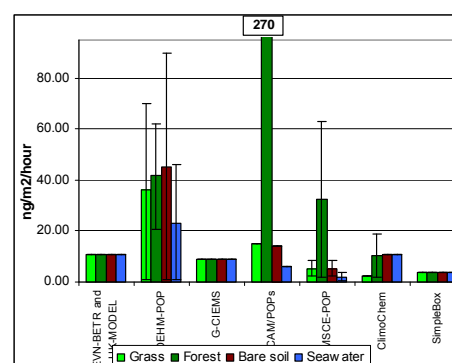


Fig. 8. Particulate dry deposition flux from the atmosphere to different types of underlying surface, ng/m²/h

Since there is large dispersion in the values of the deposition flux calculated by different models (See Table 27) we do not use statistical parameters for determining average levels of dry deposition flux but restrict ourselves by comparison of the values themselves. The additional reason for such an approach is that in two models from seven the range of calculated values of deposition flux are given and it is reasonable to include these ranges into consideration instead of comparison of mean values only. Short comments to the calculations made by participants can be found in Table 28.

Table 27. Particulate dry deposition flux from the atmosphere to different types of underlying surface, ng/m²/h

| Type of underlying surface | EVN-BETR and UK-MODEL | DEHM-POP | | | G-CIEMS | CAM/POPs | MSCE-POP | | | CliMoChem | SimpleBox |
|----------------------------|-----------------------|----------|-----|-------|---------|----------|----------|-------|-------|--------------------|-----------|
| | | Min | Max | Aver* | | | Min | Max | Aver* | | |
| Grass | 11 | 0.93 | 70 | 36 | 9 | 15 | 2.52 | 8.28 | 5.40 | 2.33 | 3.6 |
| Forest | 11 | 20.9 | 62 | 42 | 9 | 270 | 1.80 | 63.00 | 32.40 | 1.80** 18.65*** | 3.6 |
| Bare soil | 11 | 0.93 | 90 | 45 | 9 | 14 | 2.52 | 8.28 | 5.40 | 10.83 | 3.6 |
| Seawater | 11 | 0.76 | 46 | 23 | 9 | 6.1 | 0.36 | 3.60 | 1.98 | 10.83 | 3.6 |

* - calculated as arithmetic mean between minimum and maximum;

** - for coniferous forest;

*** - for deciduous forest.

Table 28. Comments

| Models | Comments |
|-----------------------|---|
| EVN-BETR and UK-MODEL | Independent on underlying surface type; Calculations are made for all considered PCB congeners together |
| SimpleBox | Independent on underlying surface type; SimpleBox works with one single deposition velocity (10-3 m/s) of aerosol particles, regardless character of aerosol or surface. Calculations are made for all considered PCB congeners together; No TSP used in model. Assumed that 'standard' specific aerosol surface of 0.00015 m ² /m ³ corresponds with TSP 30 mg/m ³ , so that Drydep flux = drydep velocity · TSP = 0.001 m/s · 30 mg/m ³ · 1000 µg/mg · 3600 s/hr = 108000 µg/m ² /hr |
| G-CIEMS | Independent on underlying surface type; Calculations are made for all considered PCB congeners together |
| CAM/POPs | Dependent on underlying surface type ; Calculations are made for all considered PCB congeners together |
| CliMoChem | Dependent on underlying surface type ; Calculations are made for all considered PCB congeners together; Flux = dry particle deposition velocity * air concentration of particulate phase |
| DEHM-POP | Dependent on underlying surface type ; Calculations are made for all considered PCB congeners together |
| MSCE-POP | Dependent on underlying surface type ; Calculations are made for all considered PCB congeners together |

Taking into account all calculated values, it is seen that the values of dry deposition flux for different models are mostly of the same order. The lowest value of the flux to grass is obtained by CliMoChem model. The flux to forest calculated by CAM/POPs model is essentially larger than that calculated by other models. The max/min value of fluxes to bare soil calculated by all participating models is within a factor of 13. Mean values of the flux to seawater calculated by MSCE-POP model are lower than values obtained by all other models. In general, the largest discrepancy of calculated fluxes to different types of underlying surface takes place for forest: maximum (CAM/POPs) and minimum (CliMoChem for coniferous forest) calculated values differ 150 times.

To evaluate the similarity between models we use correlation coefficients where appropriate (that is, between models where depositions to different types of underlying surface differ from one another). These correlation coefficients are presented in Table 29.

Table 29. Correlation coefficients

| | CAM/POPs | MSCE-POP | CliMoChem |
|----------|----------|----------|-----------|
| DEHM-POP | 0.40 | 0.47 | 0.01 |
| CAM/POPs | - | 1.00 | 0.25 |
| MSCE-POP | - | - | 0.21 |

The correlation coefficients between mean values of particulate dry deposition flux to different types of underlying surface calculated by DEHM-POP and MSCE-POP models and by DEHM-POP and CAM/POPs models are equal to 0.47 and 0.40, respectively. Correlation between CAM/POPs and MSCE-POP model is very high. Correlation between CliMoChem (taking into account the average value of the flux to forest) and the above three models is poor.

Values of average dry deposition flux for different models agree mostly within an order of magnitude. The type of underlying surface essentially affects deposition fluxes. For models distinguishing different types of underlying surface the best correlation is for CAM/POPs and MSCE-POP.

4.3. Wet deposition

4.3.1. Model approaches

All participating models use similar approach to the description of wet scavenging of POPs based on the calculation of separate washout for particulate and gaseous phases of a pollutant. Total dimensionless washout ratio W_T is determined by the Eq. (11):

$$W_T = W_G (1 - \phi) + W_P \phi, \quad (11)$$

where W_G is the washout ratio of the gas phase;
 W_P is the washout ratio of a substance associated with aerosol particles;
 ϕ is the substance fraction associated with aerosol particles.

Under such approach the concentration of the phase i (gaseous or particulate) in precipitation is expressed as

$$C_{p,i} = W_i \cdot C_{a,i}, \quad (12)$$

where $C_{p,i}$ - concentration of the phase i in precipitation;
 W_i - value of washout ratio for the phase i ;
 $C_{a,i}$ - concentration of the phase i in air.

For the description of gaseous phase scavenging with precipitation, the instantaneous equilibrium between the gaseous phase in the air and the dissolved phase in precipitation is assumed. For calculations of washout or scavenging ratio for gaseous phase, all the models use the inverse relation of dimensionless Henry's law constant taken in the form of temperature dependence.

For the description of particle bound phase scavenging with precipitation, the constant washout or scavenging ratio (W or Q , dimensionless) determined experimentally or estimated theoretically is used in MSCE-POP, EVN-BETR and UK-MODEL, DEHM-POP, G-CIEMS and CliMoChem models. The differences between model descriptions is mostly determined by the difference of washout or scavenging ratio values used for the calculation of particulate phase scavenging. Values of this parameter are given in Table 30.

Table 30. Scavenging ratio (washout ratio) for the particle phase of PCB-153

| Model | Description and comments | Numerical values | Reference |
|-----------------------|--|---------------------------------------|----------------------------------|
| G-CIEMS | Fixed scavenging ratio for atmospheric particles. Scavenging ratio is one and the same over all land and water surfaces. | 10,000-200,000, depending on the case | |
| EVN-BETR and UK-MODEL | Rain Scavenging ratio | 200000 | This study |
| | Snow Scavenging Ratio | 1000000 | |
| CliMoChem | scavenging ratio: the air volume scavenged by the falling rain is scavratio-times greater than the rainwater volume | 200000 | <i>Mackay and Paterson, 1991</i> |
| DEHM-POP | Λ_{bc} is the below cloud scavenging coefficient | 100000 | <i>Christensen, 1997</i> |
| | Λ_c is the in cloud scavenging coefficient | 700000 | |
| MSCE-POP | Washout ratio for the particle phase | 150000 | <i>Sweetman and Jones 2000</i> |

The scattering of scavenging ratio (or washout ratio) is rather large. For these models, its values vary from 10000 to 700000. The DEHM-POP model uses constant scavenging ratios but makes distinction between in-cloud and below-cloud scavenging. Besides in this model, description of wet deposition process is dependent on height of precipitation formation. The EVN-BETR and UK-MODEL use constant scavenging ratios for rain and snow scavenging separately.

To calculate the particulate wet deposition flux, CAM/POPs includes the value of scavenging rate (in s^{-1}) dependent on mean particle/drop collection efficiency and do not use the value of scavenging ratio. Besides, this model uses 12-bin structure of Sulphate aerosol for calculations of particulate phase scavenging. In CAM/POPs rain and snow scavenging are also considered separately. In SimpleBox model aerosol washout of a pollutant is determined with the help of constant value of aerosol collection efficiency, which varies greatly with the size of the particles and depends also on the chemical.

Below the results of model calculations of PCB-153 concentration in precipitation for different environmental conditions made by six models (EVN-BETR and UK-MODEL, G-CIEMS, CAM/POPs, SimpleBox, CliMoChem and MSCE-POP) are presented. As it will be seen, the variability of approaches to calculation of the scavenging ratio lead to essential differences in model calculations of concentrations in precipitation.

4.3.2. Input data

Six sets of input data are proposed for modelling experiments with PCB-153.

Table 31. Input data for computation experiments with PCB-153 describing wet deposition

| N | Experiment 1 | Experiment 2 | Experiment 3 | Experiment 4 | Experiment 5 | Experiment 6 |
|---|--------------|--------------|--------------|--------------|--------------|--------------|
| Precipitation intensity, mm/hour | 1 | 1 | 1 | 10 | 10 | 10 |
| Precipitation height, m | 1000 | 1000 | 1000 | 1000 | 1000 | 1000 |
| Average ambient temperature, °C | -1 | 3 | 15 | -1 | 3 | 15 |
| Air concentration, gaseous phase, pg/m ³ | 7 | 7.3 | 33.7 | 7 | 7.3 | 33.7 |
| Air concentration, particulate phase, pg/m ³ | 5.3 | 4.8 | 1.5 | 5.3 | 4.8 | 1.5 |

Output: calculated wet deposition fluxes, ng/m²/hour and total (dissolved+particulate) concentrations of PCB in precipitation, pg/l.

4.3.3. Comparison of the results

Numerical results of experiments on calculations of concentration in precipitation and wet deposition fluxes obtained by the participating models and their analysis are presented in this Section for PCB-153. The corresponding results for other substances can be found in Annexes D and E.

Analysis of the experiments. Similar to the case of gas/particle partitioning process, we use the following statistical parameters for each experiment:

- m is the average concentration in precipitation calculated by participating models;
- σ is the square deviation of results obtained by different models;

Since additional experiments on wet deposition (last three experiments) were made only by three participating models, statistical processing is performed for the calculation results of the first three experiments. It should be mentioned that results of Experiments 4, 5 and 6 calculated by G-CIEMS, MSCE-POP and SimpleBox show the same concentration in precipitation as in Experiments 1, 2, and 3, respectively. Fluxes between Experiments 1, 2, 3 and Experiments 4, 5, 6 differ ten times in accordance with the different values of precipitation intensity given (See Table 31). Calculated values of concentration in precipitation for PCB-153 together with m and σ are presented in Table 32. Comparison of absolute values of calculated wet deposition fluxes for PCB-153 and the above mentioned statistical parameters for each experiment are given in Table 33. Short comments to the calculations can be found in Table 34.

For the first two of the experiments, square deviation σ_φ between different model calculations of concentration in precipitation and wet deposition flux (see last column in Tables 32 and 33) do not exceed the averaged value of these parameters. In the third experiment square deviation to some extent overdraws the average value of both parameters. It corresponds to the fact that in the first two experiments calculated values of concentrations in precipitation vary within a factor of six whereas for the last experiment the difference between maximum and minimum values is equal to 14. The lowest values of this parameter is obtained by MSCE-POP model. Considering absolute values of wet deposition flux, it is seen that max/min ratio lies within an order of magnitude for the first two experiments and comes up to 36 times for the highest temperature. The highest values of wet deposition flux are calculated by CAM/POPs model, and the lowest ones – by CliMoChem model. Since for high temperatures the calculated fraction of gaseous phase of PCB-153 in the atmosphere is high enough (about 80% on the average, see the description of gas/particle partitioning), the maximum dispersion of calculated results between models take place for that temperature in which pollutant presents in the atmosphere mostly in the gaseous phase.

Table 32. Calculation results: total (dissolved + particulate) concentrations of PCB-153 in precipitation, pg/l

| No | T (°C) | EVN-BETR and UK model | G-CIEMS | CAM/POPs | MSCE-POP | CliMoChem | SimpleBox | m | σ |
|----|-------------|-----------------------------|---------|----------|----------|-----------|-----------|------|----------|
| 1 | -1 | 1870 | 1070 | 3042 | 808 | 2325 | 1094 | 1702 | 870 |
| 2 | 3 | 1510 | 967 | 2130 | 729 | 4424 | 984 | 1791 | 1384 |
| 3 | 15 | 1480 | 310 | 3262 | 237 | 1263 | 338 | 1148 | 1165 |

Table 33. Calculation results: wet deposition flux of PCB-153, ng/m²/hour

| No | T (°C) | EVN-BETR and UK model | G-CIEMS | CAM/POPs | MSCE-POP | CliMoChem | SimpleBox | m | σ |
|----|-------------|-----------------------------|---------|----------|----------|-----------|-----------|-------|----------|
| 1 | -1 | 1.870 | 1.070 | 3.042 | 0.808 | 0.313 | 1.094 | 1.366 | 0.964 |
| 2 | 3 | 1.510 | 0.967 | 2.130 | 0.729 | 0.283 | 0.984 | 1.100 | 0.643 |
| 3 | 15 | 1.480 | 0.310 | 3.262 | 0.237 | 0.091 | 0.338 | 0.953 | 1.237 |

Table 34. Comments

| Models | Physical-chemical data set | Comments |
|-----------------------|----------------------------|---|
| EVN-BETR and UK-MODEL | Own | Fugacity approach; $D_{air-surface} = Q \cdot \text{Surface Area} \cdot \text{Particles in air fraction} \cdot K_{QA} \cdot U_R \cdot Z_{air}$ In the case of deposition in vegetation, the percentage of rain interception due to vegetation is taken into account. U_R - rain rate = 8.84×10^{-5} m/h; |
| SimpleBox | "Reference" | Concentration in air adjusted by setting emission to air. Wet deposition flux ($\text{mol/m}^2/\text{s}$) = (GasWashout (m/s) + AerosolWashout (m/s)) \cdot CONC_{air} (mol/m^3) $\text{GasWashout} = \text{RAIN}_{rate}$ (m/s) \cdot FR_{gas} (-) / K_h (-) $\text{AerosolWashout} = \text{RAIN}_{rate}$ (m/s) \cdot (1- FR_{gas} (-)) \cdot COLLECT_{eff} (-) RAIN_{rate} = precipitation intensity from input set FR_{gas} = fraction of substance in gas phase = 1 - $\text{FR}_{aerosol}$ K_h = dimensionless Henry's Law Constant at ambient temperature = $K_h(25C) \cdot \exp((H^0_{vap} - H^0_{sol})/8.314) \cdot (1/298 - 1/T)$ H^0_{vap}, H^0_{sol} = Enthalpy of vaporization, dissolution in water = $\Delta U_a, \Delta U_w$ from reference data set COLLECT_{eff} = aerosol collection efficiency = $2 \cdot 10^5 \text{ m}^3(\text{air})/\text{m}^3(\text{rain})$ by default CONC_{air} = total PCB concentration in air (mol/m^3) |
| CAM/POPs | Own | Dependent on aerosol size distribution: a typical 12 size-bin structure of Sulphate Aerosol as additional input data in this experiment |
| CliMoChem | Own | surface fraction of grass, coniferous forest and deciduous forest of the vegetation area: 0.63; 0.17; 0.2 [Möller, 2002] fraction of rain falling on grass, coniferous forest and deciduous forest: 0.068, 0.35, 0.193 [Wania et al., 2001]; Wet gaseous deposition flux = $1/k_{AW}$ temperature dependent \cdot rainfall velocity \cdot air concentration gaseous phase Wet particle deposition flux = wet deposition velocity \cdot air concentration particulate phase (the rain fraction falling on vegetation and vegetation covered soil was considered when calculating the flux to these compartments) |
| MSCE-POP | Own | Equation (12); Washout ratio for the gaseous phase $W_g = 1/K'_H$ is calculated with the help of temperature dependent dimensionless Henry's law constant; washout ratio for particulate phase determined experimentally is used. |
| G-CIEMS | "Reference" | $F = R_{ain} \cdot C_{air}/H + (TSP/\rho) \cdot Q \cdot C_{particle}$, where F is total mass flux by this process, R_{ain} is rain rate, C_{air} is gaseous concentration of chemical, H is Henry's law constant, TSP is particulate concentration, ρ is density of particles, Q is scavenging ratio of particles, and $C_{particle}$ is volumetric chemical concentration in particles. |

Pairwise comparison of the models. Let us proceed with pairwise comparison of calculation results obtained by different models. Such comparison was made only for the values of concentrations in precipitation since the values of wet deposition fluxes are proportional to the concentrations practically in all models' results (except for CliMoChem). As in the case of gas/aerosol partitioning, the relation between calculated concentrations in precipitation c^1 and c^2 obtained by compared models for different environmental conditions (for first three experiments only) is described by the equation (9).

Below brief analysis of the correlation coefficient r_{12} of the compared models, regression coefficients α_{12} and β_{12} and residual square deviation σ^{res}_{12} is given.

Correlation coefficients for concentration in precipitation calculated by the models is presented in Table 35. The comparison of calculated values of concentrations in precipitation is also displayed in Fig. 9.

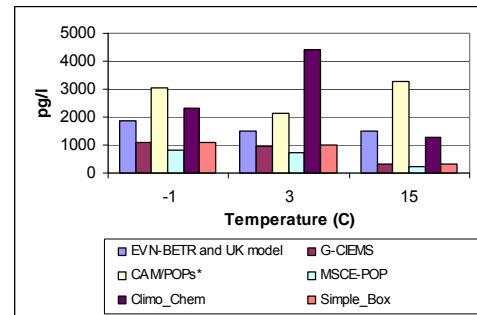


Fig. 9. Concentration in precipitation calculated by different models for different values of ambient temperatures, pg/l

Table 35. Correlation coefficients for concentration in precipitation

| | G-CIEMS | CAM/POPs | MSCE-POP | CliMoChem | SimpleBox |
|-----------------------|---------|----------|----------|-----------|-----------|
| EVN-BETR and UK model | 0.66 | 0.27 | 0.66 | -0.12 | 0.67 |
| G-CIEMS | - | -0.55 | 1.00 | 0.67 | 1.00 |
| CAM/POPs | - | - | -0.55 | -0.99 | -0.54 |
| MSCE-POP | - | - | - | 0.67 | 1.00 |
| CliMoChem | - | - | - | - | 0.66 |

Most close results are obtained by G-CIEMS and SimpleBox, by G-CIEMS and MSCE-POP models and by MSCE-POP and SimpleBox models (correlation coefficient in all cases is equal to 1.00). The values of concentrations in precipitation obtained by the rest three models are essentially higher. Temperature dependence of concentrations in precipitation obtained by EVN-BETR and UK-MODEL and G-CIEMS, by EVN-BETR and UK-MODEL and MSCE-POP are close but with some shift. Results of CliMoChem are also well correlated with G-CIEMS, MSCE-POP and SimpleBox models. No correlation is observed between CAM/POPs and all other models and between EVN-BETR and UK-MODEL and CliMoChem model.

Regression coefficients α_{12} and β_{12} (characterizing a non-random component of the regression relation) are presented in Table 36.

Table 36. Coefficients of regression dependence between the models (α / β) for concentration in precipitation

| | G-CIEMS | CAM/POPs | MSCE-POP | CliMoChem | SimpleBox |
|-------------------------------------|---------------|---------------|---------------|----------------|---------------|
| EVN-BETR and UK model | 1.250 / -1242 | 0.738 / 1616 | 0.941 / -933 | -0.871 / 4082 | 1.253 / -1225 |
| G-CIEMS | – | -0.801 / 3438 | 0.750 / 4 | 2.616 / 624 | 0.992 / 30 |
| CAM/POPs | – | – | -0.282 / 1385 | -2.649 / 10117 | -0.369 / 1844 |
| MSCE-POP | – | – | – | 3.475 / 616 | 1.322 / 24 |
| CliMoChem | – | – | – | – | 0.169 / 355 |
| Mean concentration in precipitation | 782 | 2811 | 591 | 2671 | 805 |

The differences between the models is determined by scaling coefficient α , which varies within a very wide range from –0.87 to 3.48. However, it is seen that this coefficients are very close to 1 for the most part of considered pairs of models (range from 0.8 to 1.3). Coefficients β are small enough compared with mean values of concentrations in precipitation for the most part of model pairs also (see last line in Table 36). The highest values of this parameter is obtained for the comparison of results of CAM/POPs and CliMoChem models. The lowest values of $|\beta|$ are observed for the results of the following pair of models: MSCE-POP and G-CIEMS. Taking into account both these regression coefficients' values, G-CIEMS and MSCE-POP, G-CIEMS and SimpleBox, and MSCE-POP and SimpleBox show the most close results in the experiments of wet deposition process.

Pairwise residual square deviation σ presented in Table 37 (characterizing the magnitude of random component ω_{12}) is allowed to reveal the reliability of comparative analysis given above.

Table 37. Residual square deviation, σ for concentration in precipitation

| | G-CIEMS | CAM/POPs | MSCE-POP | CliMoChem | SimpleBox |
|-----------------------|---------|----------|----------|-----------|-----------|
| EVN-BETR and UK model | 439 | 818 | 329 | 2259 | 432 |
| G-CIEMS | - | 709 | 1 | 1687 | 6 |
| CAM/POPs | - | - | 366 | 345 | 486 |
| MSCE-POP | - | - | - | 1692 | 4 |
| CliMoChem | - | - | - | - | 433 |

Values of σ vary within wide range from 1 to 2259. The highest values of the random component are characteristic of the comparisons between CliMoChem and EVN-BETR and UK-MODEL, between CliMoChem and G-CIEMS, between CliMoChem and MSCE-POP. The lowest values are obtained for G-CIEMS and MSCE-POP, G-CIEMS and SimpleBox, and MSCE-POP and SimpleBox.

The results of calculation experiments with PCB-28 and PCB-180 (see Annexes D and E) show also large dispersion between the absolute values of concentrations in precipitation and wet deposition fluxes calculated by different models. For PCB-28 there is a good correlation between results of

MSCE-POP, ClimoChem and SimpleBox (correlation coefficient is equal to 1). Calculated concentrations of PCB-180 in precipitation are also well correlated between these three models (correlation coefficient vary from 0.91 to 1) and between CAM/POPs and EVN-BETR and UK model (correlation coefficient is equal to 0.76).

For better understanding of model approaches to the description of wet deposition process, sensitivity study with respect to model descriptions and their parameterizations is reasonable. Special attention is to be paid for the description of wet scavenging of gaseous phase of POPs.

4.4. Gaseous exchange between atmosphere and soil

4.4.1. Model approaches

Within theory of intermedia diffusion, there exists a large diversity of approaches to the description of atmosphere/soil gaseous exchange. Here we present just very rough classification of similarities and distinctions of approaches used; details can be found in Table 41 and Annex C.

Gaseous exchange between atmosphere and soil is described by all participating models using resistance analogy but with some peculiarities. Processes of redistribution between different phases in soil are taken into account practically in all models (except for CAM/POPs, in which diffusion to low soil layers is considered). EVN-BETR and UK-MODEL implements fugacity approach for description of gaseous exchange between the atmosphere and soil compartments using three different diffusion transport velocity values for soil air-phase, soil water-phase and soil air boundary layer diffusion. In addition to dry gaseous deposition and revolatilization, in CliMoChem model process of bioturbation is also considered. This model takes also into consideration the percentage of vegetation coverage of soil. For the description of pollutant absorption from gas phase by soil and its volatilization from soil, SimpleBox uses two overall air-soil mass transfer coefficients (gas and soil-referenced) calculated considering processes of advection, diffusion and degradation. G-CIEMS also exploits two thin-film theory of intermedia diffusion (with restricted diffusion for soil-side mass transfer) using two mass transfer coefficients calculated with the help of molecular diffusivity and effective diffusion. For the calculation of atmosphere/soil flux, in MSCE-POP model three different resistances (turbulent air sublayer, laminar surface air sublayer and surface soil resistances) and effective diffusion coefficients are used. In addition, processes of vertical diffusion and advection with water flux and degradation of the pollutant in soil are considered in this model. The rest two models (DEHM-POP and CAM/POPs) evaluate air/soil exchange flux also using effective diffusion coefficients.

The difference between model approaches to the description of air/soil exchange is also in the number and thickness of considered soil layers. EVN-BETR and UK-MODEL, DEHM-POP, G-CIEMS, CliMoChem and SimpleBox model use one vertical layer in soil compartment which thickness varies from 5 to 15 cm. CAM/POPs uses three layers (5 cm altogether), and in MSCE-POP multi-layer approach (20 cm altogether) is used. Thus, all models consider different depth of soil compartment which varies from 5 to 20 cm.

Below the results of calculation experiments on air/soil exchange obtained by seven models are compared. Two models (G-CIEMS and MSCE-POP) presented two versions of calculations each (see below).

Since accumulation and clearance processes in soil require large time (decades), investigation of accumulation/clearance dynamics of POPs in soil is of importance. This investigation is exemplified by calculation experiments made by CAM/POPs, EVN-BETR and UK model, SimpleBox and MSCE-POP models in the end of this section.

4.4.2. Input data

Four sets of input data are proposed for modelling experiments with PCB-153.

Table 38. Input data for computation experiments with PCB-153 describing air/soil exchange

| N | Experiment 1 | Experiment 2 | Experiment 3 | Experiment 4 |
|---|--------------|--------------|--------------|--------------|
| Averaged ambient temperature, °C | 10 | 10.9 | 12.9 | 13.9 |
| Air concentration, gaseous phase, pg/m ³ | 0.8 | 5.5 | 6.8 | 2.8 |
| Bulk soil density, kg/m ³ | 1210 | 1080 | 890 | 1360 |
| Volumetric water content in soil, % | 20.6 | 41.4 | 26.4 | 16.8 |
| Volumetric air content in soil, % | 20 | 20 | 20 | 20 |
| Fraction of organic carbon in soil, % | 7.1 | 17.7 | 12.3 | 4 |

Output: calculation of PCB-153 soil concentrations, ng/g and gaseous fluxes from and to soil and/or net gaseous flux to soil, ng/m²/d.

4.4.3. Comparison of the results

Here we present numerical results of calculations of soil concentrations and net gaseous flux to soil obtained by the participating models and their analysis for PCB-153. The corresponding results for other substances can be found in Annexes D and E.

Similar to the cases of gas/particle partitioning and wet deposition, the analysis is performed into two stages. At the first stage we present an analysis of the calculated concentrations and net gaseous fluxes to soil and characterize the dispersion in these values in each experiment. At the second stage we analyze pairwise differences between participating models using the regression analysis. In addition the analysis of accumulation and clearance processes calculated by four models (CAM/POPs, EVN-BETR and UK model, SimpleBox and MSCE-POP) is performed.

Analysis of the experiments. Here we use the following statistical parameters for each experiment:

- m is the average soil concentrations for participating models;
- σ is the square deviation;

EVN-BETR and UK model, SimpleBox, and DEHM-POP models have made calculations on these experiments using steady-state approach. CliMoChem and CAM/POPs models have obtained results for equilibrium state. For G-CIEMS model two versions of calculations are presented: for steady-state (G-CIEMS 1) and at equilibrium using interim calculation parameters of the model (G-CIEMS 2). For MSCE-POP model two calculation versions are presented as well: steady-state calculations (MSCE-POP 1) and calculations from dynamic model (MSCE-POP 2). In the latter case calculations for 60 year period with air concentration roughly simulating the trend of PCB air concentrations and additional two years with constant air concentrations equal to that specified in the input data. In this case soil concentrations in the end of calculation period were used for comparison. Fig. 10 illustrates air concentration trend used in calculations for Experiment 1.

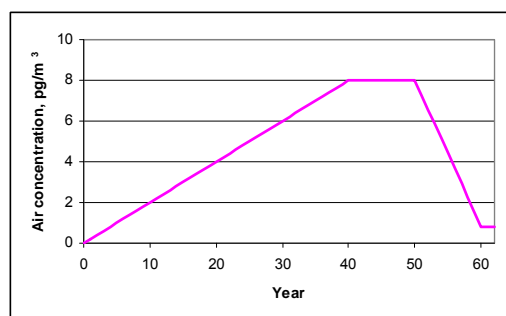


Fig. 10. Air concentration trend used for calculations for MSCE-POP model (MSCE-POP 2) for Experiment 1

Calculation results for PCB-153 soil concentrations together with m and σ are presented in Table 39. Net gaseous fluxes to soil of PCB-153 calculated by the models and statistical parameters used for its evaluation are given in Table 40. Table 41 contains appropriate comments to the calculations made by each model.

The analysis of the results submitted by participants shows that there is rather large differences between calculated both soil concentrations values and net gaseous flux values. It is confirmed by the fact that square deviation values exceed the average values in both cases. For calculated soil concentrations, results obtained by SimpleBox model are essentially lower than other ones. The comparison of calculated net gaseous fluxes shows that calculations of CAM/POPs differ from other model results in several order of magnitude. Below we analyze pairwise differences between participating models.

Table 39. Calculation results: soil concentrations of PCB-153 (ng/g) calculated by models and statistical parameters used for evaluation

| No | Air conc, pg/m ³ | EVN-BETR and UK-MODEL | DEHM-POP | G-CIEMS | | CAM/POPs | MSCE-POP | | CliMoChem | SimpleBox | m | σ |
|----|-----------------------------|-----------------------|----------|---------|--------|----------|----------|--------|-----------|-----------|------|----------|
| | | | | 1 | 2 | | 1 | 2 | | | | |
| 1 | 0.8 | 0.0020 | 0.4635 | 0.0071 | 0.0831 | 0.5719 | 0.0184 | 0.1047 | 0.0822 | 0.0001 | 0.15 | 0.21 |
| 2 | 5.5 | 0.0138 | 7.6195 | 0.0652 | 1.3089 | 8.6991 | 0.1454 | 0.8284 | 0.9207 | 0.0013 | 2.18 | 3.43 |
| 3 | 6.8 | 0.0177 | 6.3204 | 0.0652 | 0.9334 | 6.4227 | 0.2045 | 1.1675 | 1.0491 | 0.0015 | 1.80 | 2.63 |
| 4 | 2.8 | 0.0042 | 1.3987 | 0.0123 | 0.1140 | 0.7934 | 0.0518 | 0.2951 | 0.0962 | 0.0003 | 0.31 | 0.48 |

Table 40. Calculation results: net gaseous flux to soil, of PCB-153 (ng/m²/d) calculated by models and statistical parameters used for evaluation

| No | Air conc, pg/m ³ | EVN-BETR and UK-MODEL | G-CIEMS | | CAM/POPs | MSCE-POP | | CliMoChem | SimpleBox | m^* | σ^* |
|----|-----------------------------|-----------------------|----------|-----|----------|----------|-----------|-----------|-----------|----------|------------|
| | | | 1 | 2 | | 1 | 2 | | | | |
| 1 | 0.8 | 8.19E-04 | 3.71E-04 | 0.0 | 3.51E-13 | 2.98E-02 | 8.96E-03 | 0.0 | 7.16E-02 | 1.86E-02 | 2.83E-02 |
| 2 | 5.5 | 5.81E-03 | 1.66E-03 | 0.0 | 5.01E-12 | 2.29E-01 | 1.57E-01 | 0.0 | 4.95E-01 | 1.48E-01 | 1.95E-01 |
| 3 | 6.8 | 7.66E-03 | 2.56E-03 | 0.0 | 2.06E-12 | 2.54E-01 | 8.23E-02 | 0.0 | 6.08E-01 | 1.59E-01 | 2.40E-01 |
| 4 | 2.8 | 3.16E-03 | 1.49E-03 | 0.0 | 3.94E-13 | 7.66E-02 | -7.14E-02 | 0.0 | 2.48E-01 | 4.29E-02 | 1.11E-01 |

* - statistical parameters are calculated for models using steady-state and dynamic approaches.

Table 41. Comments

| Models | Physical-chemical data set | Numbers of layers in soil compartment | Thickness of considered soil layers, cm | Comments |
|----------------------|----------------------------|---------------------------------------|---|--|
| EVN-BETR and K-MODEL | Own | 1 | 10 | Steady-state Fugacity approach Redistribution between different phases in soil Individual/own dataset extremely close to the reference dataset; The flux was calculated as Gaseous flux = $D_{\text{air-soil}} \cdot \text{Fugacity (Pa)}$ $D_{\text{air-soil}} = (\text{Soil Area} \cdot Z_{\text{air}}) / [(Z_{\text{air}} / (\text{MTCas} \cdot Z_{\text{air}} + \text{MTCsw} \cdot Z_{\text{water}})) + 1 / \text{MTCsabl}]$ Soil Area = $8.36 \cdot 10^{12} \text{ m}^2$ MTCas : soil air-phase diffusion transport velocity = 0.04 m/h MTCsw : soil water-phase diffusion transport velocity = $1 \cdot 10^{-5} \text{ m/h}$ MTCsabl : soil air boundary layer transport velocity = 1 m/h |

| Models | Physical-chemical data set | Numbers of layers in soil compartment | Thickness of considered soil layers, cm | Comments | | |
|-----------------------|----------------------------|---------------------------------------|---|---|--|--|
| SimpleBox | Reference | 1 | 5 | <p>Steady-state</p> <p>Redistribution between different phases in soil and other processes;</p> <p>Concentration in air adjusted by setting emission to air.</p> <p>Transport between air and soil entirely by gas exchange. Other exchange mechanisms "switched off"; vegetation "switched off".</p> <p>Transport across air-soil interface calculated by two-resistance model. Air side: film diffusion; soil side: steady-state penetration into half-infinite porous medium with homogeneous degradation.</p> <p>Calculated concentration in soil is bulk, wet concentration in ng PCB per g of wet soil; concentration on dry weight basis added.</p> <p>Absorption from gas phase by soil (mol/m²/s) = FR_{gas} (-) · k_{as}(gas) (m/s) · CONC_{air} (mol/m³)</p> <p>Volatilization from soil (mol/m²/s) = k_{as}(soil) (m/s) · CONC_{soil} (mol/m³)</p> <p>k_{as}(gas) = overall gas-referenced air-soil mass transfer coefficient = k_{as.air} · k_{as.soil} / (k_{as.air} · (Kh/Ksw) + k_{as.soil})</p> <p>k_{as}(soil) = overall soil-referenced air-soil mass transfer coefficient = k_{as.air} · k_{as.soil} / (k_{as.air} + k_{as.soil}/(Kh/Ksw))</p> <p>k_{as.air} (m/s) = partial mass transfer coefficient for air-side of the air-soil interface = 1.05 · 10⁻³ m/s by default</p> <p>k_{as.soil} (m/s) = partial mass transfer coefficient for soil-side of the air-soil interface = Veff + Deff / PENdepth</p> <p>PENdepth (m) = penetration depth of PCB in soil = Veff + SQRT(Veff² + 4·KDEG·Deff) / 2·KDEG</p> <p>Veff (m/s) = effective (water+solids) downward advection of PCB into soil</p> <p>Deff (m²/s) = effective (gas+water+solid) diffusion coefficient of PCB in soil</p> <p>KDEG (s-1) = first-order degradation rate constant of PCB in soil</p> <p>Kh (-) = dimensionless air-water equilibrium constant</p> <p>Ksw (-) = dimensionless soil-water equilibrium constant</p> | | |
| CAM/POPs | Own | 3 | 5 (0-1, 1-3, 3-5) | <p>Equilibrium;</p> <p>Diffusion to low soil layers;</p> <p>Two transfer processes: the chemical transfer between deep soil layers and surface soil, and the exchange of the chemical vapour between the soil surface and the atmosphere.</p> | | |
| CiMoChem | Own | 1 | 10 | <p>Equilibrium;</p> <p>The concentrations are at steady-state;</p> <p>Redistribution between different phases in soil</p> <p>Dry gaseous deposition;</p> <p>Revolatilization;</p> <p>Bioturbation;</p> <p>Dry gaseous deposition flux=diffusion rate air to bare soil · (1-particle bound fraction in air) · concentration in air · air volume/(bare soil volume/ thickness of soil layer)</p> <p>Revolatilization flux = diffusion rate bare soil to air · steady state concentration in bare soil · bare soil volume/(bare soil volume/thickness of soil layer)</p> <p>(Model Geometry: box length: 100000 m; box width: 100000 m; fraction of bare soil area to total area: 0.0345)</p> | | |
| MSCE-POP ₁ | Own | 7 | 20 (0.1, 0.3, 0.6, 1, 2, 5, 11) | Steady-state; | <p>Redistribution between different phases in soil;</p> <p>Vertical diffusion and advection with water flux;</p> <p>Degradation of the pollutant.</p> <p>Gaseous exchange with the atmosphere parameterized using three-resistances approach (turbulent air sublayer, laminar surface air sublayer and surface soil resistances). Atmosphere/soil flux is calculated as follows:</p> $F_{dry}^g = \frac{C_a^g - C_s^g}{r_a + r_b + r_s},$ | |
| MSCE-POP ₂ | | | | Dynamic | | |
| G-CIEMS 1 | Reference | 1 | 5 | <p>Steady-state</p> <p>Redistribution between different phases in soil</p> <p>Diffusion to low soil layers and other processes</p> | | |
| G-CIEMS 2 | | 1 | 5 | <p>Equilibrium;</p> <p>Redistribution between different phases in soil</p> <p>Diffusion to low soil layers and other processes</p> | | |
| DEHM-POP | Own | 1 | 15 | <p>Steady-state</p> <p>Redistribution between different phases in soil</p> | | |

Pairwise comparison of the models. As in the case of gas/aerosol partitioning, the relation between calculated soil concentrations c^1 and c^2 obtained by compared models for different environmental conditions (including air concentration values) is expressed by the equation (9).

Below brief analysis of the correlation coefficient r_{12} of the compared models, regression coefficients α_{12} and β_{12} and residual square deviation σ_{12}^{res} is given.

In spite of the fact that numerical values of soil concentrations are highly different, the variations of the corresponding numerical values caused by change of environmental conditions between different experiments are similarly described by models. This can be seen from values of pairwise correlation coefficients varying in the range from 0.85 to almost 1 (Table 42).

Table 42. Correlation coefficients for soil concentrations

| | DEHM-POP | G-CIEMS 1 | G-CIEMS 2 | CAM/ POPs | MSCE-POP 1 | MSCE-POP 2 | CliMoChem | SimpleBox |
|-----------------------|----------|-----------|-----------|-----------|------------|------------|-----------|-----------|
| EVN-BETR and UK-MODEL | 0.93 | 0.98 | 0.89 | 0.90 | 1.00 | 1.00 | 0.99 | 0.99 |
| DEHM-POP | - | 0.99 | 0.99 | 0.99 | 0.90 | 0.90 | 0.96 | 0.97 |
| G-CIEMS 1 | - | - | 0.97 | 0.97 | 0.95 | 0.95 | 0.99 | 0.99 |
| G-CIEMS 2 | - | - | - | 1.00 | 0.85 | 0.85 | 0.94 | 0.93 |
| CAM/POPs | - | - | - | - | 0.86 | 0.86 | 0.95 | 0.94 |
| MSCE-POP 1 | - | - | - | - | - | 1.00 | 0.97 | 0.98 |
| MSCE-POP 2 | - | - | - | - | - | - | 0.97 | 0.98 |
| CliMoChem | - | - | - | - | - | - | - | 1.00 |

For net gaseous flux (Table 43), the best correlation is observed between SimpleBox and EVN-BETR and UK-MODEL, between MSCE-POP 1 and SimpleBox, between EVN-BETR and UK-MODEL and MSCE-POP 1, and between MSCE-POP 2 and CAM/POPs models. It is also seen that results of G-CIEMS 1 are well correlated with data of EVN-BETR and UK-MODEL, MSCE-POP 1, and SimpleBox. There is no correlation between G-CIEMS 1 and two models: MSCE-POP 2 and CAM/POPs.

Table 43. Correlation coefficients for net gaseous flux to soil of PCB-153*

| | G-CIEMS 1 | CAM/POPs | MSCE-POP 1 | MSCE-POP 2 | SimpleBox |
|-----------------------|-----------|----------|------------|------------|-----------|
| EVN-BETR and UK-MODEL | 0.96 | 0.63 | 0.97 | 0.63 | 1.00 |
| G-CIEMS 1 | - | 0.41 | 0.87 | 0.38 | 0.94 |
| CAM/POPs | - | - | 0.77 | 0.91 | 0.68 |
| MSCE-POP 1 | - | - | - | 0.79 | 0.99 |
| MSCE-POP 2 | - | - | - | - | 0.67 |

* - statistical parameters are calculated for models using steady-state and dynamic approaches.

Table 44 contains the values of regression coefficients α and β calculated for all pairs of models in terms of soil concentrations. It is seen that coefficients β are small enough compared with mean values of soil concentrations for all pairs of models (see last line in Table 44) and the differences between the models are explained mainly by scaling coefficient α . The latter varies in a very wide range (0.0002 - 486.145). The smallest value (0.0002) is characteristic for regression between DEHM-POP and SimpleBox and for regression between CAM/POPs and SimpleBox. The highest value (486.145) is obtained for regression between EVN-BETR and UK-MODEL and CAM/POPs. Pairs of models: G-CIEMS 2 and CliMoChem, MSCE-POP 2 and CliMoChem, and DEHM-POP and CAM/POPs show close results (regression coefficients α are close enough to 1).

Table 45 contains the values of regression coefficients α and β calculated for all pairs of models in terms of net gaseous fluxes to soil.

Table 44. Coefficients of regression dependence between the models (α / β) for soil concentrations

| | DEHM-POP | G-CIEMS 1 | G-CIEMS 2 | CAM/POPs | MSCE-POP 1 | MSCE-POP 2 | CliMoChem | SimpleBox |
|-------------------------|------------------|----------------|-----------------|-----------------------|-----------------|-----------------|-----------------------|------------------|
| EVN-BETR and UK-MODEL | 439.672 / -0.189 | 4.153 / -0.002 | 71.840 / -0.067 | 486.145 / -0.455 | 11.284 / -0.001 | 64.380 / -0.007 | 68.067 / -0.104 | 0.091 / -0.00005 |
| DEHM-POP | – | 0.009 / 0.002 | 0.170 / -0.063 | 1.142 / -0.391 | 0.022 / 0.019 | 0.124 / 0.108 | 0.141 / -0.021 | 0.0002 / 0.0001 |
| G-CIEMS 1 | – | – | 18.380 / -0.079 | 123.634 / -0.512 | 2.539 / 0.010 | 14.479 / 0.056 | 16.085 / -0.066 | 0.021 / 0.00001 |
| G-CIEMS 2 | – | – | – | 6.685 / 0.045 | 0.119 / 0.033 | 0.676 / 0.186 | 0.799 / 0.050 | 0.001 / 0.0002 |
| CAM/POPs | – | – | – | – | 0.018 / 0.031 | 0.103 / 0.176 | 0.121 / 0.040 | 0.0002 / 0.0002 |
| MSCE-POP 1 | – | – | – | – | – | 5.706 / -0.0004 | 5.912 / -0.084 | 0.008 / -0.00003 |
| MSCE-POP 2 | – | – | – | – | – | – | 1.036 / -0.083 | 0.001 / -0.00003 |
| CliMoChem | – | – | – | – | – | – | – | 0.001 / 0.0001 |
| Mean soil concentration | 3.9505 | 0.0375 | 0.6099 | 4.1218 | 0.1050 | 0.5989 | 0.5371 | 0.0008 |

Table 45. Coefficients of regression dependence between the models (α / β) for net gaseous flux to soil of PCB-153*

| | G-CIEMS 1 | CAM/POPs | MSCE-POP 1 | MSCE-POP 2 | SimpleBox |
|-----------------------|-----------------|----------------------|-----------------|------------------|-----------------|
| EVN-BETR and UK-MODEL | 0.29 / 2.68E-04 | 4.57E-10 / -3.97E-14 | 35.99 / -0.01 | 20.46 / -0.05 | 80.46 / 0.005 |
| G-CIEMS 1 | – | 1.01E-09 / 4.26E-13 | 107.21 / -0.02 | 41.17 / -0.02 | 252.85 / -0.03 |
| CAM/POPs | – | – | 3.90E+10 / 0.07 | 4.07E+10 / -0.04 | 7.50E+10 / 0.21 |
| MSCE-POP 1 | – | – | – | 0.69 / -0.06 | 2.15 / 0.04 |
| MSCE-POP 2 | – | – | – | – | 1.67 / 0.28 |

* - statistical parameters are calculated for models using steady-state and dynamic approaches.

The difference between the participating models in values of scaling coefficient α is even more essential for net gaseous fluxes than for concentrations. The best α value (that means the most close to 1 among others) is equal to 1.7 and is characteristic for regression between MSCE-POP 2 and SimpleBox models.

To assess the reliability of comparative analysis given above calculations of pairwise residual square deviation σ were done (Table 46 and 47).

Table 46. Residual square deviation (σ) for soil concentrations

| | DEHM-POP | G-CIEMS 1 | G-CIEMS 2 | CAM/POPs | MSCE-POP 1 | MSCE-POP 2 | CliMoChem | SimpleBox |
|-----------------------|----------|-----------|-----------|----------|------------|------------|-----------|-----------|
| EVN-BETR and UK-MODEL | 2.182 | 0.012 | 0.486 | 3.098 | 0.012 | 0.072 | 0.142 | 0.0001 |
| DEHM-POP | – | 0.009 | 0.142 | 0.820 | 0.063 | 0.361 | 0.240 | 0.0003 |
| G-CIEMS 1 | – | – | 0.269 | 1.633 | 0.044 | 0.254 | 0.104 | 0.0001 |
| G-CIEMS 2 | – | – | – | 0.171 | 0.078 | 0.449 | 0.313 | 0.0004 |
| CAM/POPs | – | – | – | – | 0.075 | 0.432 | 0.293 | 0.0004 |
| MSCE-POP 1 | – | – | – | – | – | 0.001 | 0.214 | 0.0002 |
| MSCE-POP 2 | – | – | – | – | – | – | 0.215 | 0.0002 |
| CliMoChem | – | – | – | – | – | – | – | 0.0001 |

Table 47. Residual square deviation (σ) for net gaseous flux to soil of PCB-153

| | DEHM-POP | G-CIEMS 1 | G-CIEMS 2 | CAM/POPs | SimpleBox |
|-----------------------|----------|-----------|-----------|----------|-----------|
| EVN-BETR and UK-MODEL | 4.46E-04 | 2.95E-12 | 0.04 | 0.13 | 0.03 |
| G-CIEMS 1 | – | 3.45E-12 | 0.09 | 0.16 | 0.14 |
| CAM/POPs | – | – | 0.12 | 0.07 | 0.31 |
| MSCE-POP 1 | – | – | – | 0.10 | 0.07 |
| MSCE-POP 2 | – | – | – | – | 0.31 |

It is seen that the values of residual square deviation for soil concentrations lie within the interval 0.0001 - 2.182. The highest value is obtained for the regression between EVN-BETR and UK-MODEL and DEHM-POP models. For models' results of calculated net gaseous flux, $-\sigma$ ranges from $3.45E-12$ to 0.31.

In the cases of PCB-28 and PCB-180 results (Annexes D and E), there is also a large difference in absolute values both for calculated soil concentrations and net gaseous fluxes. Correlation coefficients for soil concentration of PCB-28 vary in the range from 0.93 to almost 1 between all pairs of models; for net gaseous flux good correlation is observed between SimpleBox and EVN-BETR and UK-MODEL models. Results on soil concentrations and net gaseous fluxes of PCB-180 are well correlated for all model pairs (correlation coefficients range from 0.87 to 1.00 and from 0.85 to 1.00, respectively).

Accumulation/clearance dynamics of POPs in soil. The aim of this subsection is to analyze model descriptions of long-term processes of accumulation of selected PCB congeners in soil and clearance of soil compartment at emission termination. To do this, modelling of air/soil exchange with constant air concentration for a sufficiently long period were carried out by CAM/POPs, MSCE-POP, EVN-BETR and UK model, and SimpleBox models using first set of data presented above. In CliMoChem trend was not calculated as it takes way longer than 120 months to reach steady state in this model.

The period under simulation was split into two periods. During the first period (accumulation) air concentrations are kept at the level defined in the corresponding input data set and initial data are assumed to be zero. Soil concentrations obtained in the end of the first period were used as initial data for the second period (clearance). During this period air concentrations are set to zero.

Figs. 11, 12, 13 and 14 show the results of the experiment obtained by CAM/POPs, MSCE-POP, EVN-BETR and UK model, and SimpleBox models, respectively.

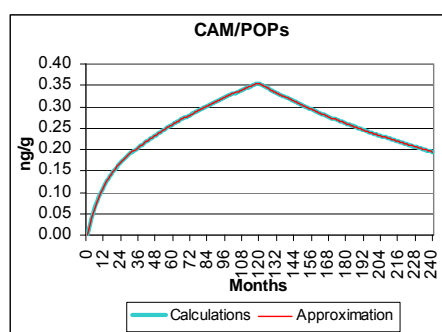


Fig. 11. Long-term trends of accumulation and clearance obtained by CAM/POPs model

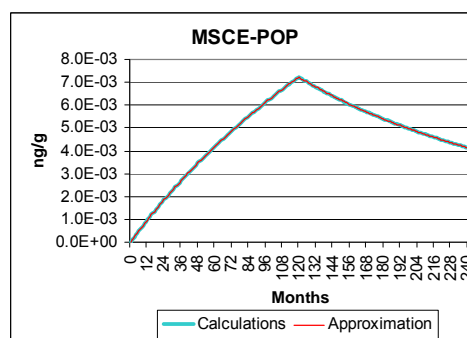


Fig. 12. Long-term trends of accumulation and clearance obtained by MSCE-POP model

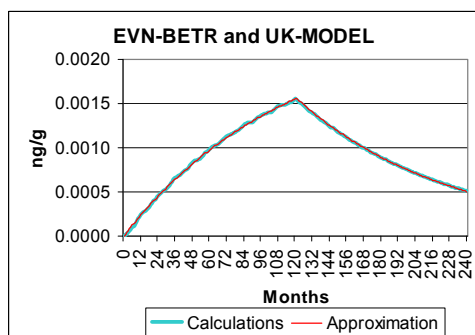


Fig. 13. Long-term trends of accumulation and clearance obtained by EVN-BETR and UK-MODEL model

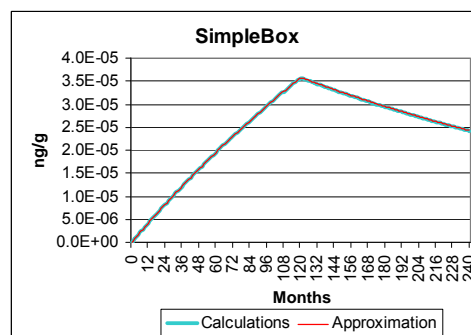


Fig. 14. Long-term trends of accumulation and clearance obtained by SimpleBox model

Together with calculated soil concentrations bi-exponential approximation of accumulation and clearance is also shown in the plots. At the accumulation stage this approximation has the form:

$$C_{soil} = C_1(1 - e^{-\lambda_1 t}) + C_2(1 - e^{-\lambda_2 t}), \quad \lambda_1 > \lambda_2$$

where t is the time, months;

λ_1 and λ_2 are exchange rate constants, month⁻¹;

C_1 and C_2 are constants determining shares of concentrations involved in fast/slow process.

Such form of the dependence of soil concentrations on time is characteristic of a process with two characteristic times of exchange: fast exchange characteristic time $T_{1/2}^1 = \ln(2)/\lambda_1$ and slow exchange characteristic time $T_{1/2}^2 = \ln(2)/\lambda_2$. At the clearance stage time dependence of soil concentrations has the form:

$$C_{soil} = C_1 e^{-\lambda_1 t} + C_2 e^{-\lambda_2 t}, \quad \lambda_1 > \lambda_2$$

where t is the time (months);

λ_1 and λ_2 are exchange rate constants, month⁻¹;

C_1 and C_2 are constants determining shares of concentrations involved in fast/slow process.

with the same interpretation of λ_1 and λ_2 .

The values of parameters obtained by the approximation with corresponding characteristic times are shown in Table 48. As seen from the plots in Figs. 11–14, bi-exponential approximation well explains the trends of soil concentrations both at accumulation and clearance phases.

Table 48. Parameters of multi-exponential approximation

| | | EVN-BETR and UK model | | CAM/POPs | | SimpleBox | | MSCE-POP | |
|--------------------|-------------------|-----------------------|----------|----------|----------|-----------|----------|----------|----------|
| | | Slow | Fast | Slow | Fast | Slow | Fast | Slow | Fast |
| Accumulation phase | λ | 8.70E-03 | 8.70E-03 | 5.90E-03 | 9.75E-02 | 3.21E-03 | 3.21E-03 | 2.84E-03 | 1.73E-02 |
| | $T_{1/2}$, years | 6.64 | 6.64 | 9.79 | 0.59 | 18.00 | 17.99 | 20.37 | 3.35 |
| Clearance phase | λ | 9.30E-03 | 9.61E-03 | 4.03E-03 | 1.00E-02 | 3.25E-03 | 3.25E-03 | 3.27E-03 | 1.00E-02 |
| | $T_{1/2}$, years | 6.21 | 6.01 | 14.32 | 5.78 | 17.79 | 17.78 | 17.68 | 5.78 |

The analysis of calculated characteristic times for all considered models shows that these models can be divided into two groups. First group (EVN-BETR and UK model and SimpleBox) are characterized by very close characteristic times for fast and slow exponentials. In essence, these models realize mono-exponential trends of POP soil contamination. Also, for these two models characteristic times of accumulation and clearance are very close to each other. The predicted characteristic times differ three times between these two models (6.6 against 18 years).

Another two models (CAM/POPs and MSCE-POP) demonstrate the presence of both fast and slow exponents in soil concentration trends at accumulation and clearance phases. The characteristic times for slow exponential vary between 10 and 20 years depending on model. The characteristic times for fast exponential (fast exchange) vary between 0.6 and 5.8 years.

The results obtained for PCB-28 and PCB-180 are similar and can be found in Annexes D and E.

Thus, there is much similarity in the description of processes of POP accumulation and clearance processes. However, the parameterization of these processes are subject to further clarification.

4.5. Gaseous exchange between atmosphere and water

4.5.1. Model approaches

Similar to the previous section, in the participating models the description of atmosphere/water gaseous exchange are based on two-film model of intermedia diffusion. Detailed descriptions of this process used in the models can be found in Table 53 and Annex C.

There also exists a large diversity of approaches for the evaluation of transfer velocities at air/water interface. In CliMoChem model diffusion rates - air to water and water to air are calculated using air-over-water and in-water transfer velocities taken from [Mackay and Paterson, 1991] and then dry gaseous deposition and revolatilization fluxes are evaluated using these velocities. For the description of air-water diffusion with the help of fugacity approach, EVN-BETR and UK-MODEL also use constant values of air-water transport velocities. In G-CIEMS air-side and water-side mass transfer coefficient are calculated as the ratio of molecular diffusivity and diffusion path length for air and water. Other participating models use mass transfer velocities, which are dependent on the values of wind speed. Thus, in DEHM-POP model exchange velocities dependent on the wind speed are calculated on the basis of the two-film layer resistance method. In CAM/POPs model the results by [Mackay et al., 1983; Schwarzenbach et al., 1993] are used for calculations of mass transfer velocities. In SimpleBox model absorption from gas phase by water and volatilization from water are calculated with the help of mass transfer coefficients also dependent on the wind speed value. In MSCE-POP model transfer velocities are also dependent on the values of wind speed. In addition, foaming process and expansion of sea area due to wave disturbance are taken into account in this model (see [Strukov, 2001]).

Of note that, EVN-BETR and UK-MODEL, SimpleBox and CAM/POPs models consider gaseous exchange between the atmosphere and freshwater. Other participating models take in consideration seawater compartment. Suspended particulate matter in water compartment is considered in SimpleBox and CliMoChem models. For all models, depth of considered water layers varies in very wide range (3-4600 metres).

Below the results of calculation experiments on air/soil exchange obtained by seven models are compared.

4.5.2. Input data

Four sets of input data are proposed for modelling experiments with PCB-153.

Table 49. Input data for calculation experiments with PCB-153 describing air/water exchange

| N | Experiment 1 | Experiment 2 | Experiment 3 | Experiment 4 |
|---|--------------|--------------|--------------|--------------|
| Average ambient temperature, °C | 10 | 13.9 | 0 | 25 |
| Air concentration, gaseous phase, pg/m ³ | 14.3 | 3.8 | 2.5 | 23 |
| Mean wind velocity, m/sec | 5 | 3.25 | 6 | 2 |

Output: calculation of PCB-153 water concentrations, pg/l and gaseous fluxes from and to water and/or net gaseous flux to water, ng/m²/d;

4.5.3. Comparison of the results

Numerical results of calculations of water concentrations and gaseous flux to water obtained by participating models and their analysis are presented for PCB-153 in this Subsection. The corresponding results for PCB-28 and PCB-180 can be found in Annexes D and E.

The analysis is also performed into two stages. At the first stage we present an analysis of the calculated concentrations and gaseous fluxes to water and characterize the dispersion in these values in each experiment. At the second stage we analyze pairwise differences between participating models using the regression analysis.

Analysis of the experiments. For evaluation of results obtained by the participating models, we use the following statistical parameters for each experiment:

- m is the average water concentrations or average gaseous flux to water for participating models;
- σ is the square deviation;

Calculated values of water concentrations for PCB-153 together with m and σ are presented in Table 50. Comparison of absolute values of calculated gaseous flux to water for PCB-153 and the above mentioned statistical parameters for each experiment are given in Table 52. Short comments to the calculations made by participants can be found in Table 53. CAM/POPs model has made calculations on these experiments using dynamic approach. Other participating models used steady-state approach.

If compare the absolute values of calculated water concentrations presented in Table 50, it is seen that there is a large dispersion of water concentration values calculated by the participating models. Results of CliMoChem model differ from other models' results more than order of magnitude. This difference leads to significant bias of averaged values of water concentrations to the maximum values obtained by this model. For each experiment, square deviation σ_ϕ between different model calculations (see last column in Table 50) substantially exceed the averaged value of water concentrations.

Table 50. Calculation results: water concentrations of PCB-153 (pg/l) calculated by all participating models and statistical parameters used for evaluation

| N | EVN-BETR and UK-MODEL | CAM/POPs | DEHM-POP | CliMoChem | G-CIEMS | SimpleBox | MSCE-POP | m | σ |
|---|-----------------------|----------|----------|-----------|---------|-----------|----------|------|----------|
| 1 | 5.56 | 8.40 | 7.10 | 8497.85 | 30.15 | 20.30 | 7.90 | 1225 | 3207 |
| 2 | 0.98 | 24.00 | 1.25 | 1514.86 | 7.44 | 3.09 | 1.44 | 222 | 570 |
| 3 | 3.11 | 4.8 | 3.74 | 4103.52 | 5.92 | 5.88 | 3.76 | 590 | 1549 |
| 4 | 2.10 | 3.0 | 2.51 | 2995.49 | 32.47 | 6.14 | 3.09 | 435 | 1129 |

In Table 51 similar statistical evaluation is presented for a group of participating models, which obtained close results of water concentration values of PCB-153. Differences in their calculated absolute values are within an order of magnitude. At that it can be seen that m values become more indicative for their comparison. In two cases (experiments 1 and 3), square deviation σ_ϕ between different results (see last column in Table 51) do not exceed the averaged values of water concentration. For other experiments, the deviations are more remarkable.

Table 51. Calculation results: statistical evaluation of PCB-153 water concentrations (pg/l) calculated by models having results of the same order

| N | EVN-BETR and UK-MODEL | CAM/POPs | DEHM-POP | G-CIEMS | SimpleBox | MSCE-POP | m | σ |
|---|-----------------------|----------|----------|---------|-----------|----------|------|----------|
| 1 | 5.56 | 8.40 | 7.10 | 30.15 | 20.30 | 7.90 | 13.2 | 9.8 |
| 2 | 0.98 | 24.00 | 1.25 | 7.44 | 3.09 | 1.44 | 6.4 | 9.0 |
| 3 | 3.11 | 4.8 | 3.74 | 5.92 | 5.88 | 3.76 | 4.5 | 1.2 |
| 4 | 2.10 | 3.0 | 2.51 | 32.47 | 6.14 | 3.09 | 8.2 | 12.0 |

Considering results of calculations of gaseous flux to water (See Table 52), we can observe much better agreement for this parameter than for water concentration results between all models calculations. Square deviation σ_{φ} presented in last column of Table 52 do not exceed the averaged value of fluxes. It testifies that all models give rather close results on calculation of gaseous fluxes to water in terms of absolute values.

Table 52. Calculation results: Gaseous flux to water of PCB-153 calculated by all participating models and statistical parameters used for evaluation, ng/m²/d

| N | EVN-BETR and UK-MODEL | CAM/POPs | CliMoChem | G-CIEMS | SimpleBox | MSCE-POP | <i>m</i> | σ |
|---|-----------------------|----------|-----------|---------|-----------|----------|----------|----------|
| 1 | 2.60 | 2.08 | 0.86 | 1.02 | 4.59 | 2.25 | 2.2 | 1.3 |
| 2 | 0.56 | 0.62 | 0.21 | 0.25 | 0.74 | 0.54 | 0.5 | 0.2 |
| 3 | 0.66 | 0.40 | 0.17 | 0.20 | 1.12 | 0.42 | 0.5 | 0.4 |
| 4 | 1.71 | 1.49 | 0.86 | 1.10 | 1.95 | 2.24 | 1.6 | 0.5 |

Table 53. Comments

| Models | Physical-chemical data set | Depth of considered water layer, metres | Comments |
|-----------------------|----------------------------|---|---|
| EVN-BETR and UK-MODEL | Own | 20 | Steady-state approach; Freshwater; Individual/own dataset extremely close to the reference dataset; The flux was calculated as Gaseous flux = $D_{\text{air-water}} \cdot \text{Fugacity (Pa)}$ $D_{\text{air-water}} = \text{Water Area} / [(1 / (\text{MTCasa} \cdot Z_{\text{air}})) + (1 / (\text{MTCass} \cdot 0.8 \cdot Z_{\text{water}}))]$ Fresh water area = $1.7 \cdot 10^{11} \text{ m}^2$ MTCasa : Air side air-water transport velocity = 30 m/h MTCass : water side air-water transport velocity = 0.03 m/h |
| SimpleBox | Reference | 3 | Steady-state approach; Freshwater; Inclusion of suspended particulate matter; Transport between air and water entirely by gas exchange. Other exchange mechanisms "switched off". Concentration in air adjusted by setting emission to air. Transport across air-water interface calculated by classical double film diffusion model. Absorption from gas phase by water (mol/m ² /s) = $\text{FR}_{\text{gas}} (-) \cdot k_{\text{aw}}(\text{gas}) (\text{m/s}) \cdot \text{CONC}_{\text{air}} (\text{mol/m}^3)$ Volatilization from water (mol/m ² /s) = $\text{FR}_{\text{water}} (-) \cdot k_{\text{aw}}(\text{water}) (\text{m/s}) \cdot \text{CONC}_{\text{water}} (\text{mol/m}^3)$ $k_{\text{aw}}(\text{gas})$ = overall gas-referenced air-water mass transfer coefficient = $k_{\text{aw.air}} \cdot k_{\text{aw.water}} / (k_{\text{aw.air}} \cdot K_{\text{h}} + k_{\text{aw.water}})$ $k_{\text{aw}}(\text{soil})$ = overall water-referenced air-water mass transfer coefficient = $k_{\text{aw.air}} \cdot k_{\text{aw.water}} / (k_{\text{aw.air}} + k_{\text{aw.water}}/K_{\text{h}})$ K_{h} = dimensionless air-water equilibrium constant $k_{\text{aw.air}}$ = partial mass transfer coefficient for air-side of the air-water interface (m/s) = $0.01 \cdot (0.3 + 0.2 \cdot \text{WINDspeed}) \cdot (0.018/\text{Molweight})^{(0.67 \cdot 0.5)}$ $k_{\text{aw.water}}$ = partial mass transfer coefficient for water-side of the air-water interface (m/s) = $0.01 \cdot (0.0004 + 0.00004 \cdot \text{WINDspeed}^2) \cdot (0.032/\text{Molweight})^{(0.5 \cdot 0.5)}$ WINDspeed = mean wind velocity from input set Molweight = molecular weight PCB-congener |
| CAM/POPs | Own | Surface water | Dynamic approach; Freshwater |
| CliMoChem | Own | 200 | Steady-state approach; Seawater; Inclusion of suspended particulate matter; Only dry gaseous deposition, revolatilization and degradation in water were considered (Model Geometry: box length: 100000 m; box width: 100000 m; fraction of water area to total area: 0.7162) Dry gaseous deposition flux=diffusion rate air to water* concentration in air*volume air/(water volume*depth of water layer) Revolatilization flux = (diffusion rate water to air+degradation rate) * steady state concentration in water * water volume/(water volume/depth of water layer) |

| Models | Physical-chemical data set | Depth of considered water layer, metres | Comments |
|----------|----------------------------|---|---|
| MSCE-POP | Own | 4600 (15 layers) | Steady-state approach; Seawater; POP flux through the sea surface: $F_z _{z=0} = \alpha_1(c_{ga} / K_{HR}(T) - c_d)((1 - \alpha_2)D_\mu / \delta + \alpha_2 K_{HR} h_f)$ $D_\mu = 5.14 \cdot 10^{-10}$ - molecular diffusion coefficient in water, m ² /s; $\delta_0 = 4 \cdot 10^{-5}$ - surface molecular layer depth at zero wind speed, m; $h_f = 8 \cdot 10^{-3}$ - foam settling rate on the sea surface, m/s; α_1 - coefficient of surface sea area expansion due to wave disturbance; α_2 - coefficient describes the relative sea surface area covered with foam at strong wind; α_1 and α_2 are dependent on wind speed absolute value near the surface; |
| G-CIEMS | Reference | 20 | Steady-state approach; Seawater |
| DEHM-POP | Own | 75 | Steady-state approach; Seawater |

Pairwise comparison of model results. The analysis of pairwise differences between calculation results obtained by all models is performed with the help of regression equation (9). Below brief analysis of the correlation coefficient r_{12} of the compared models, regression coefficients α_{12} and β_{12} and residual square deviation σ_{12}^{res} is given.

Pairwise correlation coefficients for water concentrations calculated by all participating models are presented in Table 54. It is seen that their values varies in the very wide range from -0.50 to almost 1. At that, there is no correlation between CAM/POPs and all other models. Results of G-CIEMS model are poor correlated with other models also. However, in spite of the fact that absolute values of water concentrations of EVN-BETR and UK-MODEL, DEHM-POP, CliMoChem, SimpleBox and MSCE-POP differ from each other substantially, the variations of the corresponding numerical values caused by change of environmental conditions between different experiments are similarly described by them. Correlation coefficient for these models is very close to 1.

Table 54. Correlation coefficients for water concentrations

| | CAM/POPs | DEHM-POP | CliMoChem | G-CIEMS | SimpleBox | MSCE-POP |
|-----------------------|----------|----------|-----------|---------|-----------|----------|
| EVN-BETR and UK-MODEL | -0.48 | 1.00 | 0.99 | 0.46 | 0.95 | 0.99 |
| CAM/POPs | - | -0.44 | -0.41 | -0.50 | -0.29 | -0.44 |
| DEHM-POP | - | - | 1.00 | 0.46 | 0.96 | 0.99 |
| CliMoChem | - | - | - | 0.50 | 0.98 | 1.00 |
| G-CIEMS | - | - | - | - | 0.59 | 0.54 |
| SimpleBox | - | - | - | - | - | 0.98 |

Correlation coefficients for values of gaseous flux to water calculated by all models range from 0.73 to 1 (See Table 55). It is evident that results of all participating models well correlated with each other in describing air–water gaseous exchange fluxes. Most close results are obtained between EVN-BETR and UK-MODEL and CAM/POPs, between G-CIEMS and CliMoChem, between G-CIEMS and MSCE-POP models and between MSCE-POP and CliMoChem models (correlation coefficient is all cases is equal to 1.00).

Table 55. Correlation coefficients for gaseous flux to water

| | CAM/POPs | CliMoChem | G-CIEMS | SimpleBox | MSCE-POP |
|-----------------------|----------|-----------|---------|-----------|----------|
| EVN-BETR and UK-MODEL | 0.99 | 0.92 | 0.90 | 0.96 | 0.92 |
| CAM/POPs | - | 0.95 | 0.93 | 0.92 | 0.95 |
| CliMoChem | - | - | 1.00 | 0.77 | 1.00 |
| G-CIEMS | - | - | - | 0.73 | 1.00 |
| SimpleBox | - | - | - | - | 0.78 |

For further evaluation of closeness of calculated results obtained by models, regression coefficients α_{12} and β_{12} and the residual square deviation, σ_{12}^{res} are used below.

Values of regression coefficients α and β for water concentrations calculated for all pairs of models are given in Table 56. It is seen that maximum values of coefficients α and β are characteristic for the comparison of CliMoChem with other models (α : -129.469 - 1531.35; β : -220.42 – 5579.09). It is obvious since absolute values of this model's results differ substantially from others. For the rest of pairs of the models, α varies far less (from -2.33 to 3.76). β varies not very much in comparison with mean values of water concentrations (lying in the range from -2.20 to 26.53).

Table 56. Coefficients of regression dependence between the models (α / β) for water concentrations

| | CAM/POPs | DEHM-POP | CliMoChem | G-CIEMS | SimpleBox | MSCE-POP |
|-----------------------------|---------------|--------------|--------------------|---------------|---------------|--------------|
| EVN-BETR and UK-MODEL | -2.33 / 16.89 | 1.29 / -0.13 | 1531.35 / -220.42 | 3.35 / 9.15 | 3.76 / -2.20 | 1.40 / -0.05 |
| CAM/POPs | – | -0.12 / 4.81 | -129.469 / 5579.09 | -0.75 / 26.53 | -0.24 / 11.21 | -0.13 / 5.31 |
| DEHM-POP | – | – | 1193.26 / -77.47 | 2.62 / 9.44 | 2.96 / -1.95 | 1.09 / 0.08 |
| CliMoChem | – | – | – | 0.002 / 8.90 | 0.003 / -1.91 | 0.001 / 0.14 |
| G-CIEMS | – | – | – | – | 0.32 / 2.74 | 0.10 / 2.06 |
| SimpleBox | – | – | – | – | – | 0.35 / 0.98 |
| Mean concentration in water | 10.05 | 3.65 | 4277.93 | 19.00 | 8.85 | 4.05 |

Coefficients of regression dependence between the models (α and β) for gaseous flux to water are presented in Table 57. One can see that in this case the difference between the participating models in α and β values is much less than for water concentrations. For all models α varies not substantially (from 0.37 to 3.47), and β ranges from -0.28 to 0.42. The closest results (α values are close to 1 and β values are comparable with mean values of fluxes) are obtained by the following pairs of models: CAM/POPs and EVN-BETR and UK-MODEL; G-CIEMS and CliMoChem; MSCE-POP and EVN-BETR and UK-MODEL; MSCE-POP and CAM/POPs.

Table 57. Coefficients of regression dependence between the models (α / β) for gaseous flux to water

| | CAM/POPs | CliMoChem | G-CIEMS | SimpleBox | MSCE-POP |
|----------------------------|-------------|--------------|--------------|--------------|--------------|
| EVN-BETR and UK-MODEL | 0.80 / 0.05 | 0.37 / 0.01 | 0.45 / 0.02 | 1.72 / -0.28 | 0.98 / 0.01 |
| CAM/POPs | – | 0.47 / -0.02 | 0.57 / -0.02 | 2.04 / -0.24 | 1.24 / -0.06 |
| CliMoChem | – | – | 1.25 / -0.01 | 3.47 / 0.28 | 2.63 / -0.02 |
| G-CIEMS | – | – | – | 2.62 / 0.42 | 2.10 / 0.01 |
| SimpleBox | – | – | – | – | 0.46 / 0.40 |
| Mean gaseous flux to water | 1.15 | 0.53 | 0.64 | 2.10 | 1.36 |

Calculations of pairwise residual square deviation σ given in Table 58 and 59 allow to assess the reliability of comparative analysis given above.

Table 58. Residual square deviation, σ for water concentrations

| | CAM/POPs | DEHM-POP | CliMoChem | G-CIEMS | SimpleBox | MSCE-POP |
|-----------------------|----------|----------|-----------|---------|-----------|----------|
| EVN-BETR and UK-MODEL | 14.58 | 0.20 | 537.54 | 21.96 | 4.29 | 0.61 |
| CAM/POPs | - | 3.92 | 4744.96 | 21.35 | 12.86 | 4.28 |
| DEHM-POP | - | - | 326.00 | 21.92 | 3.78 | 0.49 |
| CliMoChem | - | - | - | 21.43 | 2.96 | 0.26 |
| G-CIEMS | - | - | - | - | 10.82 | 3.99 |
| SimpleBox | - | - | - | - | - | 0.97 |

Table 59. Residual square deviation, σ for gaseous flux to water

| | CAM/POPs | CliMoChem | G-CIEMS | SimpleBox | MSCE-POP |
|-----------------------|----------|-----------|---------|-----------|----------|
| EVN-BETR and UK-MODEL | 0.23 | 0.26 | 0.37 | 0.86 | 0.68 |
| CAM/POPs | - | 0.21 | 0.32 | 1.20 | 0.55 |
| CliMoChem | - | - | 0.06 | 1.90 | 0.01 |
| G-CIEMS | - | - | - | 2.05 | 0.13 |
| SimpleBox | - | - | - | - | 1.11 |

It is seen that the values of residual square deviation are maximum for the comparison of water concentrations calculated by CliMoChem with those obtained by other models. For the rest of the model pairs σ lies within the interval 0.2 - 21.96. For results of calculations of gaseous flux to water, σ ranges from 0.01 to 2.05.

For PCB-28 (See Annex D), a difference in absolute values of calculated water concentrations is also large. However, max/min ratio of values of PCB-28 gaseous fluxes to water lies within factor 3-5 only. The results obtained for PCB-180 are similar to the results on PCB-153 and can be found in Annex E. All models (except for DEHM-POP) similarly describe the variations of water concentration values for both congeners caused by change of environmental conditions between different experiments (correlation coefficient is very close 1). Correlation coefficients for values of gaseous flux to water of PCB-28 and PCB-180 calculated by all models range from 0.84 to 1 and from 0.93 to 1.00, respectively.

4.6. Gaseous exchange between atmosphere and vegetation

4.6.1. Model approaches

Similar to the descriptions of other gaseous exchange processes considered above, in the participating models atmosphere/vegetation gaseous exchange is also described with the help of theory of intermedia diffusion. Detailed descriptions of this process used in the models can be found in Table 63 and Annex C.

Not all models include vegetation as environmental media for calculations. In description of gaseous exchange between vegetation and atmosphere on the basis of fugacity approach, EVN-BETR and UK-MODEL use constant values of air-vegetation transport velocities. In SimpleBox model absorption from gas phase by plant and volatilization from plant are calculated with the help of constant value of mass transfer coefficient. In CliMoChem models fluxes between atmosphere and vegetation are calculated via atmosphere/vegetation diffusion rates. These rates are supposed to be dependent on climatic zones. In CliMoChem three types of vegetation are considered: grass, coniferous forest and deciduous forest. MSCE-POP describes air/vegetation exchange on the basis of resistance analogy. At that mass transfer coefficient is assumed to be directly proportional to K_{oa} value. Similar to CliMoChem in MSCE-POP grass, coniferous forest and deciduous forest are treated separately. Models G-CIEMS and CAM/POPs use description of air/vegetation exchange similar to that for air/soil but with another parameter values. The model DEHM-POP does not include vegetation compartment.

At present calculation experiments with vegetation are made by EVN-BETR and UK-MODEL, SimpleBox and MSCE-POP. The comparison of the results of calculation experiments are presented below.

4.6.2. Input data

Four sets of input data are proposed for modelling experiments with PCB-153.

Table 60. Input data for calculation experiments with PCB-153 describing air/vegetation exchange

| N | Experiment 1 | Experiment 2 | Experiment 3 | Experiment 4 |
|---|--------------|--------------|--------------|--------------|
| Type of vegetation compartment: | Grass | Grass | Grass | Grass |
| Average ambient temperature, °C | 5 | 25 | 11 | 18 |
| Air concentration, gaseous phase, pg/m ³ | 6 | 19 | 3 | 14 |
| Mean wind velocity, m/sec | 4 | 4 | 4 | 4 |

Output: calculation of PCB-153 concentration in vegetation, ng/g dry weight and gaseous fluxes from and to vegetation and/or net gaseous flux to vegetation, ng/m²/d;

4.6.3. Comparison of the results

Numerical results of experiments on calculations of concentration in vegetation and net gaseous flux to vegetation obtained by participating models and their analysis are presented in this Section for PCB-153. The corresponding results for other substances can be found in Annexes D and E.

Since optional experiments on gaseous exchange between atmosphere and vegetation were made by three participating models only, such statistical parameters as the average concentration in vegetation and net gaseous flux to vegetation and square deviation of these results can not be useful in the analysis of results. It is more reasonable to make comparison of the absolute values themselves. Calculated values of concentration in vegetation for PCB-153 are presented in Table 61. Comparison of absolute values of calculated net gaseous flux to vegetation for PCB-153 are given in Table 62. Short comments to the calculations can be found in Table 63.

It is seen that dispersion of absolute values of concentrations in vegetation calculated by the models is rather large. The difference between maximum and minimum values of this parameter varies within wide range from 3 to 10. Comparing the results on net deposition flux calculations, we can see that in EVN-BETR and UK-MODEL volatilization flux from vegetation exceed flux from air to vegetation for all four experiments (that is re-emissions from plant takes place) in contrary to MSCE-POP and SimpleBox models. At that the difference in absolute values is very large. However, for the last two models, absolute values are very close to each other.

Table 61. Calculation results: concentrations of PCB-153 in vegetation calculated by models, ng/g d.w

| N | Air concentration, pg/m ³ | EVN-BETR and UK-MODEL | SimpleBox * | MSCE-POP |
|--------------|--------------------------------------|-----------------------|-------------|----------|
| Experiment 1 | 6 | 0.220 | 0.401 | 0.104 |
| Experiment 2 | 19 | 0.050 | 0.483 | 0.252 |
| Experiment 3 | 3 | 0.053 | 0.159 | 0.050 |
| Experiment 4 | 14 | 0.089 | 0.529 | 0.217 |

* - ng/g wet weight.

Table 62. Calculation results: net gaseous flux of PCB-153 to vegetation calculated by models, ng/m²/d

| N | Air concentration, pg/m ³ | EVN-BETR and UK-MODEL | SimpleBox | MSCE-POP |
|--------------|--------------------------------------|-----------------------|-----------|----------|
| Experiment 1 | 6 | -0.07 | 0.40 | 0.33 |
| Experiment 2 | 19 | -0.03 | 0.82 | 0.81 |
| Experiment 3 | 3 | -0.02 | 0.18 | 0.16 |
| Experiment 4 | 14 | -0.0004 | 0.71 | 0.70 |

Table 63. Comments

| Models | Physical-chemical data set | LAI, m ² /m ² | Comments |
|-----------------------|----------------------------|-------------------------------------|--|
| EVN-BETR and UK-MODEL | Own | 4 | Steady-state approach; Individual/own dataset extremely close to the reference dataset; The flux was calculated as Gaseous flux = Dair-veg · Fugacity (Pa) Dair-veg = 1/((1/(Veg Area · Veg_airMTC · Z _{veg})) + (1/(Veg Area·Air_VegMTC · Z _{air}))) Veg_area: Vegetation area = 8·10 ¹² m ² Veg_airMTC: Vegetation side air-vegetation transport velocity = 10.8 m/h Air_VegMTC : Air side air-vegetation transport velocity = 9 m/h |
| SimpleBox | "Reference" | 3.9 | Steady-state approach; SimpleBox works with (wet) bulk vegetation densities (900 kg/m ³ by default); concentrations in vegetation expressed on wet weight basis. Specific amount of plant material given in SimpleBox as mass per unit area (1.2 kg/m ² by default). Fluxes to and from vegetation expressed per unit leaf area. Absorption from gas phase by plant (mol/m ² /s) = FRgas (-) · kav(gas) (m/s) · CONCair (mol/m ³) Volatilization from plant (mol/m ² /s) = kav(gas) (m/s) / Kva (-) · CONCair (mol/m ³) kav(gas) = overall gas-referenced air-plant mass transfer coefficient = 10 ⁻³ m/s by default Kva = dimensionless vegetation-air euilibrium constant |
| MSCE-POP | Own | 1 | Steady-state approach $\frac{dC_V}{dt} = \frac{1}{R_{tot}} \cdot (C_a^g - C_V / K_{Va}),$ where C_a^g - air concentration of a pollutant; C_V - concentration in the vegetation of a given type; K_{Va} - bioconcentration factor (BCF); R_{tot} - total resistance to the gaseous exchange given by the formula. $R_{tot} = R_a + a_v / k,$ where R_a - aerodynamic resistance of turbulent atmospheric layer; k - mass transfer coefficient, m/s; a_v - specific surface area of vegetation, m ² /m ³ (assumed value is 8000, see [Duyzer and van Oss, 1997]) |

The comparison of calculated values of concentrations in vegetation is also displayed in Fig. 15. Calculation results of Simple Box and MSCE-POP models show very close character of variability of concentration values in dependence with variability of input data for each experiments. For these models' result on calculation of net gaseous fluxes, we can see the same tendency.

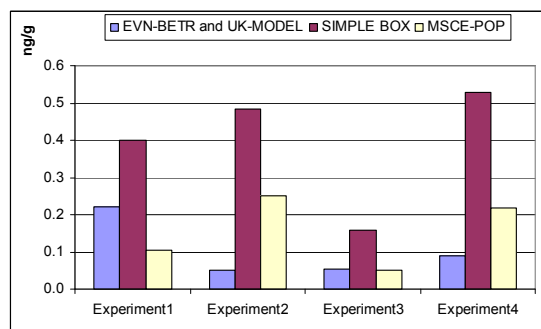


Fig.15. The comparison of calculated values of concentrations in vegetation

Correlation coefficients for concentration in vegetation and net gaseous flux calculated by the models are presented in Tables 64 and 65.

Table 64. Correlation coefficients for concentrations in vegetation

| | SimpleBox | MSCE-POP |
|-----------------------|-----------|----------|
| EVN-BETR and UK-MODEL | 0.15 | -0.30 |
| SimpleBox | — | 0.88 |

Table 65. Correlation coefficients for net gaseous flux

| | SimpleBox | MSCE-POP |
|-----------------------|-----------|----------|
| EVN-BETR and UK-MODEL | 0.27 | 0.34 |
| SimpleBox | — | 1.00 |

According to the values of pairwise correlation coefficients for both parameters, only two models SimpleBox and MSCE-POP describe tendency of gaseous exchange variability similarly. Correlation coefficients for concentrations and fluxes are equal to 0.88 and 1.0, respectively. It is evident that results of EVN-BETR and UK-MODEL are not correlated with other models.

The values of coefficients α and β calculated for the regression between SimpleBox and MSCE-POP models in values of calculated concentration in vegetation and net gaseous flux are presented in Table 66 and 67.

Table 66. Coefficients of regression dependence between the models (α / β) for concentrations in vegetation

| | SimpleBox |
|----------|---------------|
| MSCE-POP | 0.51 / -0.044 |

Table 67. Coefficients of regression dependence between the models (α / β) for net gaseous flux

| | SimpleBox |
|----------|---------------|
| MSCE-POP | 1.04 / -0.045 |

Considering concentration in vegetation, the differences between these models is determined by scaling coefficient α , which totals to 0.51 in this case. However, it is seen that α is very close to 1 for net gaseous flux results. Coefficients β are small enough in both cases compared with mean values of concentrations and fluxes.

For results on PCB-28 and PCB-180 (see Annexes D and E), a dispersion in absolute values of concentrations in vegetation and net deposition fluxes calculated for all experiments by three participating models is also large. However, values of PCB-180 concentrations are closer to each other than results for PCB-28. Thus, the differences between maximum and minimum values of this parameter calculated by the participating models vary within ranges from 3 to 7 and from 13 to 41, respectively. The difference in absolute values of fluxes of both congeners are more substantial than the dispersion of their concentrations. Correlation coefficients for PCB-180 concentration in vegetation vary in the range from 0.63 to 1.00 between all pairs of models; for PCB-28 a good correlation is observed between SimpleBox and EVN-BETR and UK-MODEL and between SimpleBox and MSCE-POP models. Results on net gaseous fluxes of PCB-28 and PCB-180 are well correlated for SimpleBox and MSCE-POP models.

Conclusions

At the preliminary stage of POP models intercomparison study short descriptions of 13 models were submitted by participants. On the basis of these descriptions a short summary of model types participating in the intercomparison study with indication of model type, spatial and temporal resolution, environmental media used, and processes taken into account was compiled. This analysis was used for the determination of the intercomparison procedure at Stage I.

Stage I of the intercomparison study of POP models was aimed at the comparison of:

- modelling approaches to the description of main processes determining POP fate in the environment, namely:
 - gas/particle partitioning in the atmosphere;
 - dry deposition;
 - wet deposition;
 - gaseous exchange between the atmosphere and different types of underlying surface (soil, seawater, vegetation);
 - degradation;
- values of physical-chemical parameters used for modelling;
- results of calculation experiments on the above processes carried out by participating models.

Values of physical-chemical parameters used by participants for the Stage I calculations strongly affect the results of calculation experiments. Comparison of physical-chemical parameters used in participating models and statistical processing of these data is made. Physical-chemical data sets of individual models are compared also with “reference data sets”, which will be used at follow-up Stage II within sensitivity study with respect to basic processes. Thus, analysis of physical-chemical parameters of PCB-153, PCB-28 and PCB-180 shows the following:

- Henry's law constant and air-water partition coefficient :
 - All models use temperature dependent Henry's law constant and air-water partition coefficient (except H value of EVN-BETR and UK-MODEL). Differences in absolute values of Henry's law constant between all models are very large for PCB-153 and PCB-180. These values differ from each other more than an order of magnitude. Difference in H values for PCB-28 is much less than for other congeners. Scattering is going down with temperature.
 - If temperature independent H values of EVN-BETR and UK-MODEL are not taken into account, max/min ratio of H and K_{aw} values for PCB-153 varies within factor 8-9; for PCB-28 - within factor 1-2; and for PCB-180 - within factor 12-22.
- Subcooled liquid vapour pressure:
 - All models use temperature dependent subcooled liquid vapour pressure (except EVN-BETR and UK-MODEL). Differences in absolute values of p_{ol} between all models are more substantial for PCB-153 and PCB-180 than that for PCB-28.
 - For PCB-153 and PCB-28 there is a high similarity between the values of subcooled liquid vapour pressure presented by models using temperature dependence of this parameter (max/min ratio is about 1.1 and 1.3, respectively). For PCB-180 max/min ratio of p_{ol} values lies within factor 7.
- Octanol/water partition coefficient:

- Difference in absolute values of octanol/water partition coefficient between all models is not large. Max/min ratio of K_{ow} values for PCB-153 varies from 2 to 5; for PCB-28 - from 2 to 4; and for PCB-180 – from 2 to 3. If not take into account the temperature independent value of MSCE-POP, max/min ratio for all considered congeners to a variable degree comes down.
- This parameter is changing with temperature within factor 3-4 for considered interval of temperatures (-10-25°C).
- Scattering of coefficients of temperature dependences among all models lies within factors 1 – 4.
- Octanol/air partition coefficient:
 - There is a large similarity in values of octanol/air partition coefficient obtained with the use of existing temperature dependencies.
 - Max/min ratios between absolute values of K_{oa} used by all participants at different temperatures range from 5 to 6 for PCB-153; from 2 to 5 for PCB-28 and from 6 to 8 for PCB-180.
 - Max/min ratio of coefficients of temperature dependences of K_{oa} for the considered congeners equals practically to 1.0.
- Organic carbon/water partition coefficient:
 - Difference between the highest and the lowest values of organic carbon/water partition coefficient is less than an order of magnitude. For the considered temperature interval, max/min ratio for PCB-153 comes down from 9 to 7.
 - For models using close values of regression coefficients for recalculation of K_{oc} from K_{ow} (all models except for G-CIEMS), its values differ within factors of 2-5 for PCB-153; and within factors 2-4 for PCB-28 and PCB-180.
- Water solubility:
 - Values of water solubility used in EVN-BETR and UK-MODEL, SimpleBox and G-CIEMS models are of the same order. Other models do not use this parameter directly.
- Degradation:
 - There is a large difference in absolute values of first order rate constant for the considered media between the models. For all media max/min ratios for PCB-153 vary within the range of 4-10; for PCB-28 – within the range of 2-12; and for PCB-180 – within the range of 3-10.
 - Degradation in air, soil and water is considered in all models. Max/min ratios for PCB-153 vary from 4 to 5; for PCB-28 – from 2 to 12; and for PCB-180 – from 3 to 10.
 - Degradation in vegetation is included in CliMoChem and EVN-BETR and UK-MODEL. Difference of rate constants between the models (max/min ratio) for PCB-153 is around 10; for PCB-28 it equals to 7 and for PCB-180 it is around 6. Degradation in sediments is considered in EVN-BETR and UK-MODEL only.
 - Temperature dependence of rate constant for degradation in air are considered in CAM/POPs, CliMoChem and MSCE-POP models. The difference between temperature dependent values for the considered congeners is within factors 1-2.
 - Degradation in other media than air is temperature dependent in CliMoChem model only.

In order to analyze similarities and distinctions in model descriptions and parameterisations of the above listed processes and to find out “hot spots” in modelling, a number of calculation experiments

with PCB-153 (first priority) and PCB-28 and PCB-180 (second priority) were carried out by the participating models. The analysis of the results of these experiments revealed that:

- Gas/particle partitioning:
 - For the description of gas/particle partitioning, the models mostly use adsorption and absorption approaches. There is not a large difference in values of particulate fraction calculated by both methods.
 - Tendency in variability of calculated particulate fraction of PCB-153 with temperature is described by all models rather closely and the difference in its absolute values is not substantial. The difference of model results can be explained by the difference in K_{oa} or p_{ol} values used. Correlation coefficients for PCB-153 are very high for all pairs of models (from 0.83 to 1.00). The main difference between models is determined by scaling factors (from 0.13 to 3.78).
 - The results obtained for PCB-180 and PCB-28 are similar to the results on PCB-153. Dispersion of their absolute values are not large. Correlation coefficients between all pairs of models for PCB-180 vary from 0.75 to 1.00; and for PCB-28 - from 0.98 to 1.00.
- Dry deposition of the particulate phase:
 - The difference between models in the description of this process lies in different methods of calculation of deposition velocity used by the participating models. A large dispersion in calculated values of dry deposition flux is mainly explained by the high scattering of dry deposition velocity values used. The type of underlying surface essentially affects deposition fluxes. According to descriptions of dry deposition accepted in the participating models, parameterizations of the flux are one and the same for all PCB congeners.
 - The values of dry deposition flux for different models are mostly of the same order. A discrepancy in calculated deposition fluxes comes up to an order of magnitude for models distinguishing different types of underlying surface. The largest discrepancy of calculated fluxes to different types of underlying surface takes place for forest: maximum and minimum calculated values differ 150 times. For models distinguishing different types of underlying surface the best correlation is observed for CAM/POPs and MSCE-POP.
- Wet deposition:
 - All models use the inverse dimensionless Henry's law constant for the calculations of washout or scavenging ratio of gaseous phase. A difference in this parameter values used by the models affects the calculation results. The scattering of constant values of scavenging ratio (or washout ratio) used by the most part of participating models for the description of wet deposition of particle bound phase is rather large. CAM/POPs and SimpleBox do not include scavenging ratio in their parameterizations and use the values of aerosol collection efficiency to evaluate scavenging or washout rate of a pollutant.
 - There is a large difference between model calculations made for experiments on wet deposition process. Values of PCB-153 concentrations in precipitation vary within a factor 6-14. Max/min ratio of absolute values of wet deposition flux lies within an order of magnitude for the first two experiments and comes up to 36 times for the highest temperature. For PCB-153, the best correlations are obtained between G-CIEMS and SimpleBox, between G-CIEMS and MSCE-POP models and between MSCE-POP and SimpleBox models (correlation coefficient in all cases is equal to 1.00). Taking into account regression coefficients' values also, these models show the closest results in the experiments of wet deposition process.

- The results of calculation experiments with PCB-28 and PCB-180 show also a large dispersion between the absolute values of concentrations in precipitation and wet deposition fluxes calculated by different models. For PCB-28 there is a good correlation between results of MSCE-POP, ClimoChem and SimpleBox (correlation coefficient is equal to 1). Calculated concentrations of PCB-180 in precipitation are also well correlated between these three models (correlation coefficient vary from 0.91 to 1) and between CAM/POPs and EVN-BETR and UK model (correlation coefficient is equal to 0.76).
- Gaseous exchange between atmosphere and soil
 - All models use one and the same philosophy for the description of atmosphere/soil gaseous exchange – resistance analogy. The difference between model approaches to the description of air/soil exchange is mostly determined by the variability of mass transfer coefficient or diffusion transport velocity values used by the models. The difference between models is also in the number and thickness of considered soil layers.
 - There is rather large difference in absolute values both for calculated soil concentrations and net gaseous flux of PCB-153. However, all models similarly describe the variations of soil concentration values caused by change of environmental conditions between different experiments. Correlation coefficients vary within the range from 0.85 to almost 1. Results on net gaseous flux of PCB-153 are also well correlated for the most part of model pairs except for pairs between G-CIEMS 1 and two models: MSCE-POP 2 and CAM/POPs.
 - For PCB-28 and PCB-180, a large difference in absolute values also takes place both for calculated soil concentrations and net gaseous flux. Correlation coefficients for soil concentration of PCB-28 vary within the range from 0.93 to almost 1 between all pairs of models; for net gaseous flux, a good correlation is observed between SimpleBox and EVN-BETR and UK-MODEL models. Results on soil concentrations and net gaseous fluxes of PCB-180 are well correlated for all model pairs (correlation coefficients range from 0.87 to 1.00 and from 0.85 to 1.00, respectively).
 - Within the optional experiment on POP accumulation and clearance dynamics in soil, the analysis of calculated characteristic times for four considered models shows that these models can be divided into two groups. First group (EVN-BETR and UK model and SimpleBox) are characterized by very close characteristic times for fast and slow exponentials. In essence, these models realize mono-exponential trends of POP soil contamination. Another two models (CAM/POPs and MSCE-POP) demonstrate the presence of both fast and slow exponents in soil concentration trends at accumulation and clearance phases.
- Gaseous exchange between atmosphere and water:
 - The description of atmosphere/water gaseous exchange in all models is based on two-film model of intermedia diffusion. There exist a large diversity of approaches to the evaluation of transfer velocities at air/water interface.
 - For results on PCB-153, a dispersion in absolute values of water concentrations obtained by all models is large. However, EVN-BETR and UK-MODEL, DEHM-POP, ClimoChem, SimpleBox and MSCE-POP similarly describe the variations of water concentration values caused by change of environmental conditions between different experiments. Correlation coefficient for these models is very close to 1. For calculated PCB-153 gaseous fluxes to water, a better agreement between all models calculations is observed than for water concentration results. Correlation coefficients for values of gaseous flux to water calculated by all models range from 0.73 to 1. It is evident that results of all models are well correlated with each other describing air –water gaseous exchange fluxes.

- For PCB-28, a difference in absolute values of calculated water concentrations is also large. However, max/min ratio of values of PCB-28 gaseous fluxes to water lies within factor 3-5 only. The results obtained for PCB-180 are similar to the results on PCB-153. The most part of models similarly describe the variations of water concentration values for both congeners caused by change of environmental conditions between different experiments (correlation coefficient is very close 1). Correlation coefficients for values of gaseous flux to water of PCB-28 and PCB-180 calculated by all models range from 0.84 to 1 and from 0.93 to 1.00, respectively.
- Gaseous exchange between atmosphere and vegetation (optional):
 - Atmosphere/vegetation gaseous exchange is described in all models with the help of theory of intermedia diffusion. Not all models include vegetation as environmental media for calculations. The difference between models is determined by the difference of mass transfer coefficient or diffusion transport velocity values used.
 - A dispersion of absolute values of PCB-153 concentrations in vegetation and net deposition flux calculated for all experiments by three participating models is large. The difference between maximum and minimum values of concentrations varies within wide range from 3 to 10. Absolute values of PCB-153 fluxes are very close to each other in MSCE-POP and SimpleBox models. In addition, Simple Box and MSCE-POP models show very close character of variability of both calculated parameters in dependence with variability of input data for each experiment.
 - A difference in absolute values of concentrations in vegetation and net deposition fluxes calculated for all experiments is also large both for PCB-28 and PCB-180. However, values of PCB-180 concentrations obtained by the models are closer to each other than results for PCB-28. The difference in absolute values of fluxes of both congeners are more substantial than the dispersion of their concentrations. Correlation coefficients for PCB-180 concentration in vegetation vary within the range from 0.63 to 1.00 between all pairs of models; for PCB-28 a good correlation is observed between SimpleBox and EVN-BETR and UK-MODEL and between SimpleBox and MSCE-POP models. Results on net gaseous fluxes of PCB-28 and PCB-180 are well correlated for SimpleBox and MSCE-POP models.

On the basis of the analysis of physical-chemical properties and of the results of calculation experiments, it was found that maximum differences in model output absolute values takes place for deposition processes (dry deposition of particles and wet deposition), and gaseous exchange processes with underlying surfaces. It is seems reasonable to carry out sensitivity study for their model descriptions at the next stages of model intercomparison.

The results obtained at Stage I of the POP model intercomparison study show that all the participating models are able to simulate main processes determining POP fate in the environment. However, our current understanding of POP behaviour is still incomplete and needs further improvement.

References

- Achman, Hornbuckle, Eisenreich [1993]
- Atmosphere Handbook, Leningrad [1991] p. 22
- Bamford, H. A., D. L. Poster, and J. E. Baker [2000] Henry's law constants of polychlorinated biphenyl congeners and their variation with temperature. *Journal of Chemical & Engineering Data*, v.45, pp. 1069–1074.
- Bennett D.H., Scheringer, M., McKone, T.E. and K. Hungerbühler [2001] Predicting Long Range Transport: A Systematic Evaluation of Two Multimedia Transport Models, *Environmental Science and Technology*, v. 35, No. 6, pp.1181-1189.
- Beyer A. and M.Matthies [2001] Criteria for Atmospheric Long-range Transport Potential and Persistence of Pesticides and Industrial Chemicals. Umweltforschungsplan des Bundesministerium für Umwelt, Naturschutz und Reaktorsicherheit. Stoffbewertung, Gentechnik, Forderkennzeichen (UFOPLAN) 299 65 402.
- Beyer A., F. Wania, T. Gouin, D. Mackay and M. Matthies [2002] Selecting internally consistent physicochemical properties of organic compounds. *Environmental Toxicology and Chemistry*, v.21, No.5, pp. 941–953.
- Bidleman, T. F., Falconer, R. L. and T. Harner [1998] "Particle/Gas Distribution of Semivolatile Organic Compounds: Field and Laboratory Experiments with Filtration Samplers", in *Gas and Particle Partition Measurements of Atmospheric Organic Compounds*, edited by D. A. Lane. Gordon and Breach Publishers, Newark, New Jersey.
- Brandes L.J. H. den Hollander and D. van de Meent [1996] SimpleBox 2.0: a nested multimedia fate model for evaluating the environmental fate of chemicals. Report no. 719101029. National Institute of Public Health and the Environment (RIVM), P.O. Box 1, 3720 BA Bilthoven, the Netherlands.
- Breivik K., F. Wania [2002a] Evaluating a model of the historical behavior of two hexachlorocyclohexanes in the Baltic Sea environment. *Environ. Sci. Technol.* v.36, pp.1014-1023.
- Breivik K., F. Wania [2002b] Mass budgets, pathways and equilibrium states of two hexa-chlorocyclohexanes in the Baltic Sea environment. *Environ. Sci. Technol.* v.36, pp.1024-1032.
- Breivik K., Sweetman A., Pacyna J.M., Jones K. [2002] Towards a global historical emission inventory for selected PCB congeners – a mass balance approach. 2. Emissions. *The Science of the Total Environment*, v. 290, pp. 199-224.
- Burkhard L.P., Armstrong D.E. and A.W. Andren [1985] Henry's Law Constants for the Polychlorinated Biphenyls. *Environ. Sci. Technol.*, v.19, pp.590-596.
- Christensen J. [1999] An overview of modelling the Arctic mass budget of metals and sulphur: Emphasis on source apportionment of atmospheric burden and deposition. In: *Modelling and sources: A workshop on Techniques and associated uncertainties in quantifying the origin and long-range transport of contaminants to the Arctic*. Report and extended abstracts of the workshop, Bergen, 14-16 June 1999. AMAP report 99:4. see also <http://www.amap.no/>
- Christensen J. H. [1997] The Danish Eulerian Hemispheric Model – a three-dimensional air pollution model used for the Arctic. *Atmospheric Environment*, v.31, No. 24, pp.4169–4191.
- Dunnivant F.M., Elzerman A.W., Jurs P.C., M.N. Hasan [1992] Quantitative Structure-Property Relationships for Aqueous Solubilities and Henry's Law Constants of Polychlorinated Biphenyls, *Environ. Sci. Technol.*, v. 23, No. 10, pp. 1250 – 1253.
- Duyzer J.H., van Oss R.F., Verhagen H.L.M., Vervaart M. and B.Boeke [1997] Determination of deposition parameters of a number of persistence organic pollutants by laboratory experiments. TNO-report TNO-MEP-R97/150.
- ENV/JM/MONO(2002)15 [2002] Report of the OECD/UNEP Workshop on the Use of Multimedia Models for Estimating Overall Environmental Persistence and Long range Transport in the Context of PBTS/POPS Assessment. OECD Environment, Health and Safety Publications Series on Testing and Assessment, No.36. Environment Directorate OECD, Paris.
- Falconer R.L. and T.F. Bidleman [1994] Vapor pressures and predicted particle/gas distributions of polychlorinated biphenyl congeners as functions of temperature and ortho-chlorine substitution. *Atmos. Environ.*, v.28, pp.547-554
- Falconer R.L. and T. Harner [2000] Comparison of octanol-air partition coefficient and liquid-phase vapor pressure as descriptors for particle/gas partitioning using laboratory and field data for PCBs and PCNs. *Atmospheric Environment*, v. 34, pp. 4043–4046.
- Falconer R.L. and T.F. Bidleman [1994] Vapor Pressures and Predicted Particle/Gas Distributions of Polychlorinated Biphenyl Congeners as Functions of Temperature and Ortho-Chlorine Substitution, *Atmospheric Environment*, v. 28, No. 3, pp. 547-554.
- Falconer R.L. and T.F. Bidleman, Cotham and E.William [1995] Preferential Sorption of Non-and-Mono-ortho-polychlorinated Biphenyls to Urban Aerosols, *Environ. Sci. Technol.*, v. 29, No. 6, pp. 1666-1673.

- Falkowski P.G., Barber R.T., and V.Smetacek [1998] Biogeochemical Controls and Feedbacks on Ocean Primary Production, *Science*, v.281, pp.200-205.
- Finizio A., D. Mackay T. Bidleman and T. Harner [1997] Octanol-Air Partition Coefficient as a Predictor of Partitioning of Semi-Volatile Organic Chemicals to Aerosols. *Atmospheric Environment*, v.31, No.15, pp.2289-2296.
- Frohn L.M., J.H. Christensen and J. Brandt [2002] Development of a high-resolution nested air pollution model – the numerical approach. *Journal of Computational Physics*, v.179, pp. 68–94.
- Geels C., J.H. Christensen, A.W. Hansen, S. Kiilsholm, N.W. Larsen, S.E. Larsen, T. Pedersen and L.L. Sørensen [2001] Modeling concentrations and fluxes of atmospheric CO₂ in the North East Atlantic Region. *Physics and Chemistry of the Earth (B)*, v.26, No.10, pp. 763–768.
- Gong S.L., Barrie L.A. and J.-P. Blanchet [2003] Canadian Aerosol Module: A size-segregated simulation of atmospheric aerosol processes for climate and air quality models 1.Model Development", *Journal of Geophysical Research*, v. 108, No. D1, pp. 4007, doi:10.1029/2001JD002002,2003.
- Gong S.L., Barrie L.A. and J.-P. Blanchet [1997b] Modeling Sea-salt Aerosols in the Atmosphere, 1.Model Development", *Journal of Geophysical Research*, v. 102, No. D3, pp. 3805-3818.
- Granier L.K. and Chevreuil M. [1997] Behaviour and spatial and temporal variations of polychlorinated biphenyls and lindane in the urban atmosphere of the Paris area, France. *Atmospheric Environment*, v.31, No.22, pp.3787-3802.
- Grell, G. A., J. Dudhia, and D. R. Stauffer [1995] A description of the fifth-generation Penn State/NCAR Mesoscale Model (MM5). NCAR/TN-398+STR. NCAR Technical Note. Mesoscale and Microscale Meteorology Division. National Center for Atmospheric Research. Boulder, Colorado. Pp. 122.
- Gusev A., I. Ilyin, G. Petersen, A. van Pul, D.Syrakov and M. Pekar [2000] Long-range transport model Intercomparison studies: Model intercomparison study for cadmium; About EMEP/MS-C-E participation in ATMES-II, EMEP/MS-C-E Technical Note 2/2000.
- Harner et al, 1998
- Harner T. and T.F. Bidleman [1996] Measurements of octanol-air partition coefficients for polychlorinated biphenyls. *Chem. Eng. Data*, v.41, pp.895-899.
- Hawker D.W. and D.W.Connell [1988] Octanol-water partition coefficients of polychlorinated biphenyl congeners. *Environ. Sci. Technol.*, v.22, pp.382-387.
- Horstmann M. and M.S. McLachlan [1998] Atmospheric Deposition of Semivolatile Organic Compounds to Tow Forest Canopies, *Atmospheric Environment*, v.32, No. 10, pp.1799-1809.
- Jacobs C.M.J. and W.A.J. van Pul [1996] Long-range atmospheric transport of persistent organic pollutants, I: Description of surface - atmosphere exchange modules and Implementation in EUROS. National institute of public health and the environment, Bilthoven, the Netherlands. Report No722401013.
- Junge C.E. [1977] Basic considerations about trace constituent in the atmosphere is related to the fate of global pollutant. In: Fate of pollutants in the air and water environment. Part I, I.H. Suffet (ed.) (Advanced in *Environ. Sci. Technol.*, v.8), Wiley-Interscience, New York.
- Kalnay E., Kanamitsu M., Kistler R., Collins W., Deaven D., Gandin L., Irdell M., White S., Sh. G., Wollen J., Zhu Y., Chelliah M., Ebisuzaki W., Higgins H., Janowiak J., Ropelewski K.C., Mo. C., Wang J., Leetmaa A., Reynolds R., Jenne R. and D. Joseph [1996] The NCEP/NCAR 40-year reanalysis project. *Bull. Amer. Meteor. Soc.* v.77, pp. 437-471.
- Karickhoff S.W. [1981] Semiempirical estimation of sorption of hydrophobic pollutants on natural sediments and soil, *Chemosphere*, v.10, pp.833-846.
- Koziol A. and J. Pudykiewicz [2001] Global scale transport of persistent organic pollutants, *Chemosphere*, v. 45/8, pp. 1181-1200.
- Li Y.F., M.T. Scholtz, and B.J. van Heyst [2000] Global gridded emission inventories of α -hexachlorocyclohexane. *Journal of Geophysical Research*, v.102, No.D5, pp. 6621–6632.
- Li Y.-F., McMillan A., Scholtz M. T. [1996] Global HCH usage with 1 x 1 degree longitude/latitude resolution. *Environ. Sci. Tech.* v.30, pp.3525-3533.
- Li N., Wania F., Lei D.Y., Daly G.L. [2003] A comprehensive and critical compilation, evaluation and selection of physical chemical property data for selected polychlorinated biphenyls, *J. Phys. Chem. Ref. Data*, v. 32, No. 4, pp. 1545-1590.
- Lindfors V., S.M.Joffe and J.Damski [1991] Determination of the wet and dry deposition of sulphur and nitrogen compounds over the Baltic sea using actual meteorological data. Finnish Meteorological Institute Contributions N 4, Helsinki.
- Mackay D. [1999] Multimedia Environmental Models – The Fugacity Approach, second edition, Lewis Publishers.
- Mackay D., Shiu, W.Y., Ma, K.C. [1992] Illustrated Handbook of Physical-Chemical properties and environmental fate for organic chemicals, v.1: Monoaromatic Hydrocarbons, Chlorobenzenes, and PCBs. Lewis Publishers, INC.

- Mackay D. and Yeun A.T.K. [1983] Mass Transfer Coefficient Correlations for Volatilization of Organic Solutes from Water, *Environmental Science and Technology*, v. 17, pp. 211-217.
- Mackay D. and S. Paterson [1991] Evaluating the Multimedia Fate of Organic Chemicals: A Level III Fugacity Model, *Environmental Science and Toxicology*, v. 25, pp.427-436.
- Malanichev A., V. Shatalov N. Vulykh, B. Strukov [2002] Modelling of POP Hemispheric Transport, MSC-E Technical Report 8/2002.
- McLachlan M. and M. Horstmann [1998] Forests as filters of airborne organic pollutants: a model. *Environ. Sci. Technol.*, v.32, pp. 413-420.
- McLachlan, M., G. Jeczub and F. Wania [2002] The Influence of Vertical Sorbed Phase Transport on the Fate of Organic Chemicals in Surface Soils, *Environ. Sci. Technol.*, v.36, pp.4860-4867.
- Möller M. [2002] Einfluss der Vegetation auf das Verteilungsverhalten von organischen Schadstoffen in einem Umweltmodell, Diplomarbeit ETHZ Zürich, Swiss Federal Institut of Technology Zurich (ETHZ) (ISBN 3-906734-27-7).
- Murray J.W. [1992] The Oceans, in: Butcher, S.S., Charlson, R.J., Orians, G.H., Wolfe, G.V. (Eds.): *Global Biogeochemical Cycles*. Academic Press, pp.175-211.
- Pacyna, J.M. et al. [1999] Final Report for Project POPCYCLING-Baltic. NILU, P.O. Box 100, N-2007 Kjeller, Norway. CD-ROM.
- Pankow J.F. [1987] Review and comparative analysis of the theories on partitioning between the gas and aerosol particulate phases in the atmosphere. *Atmos. Environ.*, v.21, pp.2275-2283.
- Pekar M., N. Pavlova, A. Gusev, V. Shatalov, N. Vulykh, D. Ioannisian, S. Dutchak, T. Berg and A.-G. Hjelbrekke [1999] Long-range transport of selected persistent organic pollutants. Development of transport models for polychlorinated biphenyls, benzo[a]pyrene, dioxins/furans and lindane Joint report of EMEP Centres: MSC-E and CCC, EMEP Report 4/99.
- Report of the OECD/UNEP Workshop on the Use of Multimedia Models for Estimating Overall Environmental Persistence and Long-Range Transport in the context of PBTs/POPs assessment. [2002] ENV/JM/MONO(2002)15.
- Ruijgrok, W. Tieben H. and P. Eisinga [1997] The dry deposition of particles to a forest canopy: a comparison of model and experimental results. *Atmospheric Environment*, v.31, pp. 399-415.
- Ryaboshapko A., I. Ilyin, R. Artz, R. Bullock, J. Christensen, M. Cohen, A. Dastoor, D. Davignon, R. Draxler, R. Ebinghaus, J. Munthe, G. Petersen, D. Syrakob [2002] Progress report on Intercomparison study of numerical model for long range atmospheric transport of mercury. MSC-E Technical Note 10/2002.
- Ryaboshapko A., R. Artz, R. Bullock, J. Christensen, M. Cohen, A. Dastoor, D. Davignon, R. Draxler, R. Ebinghaus, I. Ilyin, J. Munthe, G. Petersen, D. Syrakov [2003] Intercomparison Study of numerical models for long-range atmospheric transport of mercury. Stage II. Comparison of modeling results with observations obtained during short-term measuring campaigns. MSC-E Technical report 1/2003.
- Scheringer M., Wegmann F. and M. Salzmänn [2003] POP model intercomparison study. Stage 1: Process Description and Parameterization for the Models ChemRange and CliMoChem. ETH-Logo. Postadresse und Buwalreferenz.
- Scheringer M. [1996] Räumliche und Zeitliche Reichweite als Indikatoren zur Bewertung von Umweltchemikalien, Diss. ETH Nr.11746, Swiss Federal Institut of Technology Zurich (ETHZ).
- Schwarzenbach, R. P., Gschwend, P. M. and D.M. Imboden [1993] *Environmental Organic Chemistry*. John Wiley & Sons, Inc., New York.
- Sehmel G.A. [1980] Particle and gas dry deposition: a review. *Atmos. Environ.* v.14, pp. 983-1011.
- Seinfeld J.H. [1986] *Atmospheric Chemistry and Physics of Air Pollution*, J. Wiley & Sons, N.Y., pp. 738
- Sellers P. J., Meeson B. W., Closs J., Collatz J., Corprew F., Dazlich D., Hall F. G., Kerr Y., Koster R., Los S., Mitchell K., McManus J., Myers D., Sun K.-J. and P. Try [1995] An Overview of the ISLSCP Initiative Global data sets. On: ISLSCP Initiative Global data sets for land-atmosphere models, 1987-1988, Vol. 1-5. Published on CD by NASA, Vol. 1, USA-NASA-GDAAC-ISLSCP-001, OVERVIEW.DOC.
- Seth R., Mackay D., Muncke J. [1999] Estimating the Organic Carbon Partition Coefficient and its Variability for Hydrophobic Chemicals, *Environmental Science and Technology*, v. 33, pp. 2390-2394.
- Shatalov V., A. Malanichev, N. Vulykh (MSC-E), T. Berg, S. Manø (CCC) [2002] Assessment of POP Transport and Accumulation in the Environment, MSC-E/CCC Technical Report 7/2002
- Shatalov V., A. Malanichev, N. Vulykh, T. Berg and S. Mano [2001] Assessment of POP transport and accumulation in the environment. EMEP Report 4/2001
- Shatalov V., A. Malanichev, T. Berg and R. Larsen [2000] Investigation and assessment of POP transboundary transport and accumulation in different media, EMEP-MSC-E, Report 4/2000, Part 1,2.
- Siegenthaler U. and F. Joos, [1992] Use of a simple model for studying oceanic tracer distribution and the global carbon cycle. *Tellus* 44B, pp.186-207.

- Sinkkonen S. and J.Paasivirta [2000] Degradation half-life times of PCDDs, PCDFs and PCBs for environmental fate modeling. *Chemosphere*, v. 40, pp.943-949.
- Sofiev M., Maslyayev A. and A. Gusev [1996] Heavy metal model intercomparison. Methodology and results for Pb in 1990, MSC-E Report 2/96.
- Strand A., and Ø. Hov [1996] A model strategy for the simulation of chlorinated hydrocarbon distributions in the global environment. *Water, Air and Soil Pollution*, v.86, pp. 283–316.
- Struijs J. and Van den Berg R. [1995]. Standardized biodegradability tests: extrapolation to aerobic environments. *Water Research*, v 29, Issue 1, Pages 255-262.
- Strukov B., Resnyansky Yu., Zelenko A., Gusev A. and V.Shatalov [2000] Modelling long-range transport and deposition of POPs in the European region with emphasis to sea currents. EMEP/MSC-E Report 5/2000.
- Strukov B.S. [2001] Dynamics of POPs distribution in Sea Water between Different Phases. EMEP/MSC-E Technical Note 1/2001, Meteorological Synthesizing Centre - East, Moscow, Russia.
- Sweetman A.J. and Jones K.C. [2000] Declining PCB concentrations in the U.K. atmosphere: evidence and possible causes. *Environmental Science and Technology*, v.34, No. 5, pp.863-869.
- Vassilyeva G. and V. Shatalov [2002] Behaviour of persistent organic pollutants in soil. MSC-E Technical Note 1/2002.
- Wania F and D. Mackay [2000] The global distribution model. A non-steady state multi-compartmental mass balance model of the fate of persistent organic pollutants in the global environment. Technical Report (www.uts.utoronto.ca/~wania)
- Wania F. and C.Dugani [2003] Assessing the long-range transport potential of polybrominated diphenyl ethers: A comparison of four multimedia models. *Environ. Toxicol. Chem.*, v. 22, No. 6, p.1252-1261.
- Wania F. and D. Mackay [2000] A Comparison of Overall Persistence Values and Atmospheric Travel Distances Calculated by various Multi-Media Fate Models. WECC Wania Environmental Chemists Corp., WECC Report 2/2000.
- Wania F. and D. Mackay [1993] An approach to modelling the global distribution of toxaphene: A discussion of feasibility and desirability. *Chemosphere*, v. 27, pp.2079-2094.
- Wania F. and D. Mackay [1995] A global distribution model for persistent organic chemicals. *Sci.Total Environ.* v.160/161, pp.211-232.
- Wania F. and D. Mackay [1999] Global chemical fate of α -hexachlorocyclohexane. 2. Use of a global distribution model for mass balancing, source apportionment, and trend predictions. *Environ. Toxicol. Chem.*, v.18, pp. 1400-1407.
- Wania F., D. Mackay Y.-F. Li T.F. Bidleman and A.Strand [1999] Global chemical fate of α -hexachlorocyclohexane. 1. Evaluation of a global distribution model. *Environ. Toxicol. Chem.* v.18, pp.1390-1399.
- Wania F. and G. Daly [2002] Estimating the contribution of degradation in air and deposition to the deep sea to the global loss of PCBs. *Atmos. Environ.*, v.36., iss.36-37, pp. 5581-5593.
- Wania F. and M.S. McLachlan [2001] Estimating the influence of forests on the overall fate of semivolatile organic compounds using a multimedia fate model, *Environmental Science and Technology*, v.35, No. 3, pp. 582-590.
- Wania F., J.Persson A. Di Guardo and M.S. McLachlan [2000] CoZMO-Pop: A Fugacity-Based Multi-Compartmental Mass Balance Model of the Fate of Persistent Organic Pollutants in the Coastal Zone, WECC-Report 1/2000
- Whitby K.T. [1978] The Physical Characteristics of Sulphur Aerosols. *Atmos. Environ.*, v.12, pp.135 – 159.
- WOCE Data Products Committee, 1998: WOCE Global Data, Surface Velocity Programme, Version 1.0, WOCE IPO Report No. 158/98, Southampton, U.K.).
- Yu Lu and M.A.K. Khall [1991] Tropospheric OH: model calculation of spacial, temporal and secular variations. *Chemosphere*, v. 23, pp.397-444.

